AD_____

Award Number:
 W81XWH-12-1-0311

TITLE:
Early Intervention with Cdk9 Inhibitors to Prevent Post-Traumatic Osteoarthritis

PRINCIPAL INVESTIGATOR:
Dominik R. Haudenschild. Ph.D.

CONTRACTING ORGANIZATION:
University of California, Davis
Davis CA 95618-6134

REPORT DATE:
October 2013

TYPE OF REPORT:
Annual

PREPARED FOR: U.S. Army Medical Research and Materiel Command
                         Fort Detrick, Maryland 21702-5012

REPORT DOCUMENTATION PAGE

Form Approved
OMB No. 0704-0188

Public reporting burden for this collection of information is estimated to average 1 hour per response, including the time for reviewing instructions, searching existing data sources, gathering and maintaining the data needed, and completing and reviewing this collection of information. Send comments regarding this burden estimate or any other aspect of this collection of information, including suggestions for reducing this burden to Department of Defense, Washington Headquarters Services, Directorate for Information Operations and Reports (0704-0188), 1215 Jefferson Davis Highway, Suite 1204, Arlington, VA 22202-4302. Respondents should be aware that notwithstanding any other provision of law, no person shall be subject to any penalty for failing to comply with a collection of information if it does not display a currently valid OMB control number. **PLEASE DO NOT RETURN YOUR FORM TO THE ABOVE ADDRESS.**

1. REPORT DATE	2. REPORT TYPE	3. DATES COVERED
October 2013	Annual	30 September 2012-29 September 2013

4. TITLE AND SUBTITLE

Early Intervention with Cdk9 Inhibitors to Prevent Post-Traumatic Osteoarthritis

5a. CONTRACT NUMBER

5b. GRANT NUMBER
W81XWH-12-1-0311

5c. PROGRAM ELEMENT NUMBER

6. AUTHOR(S)
Dominik R. Haudenschild

5d. PROJECT NUMBER

5e. TASK NUMBER

5f. WORK UNIT NUMBER

E-Mail: Dominik.Haudenschild@ucdmc.ucdavis.edu or drhaudenschild@ucdavis.edu

7. PERFORMING ORGANIZATION NAME(S) AND ADDRESS(ES)

AND ADDRESS(ES)
University of California, Davis

Davis, CA 95618-6134

8. PERFORMING ORGANIZATION REPORT NUMBER

9. SPONSORING / MONITORING AGENCY NAME(S) AND ADDRESS(ES)
U.S. Army Medical Research and Materiel Command
Fort Detrick, Maryland 21702-5012

10. SPONSOR/MONITOR'S ACRONYM(S)

11. SPONSOR/MONITOR'S REPORT NUMBER(S)

12. DISTRIBUTION / AVAILABILITY STATEMENT
Approved for Public Release; Distribution Unlimited

13. SUPPLEMENTARY NOTES

14. ABSTRACT

We proposed to test (in aim 1) whether inhibition of Cdk9 would reduce the early transcriptional response to joint injury, and (in aim 2) whether this would delay or prevent the subsequent development of post-traumatic osteoarthritis. We made significant progress on aim 1 during the past 18 months. The first manuscript describing the in-vitro results on the chondroprotective effects of Cdk9 inhibitors is published in Arthritis&Rheumatology. We next began testing whether inhibition of Cdk9 in mouse knees protects against the acute inflammatory response at early times post-injury. At first we tested the transcription of early response genes since that process is directly controlled by Cdk9. These tests were very successful: a single intraperitoneal injection of Cdk9 inhibitor significantly reduced the acute response, and multiple injections reduced the acute response to baseline levels. Next, we looked at proteinase activity within the joints, which is initiated by the acute response and is responsible for cartilage degeneration. These tests were also successful. We are currently following through with additional analyses including in-vivo imaging and cytokine profiling as described in the proposal. This will be the material for our second manuscript, which we also expect to submit to Arthritis&Rheumatology. Given these positive results during the acute phase, we are well-positioned to initiate the longer-term studies we proposed in aim 2 in the near future.

15. SUBJECT TERMS
PTOA, acute injury response, inflammation, transcriptional elongation, Cdk9

16. SECURITY CLASSIFICATION OF:			17. LIMITATION OF ABSTRACT	18. NUMBER OF PAGES	19a. NAME OF RESPONSIBLE PERSON USAMRMC
a. REPORT	b. ABSTRACT	c. THIS PAGE	UU	136	19b. TELEPHONE NUMBER *(include area code)*
U	U	U			

TABLE OF CONTENTS

INTRODUCTION:

We propose that a <u>fundamental flaw</u> in current OA management is its focus on treating an irreversibly damaged joint during end-stage organ failure, rather than preventing the onset of cartilage and bone degeneration following traumatic joint injury. Our **GLOBAL HYPOTHESIS** is that OA is initiated at the molecular and cellular level shortly after an injury occurs, thus the optimal time frame for therapeutic intervention is also shortly after the injury. The **goal** of this research proposal is to develop an early therapeutic strategy, delivered just after a joint injury, which will prevent or delay the onset of joint degradation and OA.

Joint Injury induces an acute cellular response, which occurs on a time-scale of minutes to hours after injury. This acute cellular response is characterized by mRNA transcription of early response genes and release of inflammatory mediators, which initiate a destructive cascade of events leading to the degradation of joint matrix and osteoarthritis. The mRNA transcription of these early response genes is controlled by a central checkpoint, where Cdk9 kinase activity is the rate-limiting step. We hypothesized that inhibitors of Cdk9 would reduce mRNA transcription of the early response genes, and therefore prevent the destructive cascade of events leading to osteoarthritis.

In aim 1of this proposal we test whether inhibition of Cdk9 reduces the early mRNA transcriptional response to joint injury. For aim 1 we examine early responses (1 hour to 1 week after joint injury), and we test short-term outcomes (mRNA expression, local protease activity, cytokine production). The goal of aim 1 is to determine a treatment window (time and dose) wherein we can reduce the acute response to injury by inhibition of Cdk9. In aim 2 we test whether this early intervention delays or prevents the subsequent development of post-traumatic osteoarthritis using long-term outcomes (joint degradation, arthritis grade, proteoglycan loss). These experiments are performed in our recently developed non-invasive mouse model of joint injury in mice.

BODY:

Scientifically we made significant progress on Aim 1.

The first manuscript describing the in-vitro results on the chondro-protective effects of Cdk9 inhibitors is published in Arthritis & Rheumatology (A&R), which is the <u>highest-impact journal</u> dedicated to arthritis research and has stringent peer review. Many of these results in this manuscript were preliminary data of this grant application, but a good number of additional experiments were still required to get the story published in A&R. Many of these experiments are included in the Statement of Work as Task 1.

As proposed in Aim 1, we began testing whether inhibition of Cdk9 in mouse knees protects against the acute inflammatory response at early times post-injury. At first we tested the transcription of early response genes since that process is directly controlled by Cdk9. *These tests were very successful: a single intraperitoneal injection of Cdk9 inhibitor significantly reduced the acute response, and multiple injections reduced the acute response to baseline levels.* We are currently following through with additional analyses as described in the proposal, namely the production of inflammatory cytokines, the activity of catabolic proteases within the joints, and the remodeling of subchondral bone microstructure. A preliminary write-up of these results was presented as an abstract to the Orthopaedic Research Society's 60th Annual Meeting, held in New Orleans from March 15-18, 2014. This ORS poster is included as Appendix 2. A more detailed description of the observations and results is presented in bullet format in the next section.

KEY RESEARCH ACCOMPLISHMENTS
SPECIFIC AIM 1 – SHORT TERM EXPERIMENTS TO REDUCE INJURY-RESPONSE
TASK 1 – GENE EXPRESSION ANALYSIS AT BASELINE AND AT 1-240 HOURS POST-INJURY

A. Injure Mice According to the Schedule, with n=6 for each data point.

   Progress: We have completed most of this task. See notes below.

B. Sacrifice mice at given times and dissect out the injured and contralateral uninjured knee joints, and also harvest and store blood for Task 2.

   Progress: We have completed most of this task. Mice were injured according to the schedule provided in the proposal, and joints harvested for RNA extraction at hours 1, 2, 3, 4, 6, and days 1, 2, 3, 5, 7, and 10 after injury. We have not yet performed the 12, 18 hour time points.

C. Isolate total RNA and perform PCR-Array quantitative gene expression analysis on 84 NFkB dependent primary response genes.

   Progress: We have successfully isolated total RNA from all the harvested joints, and used this total RNA to synthesize cDNA. We performed quantitative RT-PCR on select primary response genes to determine the quality of the RNA, and estimate the responsiveness of the genes. The results are presented in the appendices. Specifically, Appendix 2 (Fig 1, 2) and Appendix 3 (Fig 3, 4)

D. Perform statistical analysis of the results.

   Progress: Complete for the data collected.

Milestone: We identified a peak response of gene expression at 4-6 hours post-injury. This peak response is rapidly induced by the injury, with some genes (such as IL-6) responding with approximately 80-fold induction in the injured leg compared to the uninjured contralateral knee. The peak is also rapidly resolved by 8 hours for most genes analyzed to date, with gene expression returning to 1-5 times that in the uninjured contralateral knee. Inhibition of Cdk9 with a single dose of inhibitor greatly reduces the injury-related increase of primary response gene expression. Two injections, 0 and 6 hours post-injury, effectively prevents the injury-related increase of the primary response genes assayed.

TASK 2 – ANALYSIS OF SERUM CYTOKINE LEVELS AT BASELINE AND AT 1-240 HOURS POST-INJURY

A. Blood/serum has been collected as part of Task 1A, with n=6 for each data point

   Progress: Blood/serum has been collected and stored appropriately

B. Multiplexed bead immunoassay analysis to quantify 32 pro-and anti-inflammatory cytokines

   Progress: Analysis is underway, see notes below.

C. Statistical analysis of the results

   Progress: Initial results showed statistically insignificant changes of circulating cytokines in the plasma samples, with the exception of IL-6 that showed a mild increase. This is shown in Supporting Data 1. In light of this, we propose a revised approach using homogenized knee joints to extract cytokines. This data would provide insight into the local cytokine response, presumably with greater sensitivity because only local tissue is analyzed (not diluted into the systemic circulation). The revised approach has not yet been started.

Milestone: We identified a mild increase in serum levels of IL-6, but not other cytokines, in response to joint injury.

TASK 3 – IN-VIVO IMAGING OF JOINT PROTEASE ACTIVITY AT BASELINE AND AT 1-240 HOURS POST-INJURY

    A. Mice will be injected with Imaging Reagents prior to imaging

        Progress: Done for most time points.

    B. Mice will be injured according to the protocol

        Progress: Done for most time points.

    C. Non-invasive functional imaging of Joint Protease activity will be performed on live mice.

        Progress: Done for most time points. Data is shown in Appendix 2 (fig 3), Appendix 4, Appendix 6 (fig 6), and Appendix 7 (fig 2, 4, 5).

    D. Mice will be sacrificed for uCT analysis in Task 4.

    Milestone: Protease activity within the joint is induced within 1 hour, peaks at 2-4 days post-injury, and remains elevated out to at least 8 weeks after injury. Inhibition of Cdk9 at the time of injury effectively prevents joint protease activity for the first 24 hours. Based on our experience (Task 2) with gene expression, we expect that multiple injections will be required to reduce injury-induced joint protease activity.

TASK 4 – MICROCT ANALYSIS OF THE REMODELING IN SUBCHONDRAL BONE AT BASELINE AND AT 1-240 HOURS POST-INJURY

    A. The same mice will be used for both imaging studies (tasks 3 and 4), n=5 for each data point.

        Progress: Done for most time points.

    B. Mice will be scanned 1 day before injury to obtain a baseline measurement, and then again at the indicated times.

        Progress: Partially done. Our in-vivo uCT does not have sufficient resolution to obtain adequate the baseline measurement. Our revised approach is to scan both the injured and contralateral uninjured leg of the same animal, and perform paired analysis. This has a disadvantage of possibly underestimating the bone loss in the injured leg, due to the slight systemic bone loss we've observed in the injured animals. To address this, we are also taking uCT images of uninjured age/sex matched animals that serve as additional controls.

        Progress: A single dose of Cdk9 inhibitor significantly prevented bone loss after injury at day 3 post-injury, and analyses performed at day 7 and week 8 showed a similar trend but did not reach statistical significance. This is shown in Supporting Data 2. The Cdk9 inhibitor has an in-vivo half-life of under 6 hours. We are repeating the experiments with multiple doses of Cdk9 inhibitor.

        Milestone: Inhibition of Cdk9 activity post-injury prevents or reduces bone loss at day 3 post-injury. Day 7 analysis is inconclusive with one injection, multiple injections will be tried.

SPECIFIC AIM 2 – LONG TERM EXPERIMENTS TO PREVENT OA
TASK 1 – HISTOLOGICAL ASSESSMENT OF OA AT TIMES 2, 3, 4 MONTHS POST-INJURY

    A. Injured mice will be sacrificed at the indicated times, joints processed for histology, and stained with Safranin-O with a Fast-Green Counter-stain.

        Progress: We have encountered a difficulty in completing this aim. Specifically, because our injury model ruptures the ACL, and due to the bent position of the knee in mice, we substantially alter the biomechanics of the joint and in-effect establish a new articulation point. The result of the altered biomechanics is that all animals develop arthritis, even though the initial injury

is relatively mild. This is evident in the publication shown in Appendix 5, in figure 8. We have taken two approaches to address this: The first is to use our existing model of ACL rupture, but examine earlier time points for intervention efficacy. The second is to use an even milder mechanical injury model that does not alter the biomechanics of the knee joint. We use our existing instrumentation to apply repeated sub-rupture stress to the ACL. Two other laboratories have used such an approach to generate mild OA without altering the biomechanics of the joint.

2. SUBSTANTIAL PROGRESS TOWARDS OVERALL GOAL:

- We established a cartilage explant injury model, where we mechanically compress bovine cartilage explants to 30% strain at a rate of 100% strain/second. Using this model we observed increased expression of injury response genes within 2 hours, including IL-6 (shown on the ORS manuscript figure 1a), iNOS, and others. Treatment with flavopiridol prevented elevation of these genes by injury at 2, 6, and 24 hours after injury.
- In the cartilage explant injury model, we observed that injury causes a decrease in the mechanical properties of injured cartilage compared to uninjured control. Treatment with flavopiridol prevented this loss of mechanical properties by the simulated injury (ORS manuscript figure 1b). In fact, even uninjured controls in the presence of flavopiridol had greater mechanical properties than in the absence of flavopiridol.
- Using our in-vivo mouse model of joint injury, we found a peak of inflammatory gene expression at about 2 hours post-injury. This timing was conserved between many genes, including iNOS, IL-6, MMP13, ADAMTS, TNFa, and others, suggesting a common regulatory mechanism (we presume Cdk9 is involved). Since many of these genes follow a similar pattern of induction after joint injury, we focused on the most highly induced genes, IL-6 and iNOS, for cost saving.
- In the mouse model of joint injury, a single injection of flavopiridol reduced and delayed the activation of inflammatory genes. However, a single injection of flavopiridol did not completely prevent the activation of inflammatory genes. This is not surprising given the half-life of flavopiridol is under 6 hours.
- In the mouse model of joint injury, a single injection of flavopiridol did not reduce the extent of remodeling in subchondral bone as measured by micro-CT within 1 week. We therefore switched to multiple post-injury injections of flavopiridol from here on.
- Multiple injections of flavopiridol completely prevented the activation of pro-inflammatory cytokines and catabolic proteases at the mRNA level after knee injury at all times measured (figure 2 of ORS poster).
- In-vivo imaging of MMP activity after injury showed elevated MMP activity in the injured joint became detectable perhaps as soon as 1 hour after injury. The 1 hour time point did not quite reach statistical significance with n=8 mice, but all other time points (2h, 3h, 4h, 6h, 8h, 12h, 1day, 2day, 4days, 7 days) showed significantly elevated in-vivo MMP activity in the injured joint. (figure 3 of ORS poster, open triangles).
- A single injection of flavopiridol after injury substantially reduced in-vivo MMP activity to near baseline levels during the first 24 hours, and MMP activity remained lower at all time points tested (figure 3 of ORS poster).
- Injury-induced inflammation and synovial hypertrophy both appear reduced if flavopiridol is administered after injury. An anecdotal image is shown as figure 4 of the ORS poster, but this result is preliminary because we still need to perform a full blinded scoring of the histological sections followed by statistical analysis.
- Multiple injections of flavopiridol after injury prevents subchondral bone loss at 3 days post-injury (figure 5 of ORS poster).

In **summary**, the results from these experiments are very positive. The data conclusively demonstrates that Cdk9 inhibition strongly reduced or even completely prevented every one of the acute local responses to joint injury that we tested. Given these positive results during the acute phase, we are well-positioned to initiate the longer-term studies we proposed in aim 2, namely to ask whether reducing the acute response will slow or prevent the development of osteoarthritis.

Given these very positive results in the context of joint injury, we are pursuing a similar Cdk9-inhibition strategy in additional injury situations, such as preventing systemic inflammation upon severe trauma, etc.

2. NEGATIVE FINDINGS AND PROBLEMS IN ACCOMPLISHING TASKS:

Overall the progress has been substantial, in some respects faster and much better than anticipated. The results have been universally very positive, almost without exception. A few minor difficulties are below:

2.a: Deaths of mice: We attribute the following negative events to our own mistakes, but we feel obligated to report them for the sake of transparency. Four mice died in the groups where mice received single or multiple injections of flavopiridol, while no deaths occurred in the vehicle-control or un-injected groups. The deaths occurred at 1 to 2 days after intraperitoneal injection of flavopiridol, and we believe it was because the needle accidentally punctured an internal organ rather than staying within the intraperitoneal space. This is from a total of 519 mice used so far in the study, of which between 1/3 and ½ of received flavopiridol injections.

2.b: Effort and budget underestimated: I underestimated the amount of effort, and also the budget, required for the proposed studies.

With respect to the effort - in the first year, I was able to recruit unpaid manpower onto this project. Without the uncompensated help of these individuals, progress would not have been as fast. A student from Zhejiang University (a University with which UC Davis has a close connection) joined the project as his PhD Thesis. He was appointed a Research Associate without Salary position here for 13 months ending in December 2013, and worked full-time (>50hrs/wk) on this project. In addition, two first-year medical students in the UC Davis School of Medicine were awarded research fellowships to complete aspects of this project, and four undergraduate interns put in many hours during the school year and even more hours during the summer to help complete aspects of this project. In addition, contributions from members of other labs were required. Many of these contributors are listed as co-authors in the ORS abstract.

With respect to the budget - prices of everything increased substantially since the original budget proposal, this includes salaries & benefit rates, reagents & supplies, animals, internal recharge rates for services such as in-vivo imaging and microCT, and external services such as histology. In addition, in the original proposal I over-estimated the number of assays we could practically perform on the same animals. It turned out that transferring the mice from the vivarium near my lab in Sacramento (where we perform the injury) to the facility for in-vivo imaging in Davis was a 15-mile one-way trip. For quarantine reasons animals are not allowed back into the Sacramento vivarium, a detail that I did not realize when writing the original proposal. It was unpractical to transport sufficient laboratory equipment from my lab to the imaging facility to perform assays other than imaging at that location. Therefore, given that most of our assays are performed at short time points after injury, we had to perform these experiments on additional sets of mice. Another reason that more mice were required is that imaging the early time points (as in ORS Poster figure 3) could not practically be done on the same mice. In our initial protocol we proposed imaging the mice 3 at a time, so we thought we could easily perform n=6 images within one hour. It turned out that an unexpected limitation of the imaging instrument (IVIS200 by Perkin Elmer) introduced a systemic error based on the location of the mouse and the resulting angle of the illumination on the injured knees. After consulting with the Perkin-Elmer technicians, the only solution was to image one animal at a time, centered directly under the illumination source and camera. While this modification allowed us to get great data, it also greatly increased the number of animals required for the study, and the associated effort and costs.

In retrospect I attribute the effort/budget underestimation to my own inexperience. My original proposal was an honest (not over-inflated) estimate for doing the proposed work at the time of budget preparation. However, I did not include the additional requirements for publication of the results in high-impact journals, I did not sufficiently anticipate the steep inflation of costs, and I did not expect that the constraints of injuring mice at one facility while imaging at another facility would require the early time point experiments to be performed on as many mice.

Freezer Loss: In November we had a catastrophic failure of our -80 freezer, resulting in the loss of all archived RNA and serum samples. This is a serious setback, necessitating the repeat of several key experiments.

Long term mouse injury model: Our mouse PTOA model is ideally suited for studying short-term acute responses to injury. However, the injury inevitably leads to PTOA in 8-12 weeks due to altered biomechanics of the joint, making it less than ideal for long-term experiments to evaluate therapeutic efficacy. We are working on a new milder model, wherein the ACL is stretched repeatedly and the cartilage is impacted, but no changes in biomechanics occur because the ACL stays intact. We will use this model for long term (8-12 week studies) and use our original ACL rupture model for shorter time points (under 6 weeks).

In summary, at the end of year 1 we are scientifically on track with excellent results and only very minor setbacks, but somewhat over budget and over-worked.

REPORTABLE OUTCOMES

MANUSCRIPTS, ABSTRACTS, AND PRESENTATIONS

- Manuscript published in Arthritis & Rheumatology, title "Cyclin-Dependent Kinase 9 inhibition protects cartilage from the catabolic effects of pro-inflammatory cytokines", PMID: 24470357. Included as Appendix 1. Much of the work for this manuscript was directly funded by this award.
- Manuscript published in Journal of Orthopaedic Research, title "Comparison of Loading Rate-Dependent Injury Modes in a Murine Model of Post-Traumatic Osteoarthritis", PMID: 24019199. Included as Appendix 5. No funds from this grant were used, but the work was greatly facilitated by the expertise we developed through this grant.
- Manuscript submitted to Osteoarthritis and Cartilage, title "In-vitro and In- vivo Imaging of MMP Activity in Cartilage and Joint Injury". Included as Appendix 6. No funds from this grant were used, but the work was greatly facilitated by the expertise we developed through this grant.
- Manuscript submitted to Osteoarthritis and Cartilage, title "In Vivo Fluorescence Reflectance Imaging to Quantify Sex-Based Differences in Protease, MMP, and Cathepsin K Activity in a Mouse Model of Post-Traumatic Osteoarthritis". Included as Appendix 7. No funds from this grant were used, but the work was greatly facilitated by the expertise we developed through this grant.
- Abstracts
  - Poster presentation at Orthopaedic Research Society's 60th Annual Meeting in New Orleans, March 2014. Title "CDK9 inhibition attenuates acute inflammatory response and reduces bone loss in a non-invasive post- traumatic osteoarthritis mouse model." Included as Appendix 2.
  - Poster presentation at World Congress of Osteoarthritis (OARSI) 2013, title "Early Transient Induction of IL-6 in a Mouse Joint Injury Model." Included as Appendix 3.
  - Poster presentation at World Congress of Osteoarthritis (OARSI) 2013, title "Fluorescence Reflectance Imaging of Early Processes of Post-Traumatic Osteoarthritis in Male and Female Mice." Included as Appendix 4.
- Presentations:
  - 2012 November 20, ACL Damage as a Model for Early Osteoarthritis, UC Davis Medical Center Osteoarthritis Meeting, headed by Nancy Lane.
  - 2013 January 23, Early Molecular Events in Joint Injury, Invited Seminar at the UC Davis Veterinary Orthopaedic Research Laboratory seminar series.
  - 2013 January 28, CDK9 Inhibition Protects Cartilage from the Catabolic Effects of Pro-Inflammatory Cytokines, by Yik JHN (presenting), Kumari R, Christiansen BA, and Haudenschild DR., Session 42 - "MMP Regulation in Articular Chondrocytes" at the 2013 Meeting of the Orthopaedic Research Society in San Antonio, TX.
  - 2013 June 5, Osteoarthritis: The need for Imaging Early Stages of Disease, Given at the "Frontiers in Biomedical Imaging" seminar series held by the Radiology Department of UC Davis.
  - 2013 June 20, "Early Response to Joint Injury", University of California Davis Department of Orthopaedic Surgery Research Symposium, Lawrence J. Ellison Musculoskeletal Research Center.
  - 2013 October 15, "Early Response to Joint Injury and Osteoarthritis", UC Davis Department of Orthopaedic Surgery Grand Rounds invited Seminar

LICENSES APPLIED FOR AND/OR ISSUED

- None during the last 12 months

DEGREES OBTAINED THAT ARE SUPPORTED BY THIS AWARD

- None during the last 12 months

DEVELOPMENT OF CELL LINES, TISSUES, OR SERUM REPOSITORIES

- None during the last 12 months

INFORMATICS SUCH AS DATABASES AND ANIMAL MODELS

- None during the last 12 months

FUNDING APPLIED FOR BASED ON WORK SUPPORTED BY THIS AWARD

- We applied for an R21 grant to test whether we could reduce systemic inflammation after severe trauma, using similar inhibition of Cdk9 with flavopiridol as in this award. The grant was favorably reviewed (priority score 33) but not funded. We plan a revision.

EMPLOYMENT OR RESEARCH OPPORTUNITIES APPLIED FOR AND/OR RECEIVED BASED ON EXPERIENCE/TRAINING SUPPORTED BY THIS AWARD

- None during the last 12 months

CONCLUSION

In **conclusion**, the results from these experiments are very positive. Our goal in Aim 1 was to inhibit the early response to joint injury. The data collected thus far conclusively demonstrates that Cdk9 inhibition strongly reduced or even completely prevented every one of the acute local responses to joint injury that we tested. These results are currently being finalized, and readied for submission as a manuscript to Arthritis & Rheumatism.

Given these positive results during the acute phase, we are well-positioned to initiate the longer-term studies we proposed in aim 2, namely to ask whether reducing the acute response will slow or prevent the development of osteoarthritis.

Given these very positive results in the context of joint injury, we are pursuing a similar Cdk9-inhibition strategy in additional injury situations, for example preventing systemic inflammation upon severe trauma.

REFERENCES

None

APPENDICES

1. Arthritis & Rheumatism Manuscript, Accepted Manuscript (still in press)
2. ORS 2014 Poster on chondroprotective effect of Cdk9 inhibitors in joint injury
3. OARSI 2013 Poster on transcriptional response to joint injury
4. OARSI 2013 Poster on in-vivo imaging of joint-injury proteolytic activity
5. JOR Manuscript, Published manuscript
6. OA&C Submitted manuscript #1
7. OA&C Submitted manuscript #2

SUPPORTING DATA

All supporting data is contained in the appendices.

Authors: Jasper H. N. Yik, Ph.D. [1]

Zi'ang Hu, M.D. [2,1]

Ratna Kumari, Ph.D. [1,3]

Blaine A. Christiansen, Ph.D. [1]

Dominik R. Haudenschild, Ph.D. [1,*]

[2] Department of Orthopaedic Surgery,
Sir Run Run Shaw Hospital,
School of Medicine,
Zhejiang University,
Hangzhou, 310016 PR China

[3] KIIT School of Biotechnology,
KIIT University,
Bhubaneswar,
India

[1,*]Address correspondence to
Dominik R. Haudenschild
University of California Davis,
Department of Orthopaedic Surgery,
Lawrence J. Ellison Musculoskeletal Research Center
Research Building 1 Suite 2000
4635 Second Avenue
Sacramento, CA 95817
Tel: 916-734-5015 Fax: 916-734-5750

Email: Dominik.Haudenschild@ucdmc.ucdavis.edu

Abstract

Objective. CDK9 controls the activation of primary inflammatory response genes. We determined whether CDK9 inhibition protects cartilage from the catabolic effects of pro-inflammatory cytokines.

Methods. Human chondrocytes were challenged with different pro-inflammatory stimuli (IL-1β, lipopolysaccharides, and TNFα), in the presence or absence of the CDK9 inhibitor Flavopiridol, or siRNA. The mRNA expression of inflammatory mediators, catabolic, and anabolic genes were determined by real-time PCR. Cartilage explants were incubated with IL-1β, with or without Flavopiridol, for 6 days. Cartilage matrix degradation was assessed by the release of glycosaminoglycan (GAG) and cleaved Type II collagen (Col2a) peptides.

Results. CDK9 inhibition by Flavopiridol, or knockdown by siRNA, effectively suppressed iNOS mRNA induction by all three pro-inflammatory stimuli. Results from NFkB-targets PCR array showed that Flavopiridol suppressed the induction of a broad range of inflammatory mediator genes (59 out of 67 tested) by IL-1β. CDK9 inhibition also suppressed induction of catabolic genes MMP 1, 3, 9, 13, and ADAMTS4, 5; but did not affect the basal expression of anabolic genes such as Col2a, aggrecan, and COMP, and housekeeping genes. Flavopiridol had no apparent short-term cytotoxicity as assessed by glucose-6-phosphate dehydrogenase activity. Finally, in IL-1β-treated cartilage explants, Flavopiridol reduced the release of matrix degradation products GAG and cleaved Col2a peptides, but did not affect long-term chondrocyte viability.

Conclusion. CDK9 activity is required for the primary inflammatory response in chondrocytes. Flavopiridol suppresses the induction of inflammatory mediators and catabolic genes to protect

cartilage from the deleterious effects of pro-inflammatory cytokines, without impacting cell viability and functions.

Key words: CDK9, inflammatory cytokines, primary response genes, Flavopiridol, chondrocytes, cartilage

Introduction

Osteoarthritis (OA) affects more than half of the people over age 65 in the United States. OA is a degenerative disease of the articular joints characterized by slow but progressive lost of cartilage. The main protein component of articular cartilage is a fibrillar network of type II collagen (Col2a), which provides tensile strength to the cartilage. The compressive stiffness of the cartilage is provided by the proteoglycan components, through their attraction of water molecules. Although the etiology of OA remains incompletely understood, various inflammatory conditions that cause damage to the collagens and proteoglycans in cartilage are suspected of initiating OA.

Pro-inflammatory cytokines are induced by a variety of stress conditions in cartilage, including joint overloading and physical damage such as occurs in sports-related injuries. Pro-inflammatory cytokines, such as interleukin 1 beta (IL-1β) and tumor necrosis factor alpha (TNFα), elicit a cascade of events that activate inflammatory mediator genes and apoptosis in chondrocytes (reviewed by (1)). Pro-inflammatory cytokines can also induce the expression of proteinases that degrade cartilage matrix, including matrix metallopeptidases (MMPs), aggrecanases, and cathepsins (reviewed by (2)). Therefore, a stretagy to effectively suppress the inflammatory response in cartilage may prevent or delay the onset of osteoarthritis.

Acute tissue stress and inflammatory signaling activate primary response genes (PRG) that do not require de novo protein synthesis. Recent advances demonstrate that despite their initiation by diverse signaling pathways, the transcriptional activation of most, if not all, PRG is

similarly controlled by a general transcription factor (3, 4), namely the cyclin-dependent kinase 9 (CDK9). It was believed for many years that the rate-limiting step in transcriptional activation of PRG is the recruitment of transcription factors and RNA Polymerase II (Pol II) complex to the promoters. However, recent studies show that in order for these PRG to be activated rapidly, in their basal and unstimulated states, the Pol II complex is already pre-assembled and producing short mRNA transcripts (3, 4). In the absence of inflammatory signals, Pol II remains paused ~40 base-pair downstream of the transcription start site. Upon inflammatory stimulus, CDK9 is recruited to the transcription complex by the Bromodomain-containing protein (Brd) 4 through its associated with acetylated histones (8, 9). Once recruited, CDK9 phosphorylates Pol II to induce a conformational change that allows Pol II to enter possessive elongation to efficiently transcribe full-length mRNAs (reviewed in (5)). Thus, CDK9 regulation represents a central mechanism of activating PRG transcription and has a broad impact on many aspects of biological functions.

Given that CDK9 controls a common mechanism of all PRG activation, it is an attractive target for anti-inflammatory therapy (reviewed in (6)). The objective of this study is to determine whether CDK9 inhibition effectively suppress the inflammatory response in chondrocytes and protect cartilage from the catabolic effects of pro-inflammatory cytokines in vitro.

Methods

Articular chondrocytes and cartilage explants – Human primary chondrocytes and cartilage explants were isolated from cartilage tissues obtained from total knee arthroplasty (15 donors, age 44-80 years, all with end stage OA) with IRB approval and cultured in DMEM with 10%

FBS as described (7). The chondrocytes were used for experiments within 3-5 days without passaging to avoid dedifferentiation. A total of 5 cartilage explant donors were used for matrix degradation studies (Figure 5). All other experiments were performed with chondrocytes from at least 3 individual donors. Full thickness bovine cartilage explants were isolated from the stifle joints of young veal calves using 6-mm biopsy punches and maintained in DMEM with 10% FBS.

Treatments of chondrocytes with inflammatory stimuli and small molecule inhibitors – Primary chondrocytes were seeded in 12-well plates at a density of 2×10^4 cells/cm^2 and allowed to reach ~80% confluence (~4×10^4 cells/cm^2). The cells were treated with 10 ng/ml lipopolysaccharide (LPS) (Sigma), 10 ng/ml IL-1β (R&D System), or 10 ng/ml TNFα (R&D System) for various time, with or without pharmacological inhibitors. The inhibitors used in this study included Flavopiridol (Sigma), JQ-1 (a kind gift from Dr. James Bradner, Harvard University (8)), BS-181 HCl (Selleckchem), and SNS-032 (Selleckchem). After the treatment, the cells were washed 3 times with phosphate buffered saline and harvested for gene and protein expression analysis.

Lentiviral siRNA constructs - The CDK9-targeting siRNA used in this study (AGGGACATGAAGGCTGCTAAT) was inserted into the A*ge*I and *Eco*RI sites of the lentiviral vector pLKO.1 (plasmid #8453, www.Addgene.com). A siRNA targeting GFP was used as control. Lentiviral particles were generated and tittered as described (9). Human chondrocytes were seeded at 1×10^4 cells/cm^2 in 12-well plate. Lentiviral particles harboring CDK9- or GFP-targeting siRNA were then added at a multiplicity of infection of 10, in the

presence of 1 µg/ml polybrene (American Bioanalytical). The media was replaced after 16 hours and the cells were used for experiments after 5 days. Knockdown of CDK9 was confirmed by Western blotting.

Quantitative real-time (RT) PCR – For the determination of individual mRNA expression, cytokine/inhibitor-treated chondrocytes in 12-well plates were harvested by scraping and transferred to Eppendorf tubes, followed by cell lysis and reverse transcription to generate cDNA using the Cells-to-C_T kit (Ambion) according to the manufacturer's instructions. 2 ul of cDNA was used for quantitative RT-PCR (in a final volume of 10 ul) performed in triplicate in a 7900HT RT-PCR system with gene-specific Taqman probes (Applied Biosystem Inc.) according to the manufacturer's conditions. Results were normalized to 18s rRNA and calculated as fold-change in mRNA expression relative to untreated control, using the $2^{-\Delta\Delta CT}$ method. The probes used are as follow: iNOS, Hs01060345_m1; MMP1, Hs00899658_m1; MMP3, Hs00968305_m1; MMP9, Hs03234579_m1; MMP13, Hs0023992_m1; ADAMTS4, Hs00192708_m1; ADAMTS5, Hs00199841_m1; ACAN, Hs00202971_m1; COMP, Hs00154339_m1; COL2A, Hs01060345_m1; 18s rRNA, 4319413E.

For PCR array analysis, IL-1β/Flavopiridol-treated chondrocytes grown in 10 cm plates were harvested and total RNA was isolated using the RNeasy Mini Kit (Qiagen). RNA quality and quantity were assessed with a Nanodrop 2000 spectrophotometer (Thermo Scientific) and ~500 ng of total RNA was reverse transcribed using a Superscript First-Strand kit (Invitrogen). RT-PCR was performed in a 7900HT PCR system using the PCR Arrays for Human NFκB Signaling Targets (Qiagen, cat# 330231), according to the manufacturers' protocol. PCR array

data were analyzed by the accompanying online analysis software provided by Qiagen at www.qiagen.com.

Cytotoxicity/Viability Assays – For determining the short-term cytotoxic effects of Flavopiridol, chondrocytes were seeded in 96-well plates at 1, 5, or 10 x 10^3 cells per well and treated with 300 nM Flavopiridol for 5 hours. Cytotoxicity was assessed using the Vybrant Cytotoxicity Assay kit (Invitrogen, cat# V23111), according to the manufacturer's protocol to measure soluble and total glucose 6-phosphate dehydrogenase (G6PD) activity with resazurin as substrates. Fluorescence was detected using a Synergy HT plate reader (Bio-TEK Instruments Inc.) with excitation and emission filters set at 528 and 635 nm, respectively.

For determining long-term effects of Flavopiridol on the viability of chondrocytes in cartilage, bovine cartilage explants (6-mm disk) were cultured in 6-well plates in DMEM and 10% FBS, in the presence or absence of 300 nM Flavopiridol for 6 days, with media changed every other day. The live and dead cells were stained using the LIVE/DEAD Viability/Cytotoxicity kit (Invitrogen, cat# L3224) according to the manufacturer's protocol. The percentages of live and dead cells were determined by counting the cell numbers at three random fields of the cross-section images of explants captured using a fluorescence microscope. A total of 3 different donors were used.

Western blot analysis – Chondrocytes grown in 12-well plates were harvested and lysed with sample loading buffer (50 mM Tris-HCl, pH 6.8; 100 mM dithiothreitol; 4% 2-mercaptoethanol; 2% sodium dodecyl sulfate; 10% glycerol). Lysates were resolved by 4-12% SDS-polyacrylamide gels and transferred onto nitrocellulose membranes (BioRad). The membranes

were blocked with 3% skim milk in TBST (25 mM Tris-HCl, pH 7.5; 125 mM NaCl; 0.1% Tween 20), followed by incubation with rabbit anti-CDK9 (0.6 ug/ml) (10) mouse anti-MMP13 (1:500 dilution) (Calbiochem, cat# IM78), or mouse anti-GAPDH (1:5000) (Ambion, cat# AM4300) at 4°C overnight. Blots were then probed with horseradish peroxidase-conjugated secondary antibody (Santa Cruz Biotechnology), and reactive protein bands were visualized with Western Lightning Plus-ECL (Perkin Elmer) on radiographic films.

Assessment of cartilage degradation – Human cartilage explants (~3mm cubes) were treated with 1 ng/ml IL-1β for 6 days, in the presence or absence of 6 or 300 nM Flavopiridol (with media change on day 3). The amount of glycosaminoglycan (GAG) released into the media from day 3 to day 6 was determined by the colorimetric dimethylmethylene blue dye-assay, with chondroitin sulfate as standard (11). The release of Col2a degradation products into the media was determined by measuring the amount of cleaved Col2a peptides (12) with the C2C ELISA kit (IBEX Pharmaceuticals) according to the manufacturer's protocol.

Statistical analysis – Values of all measurements were expressed as the mean $\pm$ standard deviation. Changes in gene expression were analyzed by one-way ANOVA with SPSS 16.0 software. The fold-change in mRNA was used as variables to compare samples between different treatment groups. The least significant difference post-hoc analysis was conducted with a significance level of $P<0.05$.

Results

The role of CDK9 on the induction of the primary response gene iNOS. Although the rate-limiting step for transcriptional activation of primary inflammatory response genes in lymphocytes is controlled by CDK9 (3, 4), whether CDK9 plays a similar role in articular chondrocytes has not been investigated. Therefore, we take advantage of a widely used and well-characterized pharmacological CDK9 inhibitor, Flavopiridol, to determine the role of CDK9 in the activation of PRG in chondrocytes. To activate PRG, chondrocytes in culture were treated with IL-1β, in the presence or absence of 300 nM Flavopiridol (the effective plasma concentration determined in clinical trials (13)). The induction of the stress response gene iNOS (inducible nitric oxide synthase) (14) was determined at various time points. The results showed that iNOS mRNA was unchanged after 1 hour of IL-1β treatment, but was induced significantly after 3 and 5 hours (Figure 1A, open bars). However, co-treatment with Flavopiridol completely suppressed the induction of iNOS by IL-1β (Figure 1A, grey bars). These results indicate a time-dependent induction of iNOS by IL-1β that is sensitive to Flavopiridol treatment.

The above results demonstrated the effects of Flavopiridol administered concurrently with the inflammatory cytokines. We next tested whether a delay in the addition of Flavopiridol could still suppress iNOS induction by IL-1β. Chondrocytes were treated with IL-1β for a total of 5 hours, with either no delay, or a 1- or 3-hour delay in the addition of Flavopiridol. The data showed that when compared to no Flavopiridol treatment (~235-fold iNOS induction), the addition of Flavopiridol markedly repressed iNOS induction if Flavopiridol was administered at no delay (down to ~2.7-fold induction) and at a 1-hour delay (~4-fold) (Figure 1B). Although less effective, a 3-hour delay still allowed significant repression of iNOS induction (~18-fold) (Figure 1B). These results indicate that there is at least a 3-hour window of opportunity for administering Flavopiridol to suppress iNOS induction after the initial treatment of IL-1β. We

next demonstrated that Flavopiridol suppressed iNOS induction by IL-1β in a dose-dependent manner, with the most effective dose at 300 nM (Figure 1C). Importantly, there was no apparent cytotoxicity of Flavopiridol at the highest dose, in terms of G6PD activity, on cultured chondrocytes within the 5 hours time frame tested (Figure 1D).

Besides CDK9, Flavopiridol has off-target effects that include other CDKs (listed in Figure 1E). While these CDKs do not affect PRG activation directly, we never the less used additional CDK inhibitors to rule out their involvement in suppressing iNOS induction. To this end, we tested the abilities to suppress iNOS induction by the following three small molecule inhibitors: BS-181 HCl (specific for CDK7) (15), SNS-032 (targeting CDK2, 7, and 9) (16), and JQ-1 (specific for Brd4, which is required for CDK9's function (8)). The data showed that only SNS-032, JQ-1, and Flavopiridol, but not BS-181, suppressed iNOS induction in a dose-dependent manner (Figure 1E), thus effectively ruling out the involvement of CDK7 in IL-1β-induced iNOS transcription. It is important to note that unlike the other CDK inhibitors tested here, JQ-1 does not directly inhibit the kinase activity of CDK, but rather, it prevents the association of acetylated histones with Brd4 (8), which specifically recruits CDK9 to the promoters for activation of transcription of PRG (4,5). Therefore, the above results strongly suggest that CDK9 is involved in iNOS induction. To definitively prove this, we used siRNA to specifically knockdown CDK9 expression in chondrocytes and determined the effects on iNOS induction. The results showed that in CDK9-depleted cells (confirmed by Western blot, Figure 1F inset), IL-1β failed to induce iNOS. Similar results were obtained when other catabolic genes such as MMP1, 3, 9, 13, and ADAMTS4 were examined (Figure 1F), thus demonstrating the requirement of CDK9 in catabolic gene induction. Taken together, our results clearly show the

specific involvement of CDK9, but not other CDKs, in the induction of iNOS by IL-1β. Since Flavopiridol is the first small molecule CDK inhibitor in clinical trials with well-characterized pharmacokinetics, it has the highest potential for translation into clinical studies, and therefore, it is used exclusively in the remainder of this study.

CDK9 controls the activation of inflammatory response from diverse signals. PRG are activated by diverse inflammatory signals. However, regardless of the sources, most inflammatory signals converge onto the rate-limiting step of transcriptional elongation of PRG, which is controlled by CDK9. In order to illustrate this, three different inflammatory signaling pathways were selected; namely, IL-1β, lipopolysaccharides (LPS), and Tumor Necrosis Factor alpha (TNFα). The cellular response to IL-1β, LPS, or TNFα is mediated by three distinct pathways – activation of the IL-1Receptor, Toll-Like Receptor 4, or TNF Receptor 1, respectively (Figure 2A). Chondrocytes were treated with three inflammatory stimuli independently, in the presence or absence of the CDK9 inhibitor Flavopiridol. The mRNA expression of iNOS, a common effector gene for all three pathways (14), was then determined. The results showed that Flavopiridol greatly suppressed the activation of iNOS expression by all three pathways (Figure 2B), demonstrating the effectiveness and broad range of Flavopiridol in preventing inflammatory response from diverse signals. Thus our data confirmed previous finding in other cellular systems (4, 5) and established CDK9 as a central regulatory point for primary inflammatory response in chondrocytes.

CDK9 inhibition prevents the activation of a broad spectrum of inflammatory response genes. To further investigate the effects of CDK9 inhibition on the activation of other inflammatory

mediators, the gene expression profiles of chondrocytes treated with IL-1β for 5 hours were determined by real-time PCR arrays. The PCR array contained 84 key genes responsive to NFκB signal transduction (Qiagen), which is central to the regulation of multiple cellular processes such as inflammatory, immunity, and stress responses. The gene expression profiles from three chondrocyte donors were averaged, and are presented as heat maps in which low and high relative expressions are represented by green and red colors, respectively (Figure 3). The array data in numerical format is included as supplementary data. The results showed that IL-1β strongly activated the majority of the 84 NFκB-target genes tested (Figure 3, compared lane 1& 2), while CDK9 inhibition by Flavopiridol almost completely abolished the effects of IL-1β (lane 3). On average, across three chondrocyte donors, CDK9 inhibition repressed IL-1β activity by a magnitude of greater than 86%, and suppressed 59 out of 67 NFκB-target genes that were activated at least 1.5-fold by IL-1β. Importantly, house-keeping genes, as well as genes not induced by IL-1β, were not affected by Flavopiridol. These data demonstrated that CDK9 can be targeted to effectively suppress only the activation of a cascade of downstream inflammatory response genes, without affecting the basal expression of non-responsive genes.

CDK9 inhibition prevents the activation of catabolic genes, but has no effects on basal expression of anabolic genes in chondrocytes. Besides activating the acute phase inflammatory genes, pro-inflammatory cytokines such as IL-1β and TNFα can also stimulate the expression of catabolic genes in chondrocytes (2, 17). These catabolic genes include the various matrix MMPs and ADAMTS (a disintegrin and metalloproteinase with a thrombospondin type 1 motif) that degrade the cartilage matrix. Given the role of CDK9 in activation of inflammatory genes, we next examined the effects of CDK9 inhibition on the induction of MMPs and ADAMTS in

chondrocytes treated independently with IL-1β, LPS, and TNFα for 5 hours. The results showed that IL-1β-mediated upregulation of MMP1, 3, 9, and 13, as well as ADAMTS4 mRNAs, was markedly suppressed by co-treatment with Flavopiridol (Figure 4A). Similar trends were observed in LPS- or TNFα-treated samples (Figure 4B & C). These data indicated that CDK9 inhibition prevented the transcriptional activation of catabolic genes in chondrocytes. Next, we sought to confirm the upregulation of MMP13 mRNA at the protein level, which is implicated in collagen degradation and osteoarthritis (18). Chondrocytes were treated with IL-1β, with and without Flavopiridol, for 2 days. Cell-associated active MMP13 protein (~48 kDa) was then detected by Western blots. The data showed that MMP13 protein expression was elevated in all three donors treated with IL-1β, but remained at basal levels with IL-1β and Flavopiridol treatment (Figure 4D). Thus, the results on protein expression corroborate with the mRNA expression profiles of MMP13. On the other hand, the mRNA expression of selected anabolic genes (Aggrecan, Cartilage Oligomeric Matrix Protein (COMP), and Collagen 2a) in chondrocytes was not significantly affected by IL-1β or Flavopiridol within the same 5-hours time frame (Figure 4E). Taken together, the above results demonstrate that Flavopiridol selectively suppresses only the induction of catabolic genes by pro-inflammatory stimuli, while having negligible effects on the basal expression of anabolic genes.

CDK9 inhibition protects cartilage from the catabolic effects of IL-1β. Since CDK9 inhibition suppresses the activation of inflammatory genes and catabolic enzymes in chondrocytes, we next determined whether Flavopiridol can protect cartilage from the deleterious effects of pro-inflammatory cytokines. Human arthritic cartilage explants were isolated and cultured in media containing 1 ng/mL IL-1β, in the presence or absence of Flavopiridol for 6 days. Note that the

concentration of IL-1β was reduced from the 10 ng/ml used in short-term monolayer culture, to a level similar to those detected in the synovial fluids of inflamed joints (19-21). Degradation of cartilage matrix was then assessed by measuring the release of GAG and Col2a cleavage peptides into the culturing media. As expected, IL-1β increased the amount of both GAG (Figure 5A) and Col2a peptides (Figure 5B) released into the media (compared first and second bars). However, the concentrations of both GAG and Col2a peptides were reduced by 6 nM Flavopiridol and returned to baseline levels by 300 nM Flavopiridol (Figure 5A & B). Thus, our data provides evidence that CDK9 inhibition prevents the catabolic destruction of cartilage by IL-1β. Importantly, the percentages of live/dead cells were similar in both untreated and Flavopiridol-treated bovine cartilage explants (Figure 5C). This result indicates that prolonged treatment of cartilage with Flavopiridol did not have an adverse effect on the viability of chondrocytes in cartilage explants. Taken together, our data indicate that CDK9 inhibition protects cartilage explants from the catabolic effects of IL-1β.

Discussion

The etiology of primary OA remains incompletely understood and the involvement of the inflammatory response is somewhat controversial. However, it is well established that damage to the collagen network originates around chondrocytes at the cartilage matrix surface (22). Since inflammatory response induces chondrocyte apoptosis and cartilage matrix breakdown (2), there are several anti-OA strategies that target either specific branches of the inflammatory signaling cascade (e.g. IL-1, IL-6, TNFα, and NFκB inhibitors) (17, 23, 24), or the downstream events such as apoptosis with caspase inhibitors (1). However, because inflammation can be induced by a variety of stimuli, the above individual approaches would have limited effectiveness in

handling the diverse simultaneous challenges in a biological system, as well as limited abilities in efficiently suppressing a broad range of inflammatory mediator expression. A novel approach to addressing these limitations is to directly target CDK9, which activates transcription of primary inflammatory response genes. Using the pharmacological CDK9 inhibitor Flavopiridol, we have shown that cartilage can be protected from the harmful effects of pro-inflammatory cytokines.

Our results demonstrate for the first time in chondrocytes that Flavopiridol effectively suppresses the acute response to multiple inflammatory stimuli (Figure 2), and prevents the induction of a broad range of inflammatory mediators (Figure 3), as well as catabolic genes that contribute to the degradation of the cartilage matrix (Figure 4). In most cases, Flavopiridol almost completely abolishes the activation of inflammatory mediator expression. For example, from the PCR array data (Fig 3 and supplemental data), IL-1β induced expression of IL-6 by 492-fold, but only 4.2-fold in the presence of Flavopiridol, representing a 99.2% repression of IL-1ß-dependent transcription. Importantly, our data demonstrate the selectivity of Flavopiridol-mediated inhibition, in which only the IL-1β-inducible genes are suppressed, but not the basal expression of non-inducible genes, housekeeping genes (Figure 3), and the anabolic genes (Col2a, COMP, and aggrecan) in chondrocytes (Figure 4E). The gene expression profiles are further supported by the experiments demonstrating Flavopiridol can effectively prevent cartilage degradation induced by IL-1β (Fig 5A & B). The reduction in matrix degradation products was not due to changes in cell viability in cartilage treated with Flavopiridol, because live/dead staining revealed similar chondrocyte viabilities between control and Flavopiridol treated bovine cartilage explants (Figure 5C). Bovine cartilage was used instead of human

cartilage because normal, healthy human cartilage is not routinely available, and the live/dead ratio of arthritic human cartilage obtained from knee surgery is erratic even when adjacent areas were examined.

Flavopiridol is an ATP analog that preferentially inhibits CDK9 kinase activity (Ki=30 nM) by a high affinity interaction with its ATP-binding pocket (25). Although Flavopiridol can potentially inhibit other CDKs, numerous studies using a combination of specific inhibitors and siRNA have demonstrated that only CDK9 inhibition is responsible for the anti-inflammatory action of Flavopiridol (26, 27). We have also shown that both JQ-1-mediated inhibition of Brd4, which does not directly interact with other CDKs (10); as well as siRNA-mediated inhibition of CDK9, lead to the loss of IL-1β-mediated induction of iNOS in chondrocytes (Figure 1E & F). In addition, it is not documented that other CDKs involved in cell cycle regulation have a pronounced effect on the transcriptional activation of a broad range of PRG within the 5-hour time frame used in this study. Therefore, our results provide strong evidence that only CDK9 is responsible for the activation of PRG in chondrocytes.

Flavopiridol was originally known for its anti-proliferation properties by suppressing cell-cycle progression in rapidly dividing cells (e.g. cancers) or in cells with short life-span (e.g. neutrophils). Its pharmacological activity is well-documented over the last two decades because of its use in clinical trials as anti-proliferation/cancer agent (reviewed by (28)). Sekine et al have demonstrated that systemic administration of Flavopiridol reduces synovial hyperplasia, but does not induce apoptosis, and result in preventing the development of rheumatoid arthritis in a collagen-induced mouse model (29). However, it is not known whether the anti-arthritic activity

of Flavopiridol is due to the systematic suppression of the leukocyte-mediated immune response to the injected collagen, or the localized suppression of the inflammatory response of chondrocytes in cartilage. Our group has developed a non-invasive knee injury mouse model for post-traumatic OA (PTOA) (30). Preliminary data indicate that systemic administration of Flavopiridol effectively suppresses the production of pro-inflammatory cytokines locally at the injured knee, thus confirming our in vitro finding detailed in this study. Future experiments are needed to determine whether Flavopiridol treatment will prevent or delay the development of PTOA in our mouse model, or in other existing PTOA models (31, 32).

In summary, our data for the first time demonstrate the absolute requirement of CDK9 activity in the activation of PRG in human chondrocytes. In addition, our data strongly indicate that Flavopiridol is an effective agent to prevent the activation of acute inflammatory response and catabolic pathways in cartilage. Our results thus may provide a new strategy to prevent or delay the onset of OA.

Competing interest

The authors declare that they have no competing interest.

Acknowledgements

Figure legends

Figure 1. Characterization of the effects of CDK9 inhibition by Flavopiridol on iNOS induction. (A) Kinetics of IL-1β-induced iNOS expression. Human chondrocytes were treated with 10 ng/ml IL-1β, with and without 300 nM Flavopiridol, for the indicated time. The fold-induction of iNOS mRNA relative to untreated control was determined by quantitative RT-PCR. (B) Time window of administration of Flavopiridol for iNOS suppression. Chondrocytes were treated with IL-1β for a total of 5 hours, with Flavopiridol added at different delayed time points to determine the window of opportunity for effective suppression of iNOS induction. (C) Dose-dependent suppression of iNOS induction by Flavopiridol. Chondrocytes were treated with IL-1β for 5 hours, with co-treatments of Flavopiridol at various concentrations to determine the dose-response for suppressing iNOS induction. (D) Cytotoxicity assays. Chondrocytes seeded in 96-wells at the indicated cell density were treated with 300 nM Flavopiridol for 5 hours, followed by measurement of soluble/total G6PD activity to determine the cytotoxic effects of Flavopiridol. (E) Suppression of iNOS induction by different inhibitors. Chondrocytes were treated with IL-1β for 5 hours in the presence of various small molecule inhibitors at the indicated concentrations. The induction of iNOS mRNA by IL-1β was determined and the maximum iNOS induction by IL-1β in the absence of inhibitor was set to 100%. The selected IC_{50} of various drugs based on their kinase inhibition are: BS-181, 21 nM for CDK7; SNS-032, 60 nM for CDK7 (used in this experiment) and 4 nM for CDK9; Flavopiridol, 30 nM for CDK9. JQ-1 is not a kinase inhibitor but prevents CDK9 recruitment to PRG promoters through suppressing the binding of Brd4 to acetylated histones at an IC_{50} of 300 nM. (F) siRNA-mediated depletion of CDK9 impairs iNOS, and catabolic gene induction. Chondrocytes were transduced

with lentiviral particles harboring siRNA against CDK9, or GFP as control. After 5 days, cells were treated with IL-1β for 5 hours and harvested for Western and mRNA analysis. While IL-1β induction of iNOS was not significantly different between the control (*) and GFP siRNA (**) groups, iNOS induction was markedly suppressed by CDK9 knockdown. The IL-1β-induced mRNA expression of MMP1, 3, 9, 13 and ADAMTS4 in cells with GFP siRNA was similar to that of the control (not shown), but their induction were reduced by CDK9 siRNA. For all the above experiments, each data point was the mean +/- standard deviation from three different donors. (*, ** indicates p<0.05)

Figure 2. The CDK9 inhibitor Flavopiridol is effective against different inflammatory stimuli. (A) Activation of inflammatory genes by diverse signals. Multiple pro-inflammatory stimuli, such as IL-1β, LPS, and TNFα activate their respective cell surface receptors. These signals are then transmitted through different intracellular mediators/pathways, which ultimately converge on CDK9-dependent transcription of inflammatory genes. Brd4 functions to recruit CDK9 to activated promoters. (B) Flavopiridol is effective against multiple inflammatory stimuli. Human chondrocytes (n=3 different donors) in monolayer culture were treated with different inflammatory stimuli (10ng/ml of either IL-1β, LPS, or TNFα) with or without 300 nM Flavopiridol for 5 hours. iNOS mRNA was quantified by real-time PCR as a measure of inflammatory response. The induction of iNOS by each stimulus alone was arbitrarily set to 100% (first bar) and compared to the respective value obtained in sample co-treated with each inflammatory stimulus and Flavopiridol. Results were the mean +/- standard deviation from three different donors (*p<0.05).

Figure 3. Flavopiridol effectively suppresses the induction of a broad range of inflammatory mediators. Primary human chondrocytes (n=3 different donors) in monolayer culture were treated with 10 ng/ml IL-1β with or without 300 nM Flavopiridol for 5 hours. Gene expression was analyzed using real-time PCR Array for NFκB targets (Qiagen) and shown here as heat map (Green=minimum expression, Red=maximum expression). Of the 84 NFκB target genes tested, 67 were induced greater than 1.5-fold by IL-1β (compare lanes 1 & 2). Flavopiridol almost completely abolishes the effects of IL-1β in 59 of these 67 genes (lane 3). Importantly, housekeeping genes and non-inducible genes are unaffected by either IL-1β or Flavopiridol.

Figure 4. CDK9 inhibition prevents induction of MMP and ADAMTS expression by various inflammatory stimuli. (A-C) Primary chondrocytes (n=3 different donors) were treated with either 10 ng/ml of IL-1β, LPS, or TNFα, with or without 300 nM Flavopiridol for 5 hours, and the relative mRNA expression of the cartilage degrading enzymes MMP-1,-3,-9,-13, and ADAMTS4 and ADAMTS5 was determined by real-time PCR. (D) Flavopiridol suppresses MMP13 protein expression. Human chondrocytes (n=3 different donors) grown in 6-well plates were treated with 10 ng/ml IL-1β, with or without 300 nM Flavopiridol for 2 days. Cell-associated active MMP13 (~48kD) was detected by Western blot. (E) Flavopiridol does not affect basal expression of anabolic genes. Chondrocytes were treated with IL-1β and/or Flavopiridol for 5 hours and the mRNA expression of the cartilage matrix genes aggrecan, COMP, and Col2a were determined by RT-PCR. For all the above experiments, each data point was the mean +/- standard deviation from three different donors (*p<0.05).

Figure 5. CDK9 inhibition protects cartilage from the catabolic effects of IL-1ß. (A) GAG breakdown in cartilage explants. Human arthritic cartilage explants (3mm cubes) were treated with 1 ng/ml IL-1ß and the indicated concentrations of Flavopiridol for 6 days (media change at day 3). GAG released into the medium was measured by DMMB assays and normalized to the wet weight of the explants. Treatment with IL-1β alone caused cartilage degradation as indicated by increased GAG release. In the presence of 300nM Flavopiridol, GAG release returned to baseline. (B) Col2a degradation in cartilage explants. Human cartilage explants (n=5 donors) were treated with 1 ng/ml IL-1ß and the indicated concentrations of Flavopiridol for 6 days (media change at day 3). Cleaved Col2a peptides released into the medium was measured by C2C ELSIA and normalized to the wet weight of the explants as described in the Methods. Treatment with IL-1β alone caused cartilage degradation as indicated by increased Col2a peptides. In the presence of Flavopiridol, Col2a peptides release returned to baseline. For all the above experiments, each data point was the mean +/- standard deviation from five different donors. (*$p < 0.05$). (C) Long-term Flavopiridol treatment does not reduce chondrocyte viability. Bovine cartilage explants (6 mm full thickness disk) (n=3 different donors) were treated with 300 nM Flavopiridol for 6 days. The explants were sliced in half and stained with LIVE/DEAD stain as described in the Methods. The numbers of live and dead cells in three random fields were counted and the percentages of live cells were calculated.

References

1.   **Lotz, M. K., and V. B. Kraus.** 2007. New developments in osteoarthritis. Posttraumatic osteoarthritis: pathogenesis and pharmacological treatment options. Arthritis Res Ther **12:**211.

2.   **Goldring, M. B., M. Otero, K. Tsuchimochi, K. Ijiri, and Y. Li.** 2008. Defining the roles of inflammatory and anabolic cytokines in cartilage metabolism. Ann Rheum Dis **67 Suppl 3:**iii75-82.

3.   **Hargreaves, D. C., T. Horng, and R. Medzhitov.** 2009. Control of inducible gene expression by signal-dependent transcriptional elongation. Cell **138:**129-145.

4.   **Zippo, A., R. Serafini, M. Rocchigiani, S. Pennacchini, A. Krepelova, and S. Oliviero.** 2009. Histone crosstalk between H3S10ph and H4K16ac generates a histone code that mediates transcription elongation. Cell **138:**1122-1136.

5.   **Zhou, Q., and J. H. Yik.** 2006. The Yin and Yang of P-TEFb regulation: implications for human immunodeficiency virus gene expression and global control of cell growth and differentiation. Microbiol Mol Biol Rev **70:**646-659.

6.   **Krystof, V., S. Baumli, and R. Furst.** 2012. Perspective of cyclin-dependent kinase 9 (CDK9) as a drug target. Current pharmaceutical design **18:**2883-2890.

7.   **Li, H., D. R. Haudenschild, K. L. Posey, J. T. Hecht, P. E. Di Cesare, and J. H. Yik.** 2011. Comparative analysis with collagen type II distinguishes cartilage oligomeric matrix protein as a primary TGFbeta-responsive gene. Osteoarthritis Cartilage **19:**1246-1253.

8.   **Filippakopoulos, P., J. Qi, S. Picaud, Y. Shen, W. B. Smith, O. Fedorov, et al.** 2010. Selective inhibition of BET bromodomains. Nature **468:**1067-1073.

9.   **Dull, T., R. Zufferey, M. Kelly, R. J. Mandel, M. Nguyen, D. Trono, et al.** 1998. A third-generation lentivirus vector with a conditional packaging system. Journal of virology **72:**8463-8471.

10.   **Yang, Z., J. H. Yik, R. Chen, N. He, M. K. Jang, K. Ozato, et al.** 2005. Recruitment of P-TEFb for stimulation of transcriptional elongation by the bromodomain protein Brd4. Molecular cell **19:**535-545.

11.   **Farndale, R. W., D. J. Buttle, and A. J. Barrett.** 1986. Improved quantitation and discrimination of sulphated glycosaminoglycans by use of dimethylmethylene blue. Biochim Biophys Acta **883:**173-177.

12.   **Poole, A. R., M. Ionescu, M. A. Fitzcharles, and R. C. Billinghurst.** 2004. The assessment of cartilage degradation in vivo: development of an immunoassay for the measurement in body fluids of type II collagen cleaved by collagenases. J Immunol Methods **294:**145-153.

13.   **Fornier, M. N., D. Rathkopf, M. Shah, S. Patil, E. O'Reilly, A. N. Tse, et al.** 2007. Phase I dose-finding study of weekly docetaxel followed by flavopiridol for patients with advanced solid tumors. Clinical cancer research : an official journal of the American Association for Cancer Research **13:**5841-5846.

14.   **Maier, R., G. Bilbe, J. Rediske, and M. Lotz.** 1994. Inducible nitric oxide synthase from human articular chondrocytes: cDNA cloning and analysis of mRNA expression. Biochim Biophys Acta **1208:**145-150.

15.   **Ali, S., D. A. Heathcote, S. H. Kroll, A. S. Jogalekar, B. Scheiper, H. Patel, et al.** 2009. The development of a selective cyclin-dependent kinase inhibitor that shows antitumor activity. Cancer research **69:**6208-6215.

16. **Heath, E. I., K. Bible, R. E. Martell, D. C. Adelman, and P. M. Lorusso.** 2008. A phase 1 study of SNS-032 (formerly BMS-387032), a potent inhibitor of cyclin-dependent kinases 2, 7 and 9 administered as a single oral dose and weekly infusion in patients with metastatic refractory solid tumors. Investigational new drugs **26:**59-65.

17. **Kobayashi, M., G. R. Squires, A. Mousa, M. Tanzer, D. J. Zukor, J. Antoniou, et al.** 2005. Role of interleukin-1 and tumor necrosis factor alpha in matrix degradation of human osteoarthritic cartilage. Arthritis Rheum **52:**128-135.

18. **Wang, M., E. R. Sampson, H. Jin, J. Li, Q. H. Ke, H. J. Im, et al.** 2013. MMP13 is a critical target gene during the progression of osteoarthritis. Arthritis Res Ther **15:**R5.

19. **Fiocco, U., P. Sfriso, F. Oliviero, P. Roux-Lombard, E. Scagliori, L. Cozzi, et al.** 2010. Synovial effusion and synovial fluid biomarkers in psoriatic arthritis to assess intraarticular tumor necrosis factor-alpha blockade in the knee joint. Arthritis Res Ther **12:**R148.

20. **McNiff, P. A., C. Stewart, J. Sullivan, H. J. Showell, and C. A. Gabel.** 1995. Synovial fluid from rheumatoid arthritis patients contains sufficient levels of IL-1 beta and IL-6 to promote production of serum amyloid A by Hep3B cells. Cytokine **7:**209-219.

21. **Deirmengian, C., N. Hallab, A. Tarabishy, C. Della Valle, J. J. Jacobs, J. Lonner, et al.** 2010. Synovial fluid biomarkers for periprosthetic infection. Clinical orthopaedics and related research **468:**2017-2023.

22. **Hollander, A. P., I. Pidoux, A. Reiner, C. Rorabeck, R. Bourne, and A. R. Poole.** 1995. Damage to type II collagen in aging and osteoarthritis starts at the articular surface, originates around chondrocytes, and extends into the cartilage with progressive degeneration. J Clin Invest **96:**2859-2869.

23.	**Attur, M., J. S. Millman, M. N. Dave, H. E. Al-Mussawir, J. Patel, G. Palmer, et al.** 2011. Glatiramer acetate (GA), the immunomodulatory drug, inhibits inflammatory mediators and collagen degradation in osteoarthritis (OA) cartilage. Osteoarthritis Cartilage **19:**1158-1164.

24.	**Attur, M. G., M. Dave, C. Cipolletta, P. Kang, M. B. Goldring, I. R. Patel, et al.** 2000. Reversal of autocrine and paracrine effects of interleukin 1 (IL-1) in human arthritis by type II IL-1 decoy receptor. Potential for pharmacological intervention. J Biol Chem **275:**40307-40315.

25.	**Ni, W., J. Ji, Z. Dai, A. Papp, A. J. Johnson, S. Ahn, et al.** 2010. Flavopiridol pharmacogenetics: clinical and functional evidence for the role of SLCO1B1/OATP1B1 in flavopiridol disposition. PLoS One **5:**e13792.

26.	**Wang, K., P. Hampson, J. Hazeldine, V. Krystof, M. Strnad, P. Pechan, et al.** 2012. Cyclin-dependent kinase 9 activity regulates neutrophil spontaneous apoptosis. PLoS One **7:**e30128.

27.	**Schmerwitz, U. K., G. Sass, A. G. Khandoga, J. Joore, B. A. Mayer, N. Berberich, et al.** 2011. Flavopiridol protects against inflammation by attenuating leukocyte-endothelial interaction via inhibition of cyclin-dependent kinase 9. Arteriosclerosis, thrombosis, and vascular biology **31:**280-288.

28.	**Wang, L. M., and D. M. Ren.** 2010. Flavopiridol, the first cyclin-dependent kinase inhibitor: recent advances in combination chemotherapy. Mini Rev Med Chem **10:**1058-1070.

29.	**Sekine, C., T. Sugihara, S. Miyake, H. Hirai, M. Yoshida, N. Miyasaka, et al.** 2008. Successful treatment of animal models of rheumatoid arthritis with small-molecule cyclin-dependent kinase inhibitors. J Immunol **180:**1954-1961.

30.   **Christiansen, B. A., M. J. Anderson, C. A. Lee, J. C. Williams, J. H. Yik, and D. R. Haudenschild.** 2012. Musculoskeletal changes following non-invasive knee injury using a novel mouse model of post-traumatic osteoarthritis. Osteoarthritis Cartilage **20:**773-782.

31.   **Glasson, S. S., T. J. Blanchet, and E. A. Morris.** 2007. The surgical destabilization of the medial meniscus (DMM) model of osteoarthritis in the 129/SvEv mouse. Osteoarthritis Cartilage **15:**1061-1069.

32.   **Furman, B. D., J. Strand, W. C. Hembree, B. D. Ward, F. Guilak, and S. A. Olson.** 2007. Joint degeneration following closed intraarticular fracture in the mouse knee: a model of posttraumatic arthritis. Journal of orthopaedic research : official publication of the Orthopaedic Research Society **25:**578-592.
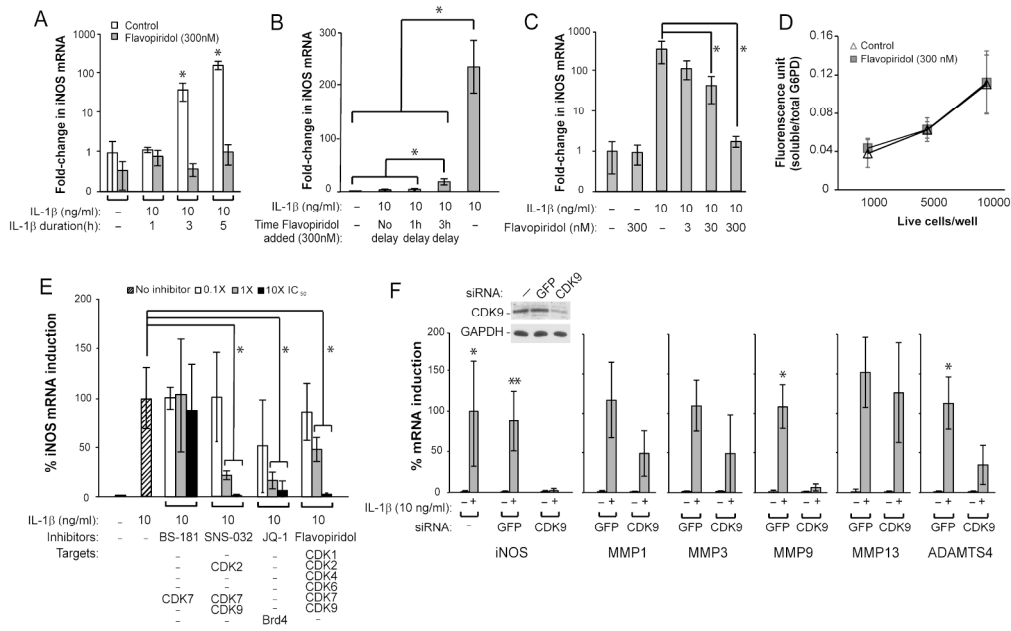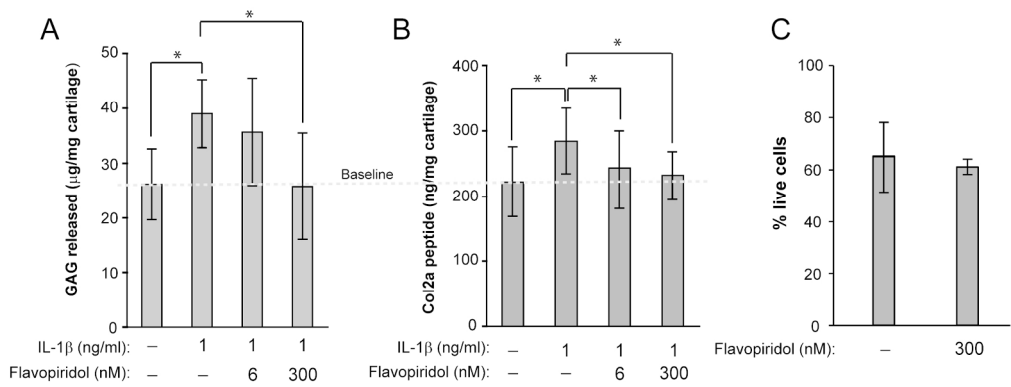
205x128mm (300 x 300 DPI)
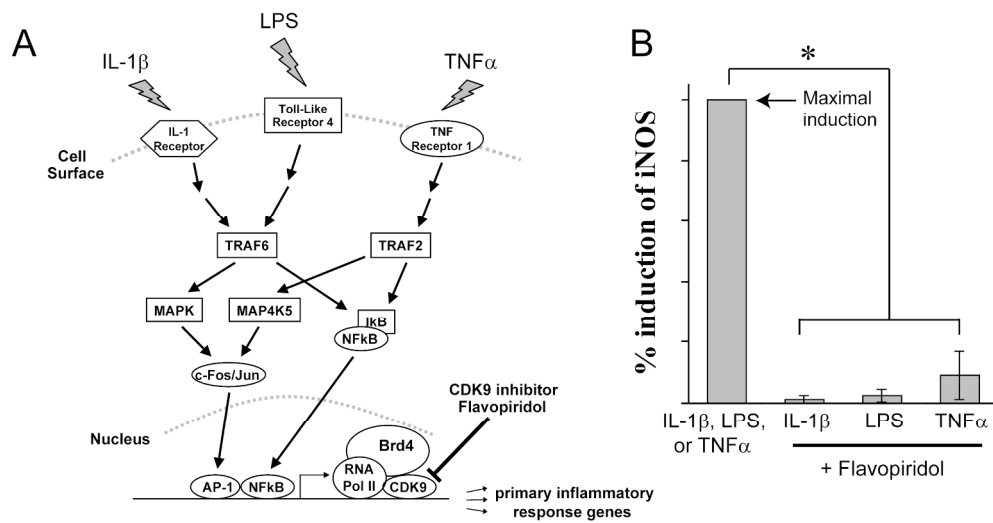
203x104mm (300 x 300 DPI)
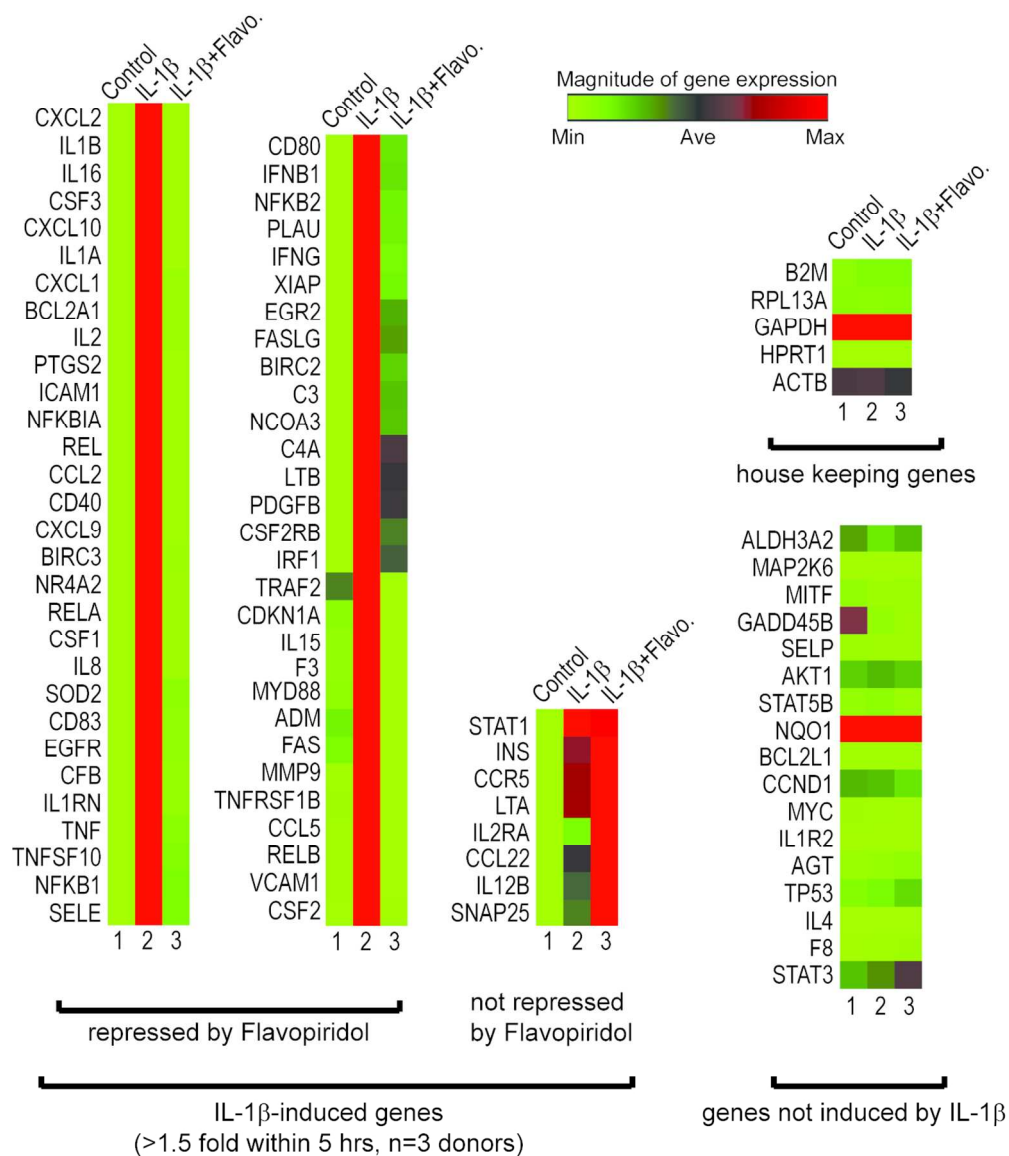
117x135mm (300 x 300 DPI)
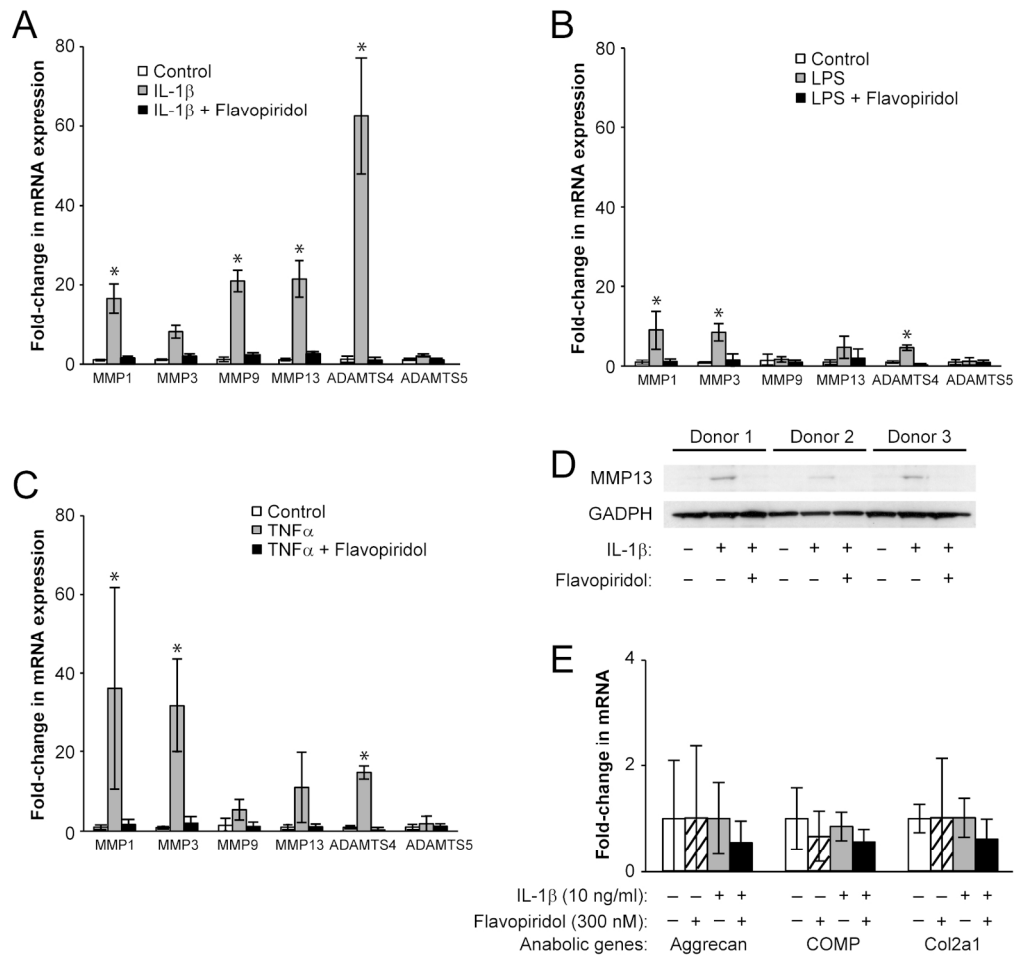
150x142mm (300 x 300 DPI)

A

B

C

179x67mm (300 x 300 DPI)

CDK9 Inhibition Attenuates Acute Inflammatory Response, Reduces Bone Loss in a Post-Traumatic Osteoarthritis Mouse Model

Hu, Z; Yik, JHN; Fong, JY; Michelier, P; Shidara, K; Liu, N; Huang, B; Cissell, D; Christiansen, BA; and Haudenschild, DR

Department of Orthopaedic Surgery, Lawrence J. Ellison Musculoskeletal Research Center, Sacramento CA 95817

UC DAVIS
UNIVERSITY OF CALIFORNIA

Objective

Although joint injuries often lead to post-traumatic osteoarthritis (PTOA), few studies have focused on the immediate effects of an acute injury response on the progression and development of PTOA. Acute injury responses are characterized by the transcriptional activation of primary inflammatory genes such as IL-1β, IL-6, and TNFα, and other inflammatory mediators. These events lead to increased production of matrix degrading enzymes that contribute to the catabolic destruction of cartilage and subchondral bone. We **hypothesize** that excessive inflammatory response to joint injuries is a major contributor to the observed cartilage and bone loss preceding the onset of PTOA. Despite being triggered by various inflammatory stimuli, diverse signaling pathways converge onto a single mechanism that activates the transcription of primary inflammatory response genes. **This rate-limiting step of inflammatory gene activation is controlled by the transcription factor cyclin-dependent kinase 9 (CDK9).** CDK9 functions to phosphorylate RNA Polymerase II to overcome its promoter proximal pausing and to stimulate transcriptional elongation of mRNAs. Thus, CDK9 is an attractive and novel target for anti-inflammatory therapy, and we showed that CDK9 inhibition protects cartilage from catabolic cytokines in vitro[1]. Here we investigated the effects of CDK9 inhibition, by the pharmacological small molecule inhibitor Flavopiridol, on:
1) suppressing the acute injury response, and 2) the subsequent cartilage/bone loss in an in vitro cartilage explant injury model, and in a non-invasive PTOA mouse model.

Methods

Cartilage explant injury: Cartilage explants were harvested by 6mm biopsy punches from bovine stifled joints obtained from a local slaughter house. The explants were trimmed to a height of 3mm and cultured in DMEM+10% FBS for 24 hrs. The explants were then subjected to a single load of compression with 30% strain, and then placed into culturing media with or without 300 nM Flavopiridol (Santa Cruz Biotech). The expression of inflammatory and catabolic/anabolic genes was determined by qPCR described below.

Mechanical properties: After 4 weeks of culture, mechanical properties were measured in a sample of the cartilage (2mm height by 3mm diameter). A Bose Enduratec instrument was used to apply 10% and 20% compressive strain and custom MatLab software to estimate the instantaneous and relaxation moduli.

PTOA mouse model: The right knees of skeletally matured C57BL6 mice were injured with a single mechanical compression as described (2), with the contralateral knees as uninjured control. These knee injuries consistently lead to a rapid bone loss at 1 week and apparent PTOA at 8 weeks. Half of these mice received intra-peritoneal injections of Flavopiridol at a dosage of 7.5mg/kg at 0- and 4-hours post-injury, and the other half received placebo injections. The knee joints and capsules were harvested and dissected at various time points (n=6/time point) and processed for gene expression, histology (H&E staining), and microCT analysis for femoral epiphysis bone volume. All animal procedures were performed according to an IACUC approved protocol.

qPCR: Total RNA from cartilage explants or dissected mouse knees were isolated by the miRNeasy Kit (Qiagen) and reverse transcribed by the QuantiTect Reverse Transcription Kit (Qiagen). Expression of pro-inflammatory cytokines, catabolic and anabolic genes were determined by qPCR in a 7900HT PCR system with gene-specific probes (ABI) and normalized to 18s rRNA.

In vivo Functional Imaging of MMP activity: MMP activities at the knee joints were determined by in vivo fluorescence imaging at 1-hour to 7-days post injury. MMP-Sense 680 probe was systemically administered, the animals were imaged in an IVIS imaging system under isoflurane anesthesia while held in place by a custum built adaptor. For each mouse, fluorescence (MMP activity) was expressed as a ratio of the injured to uninjured knee.

Statistical analysis: One-way ANOVA with Tukey's correction for multiple comparisons was used to determine significance.
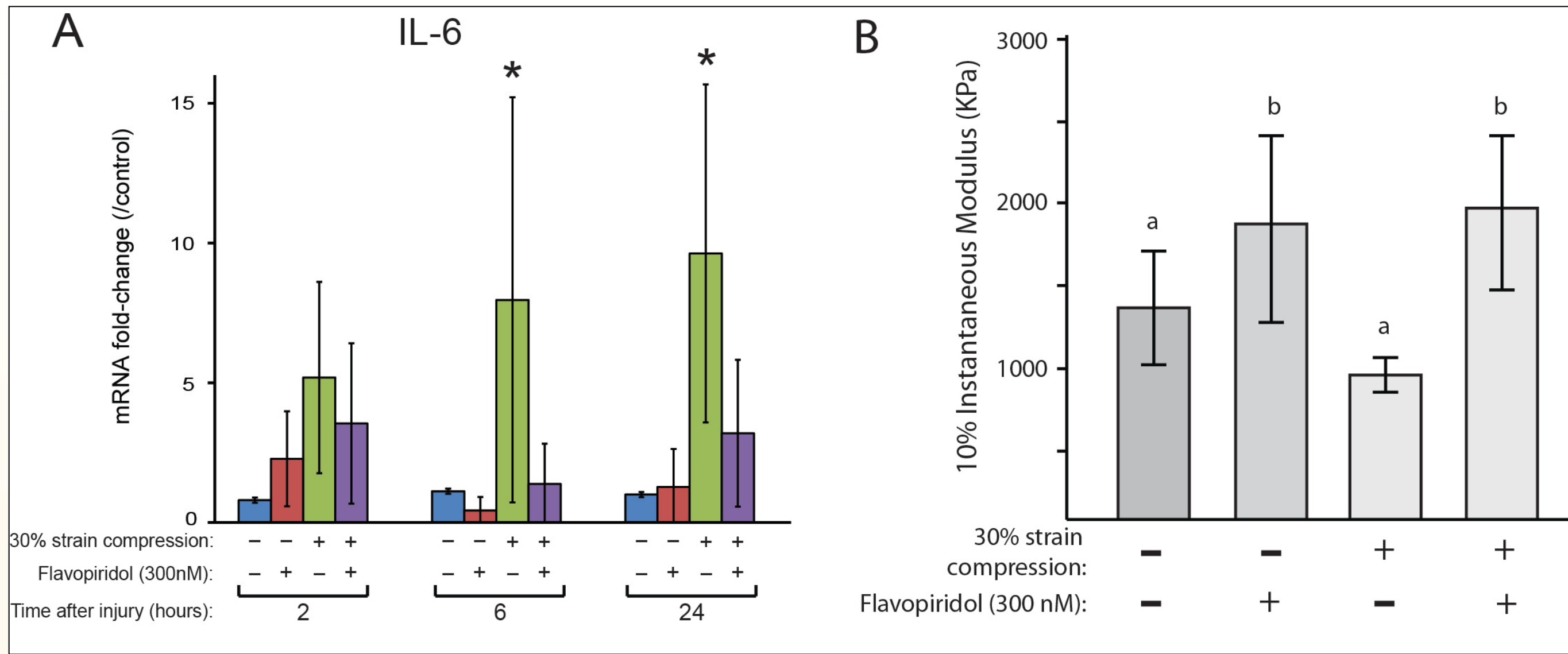
Results

Fig. 1. Mechanically injured cartilage explants express pro-inflammatory cytokines.
A) **CDK9 inhibition suppressed IL-6 induction.** Bovine cartilage explants were compressed by a single load of 30% strain rate and analyzed for the mRNA expression of the injury marker IL-6. The results showed that IL-6 expression was markedly increased at 6 and 24 hours post-injury, but the increase was suppressed by Flavopiridol (P<0.05). Importantly, Flavopiridol did not affect anabolic genes expression nor chondrocyte viabilities (not shown).
B) **CDK9 inhibition preserved cartilage mechanical properties.** The mechanical properties of the explants were determined 4 weeks post-injury. The results showed that injury caused a reduction in the instantaneous modulus but the effects were reversed by Flavopiridol.
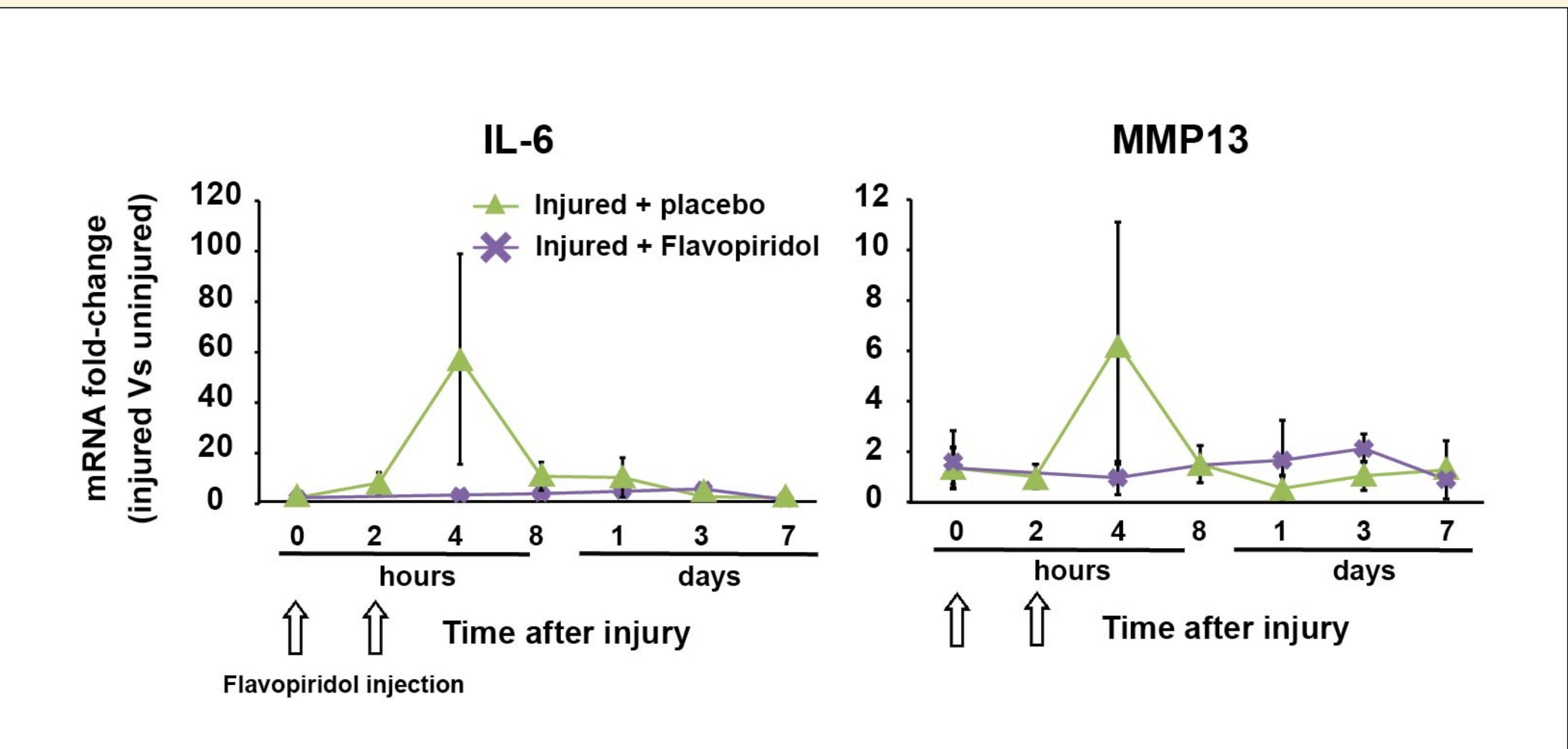

Fig. 2. In vivo CDK9 inhibition suppresses pro-inflammatory cytokine and catabolic gene mRNA induction after traumatic knee injury. In the PTOA mouse model, the expression of IL-6 and MMP13 mRNA increased rapidly 2 hrs after knee injury and peaked at 4 hrs, then returned gradually to baseline after 3-7 days. However, their induction was greatly reduced by Flavopiridol (*P<0.05). Similar results were seen in other catabolic genes such as IL-1β and ADAMTS4 (not shown). In contrast, at these time points the expression of anabolic genes Col2a1 and aggrecan were not affected by knee injury or Flavopiridol.
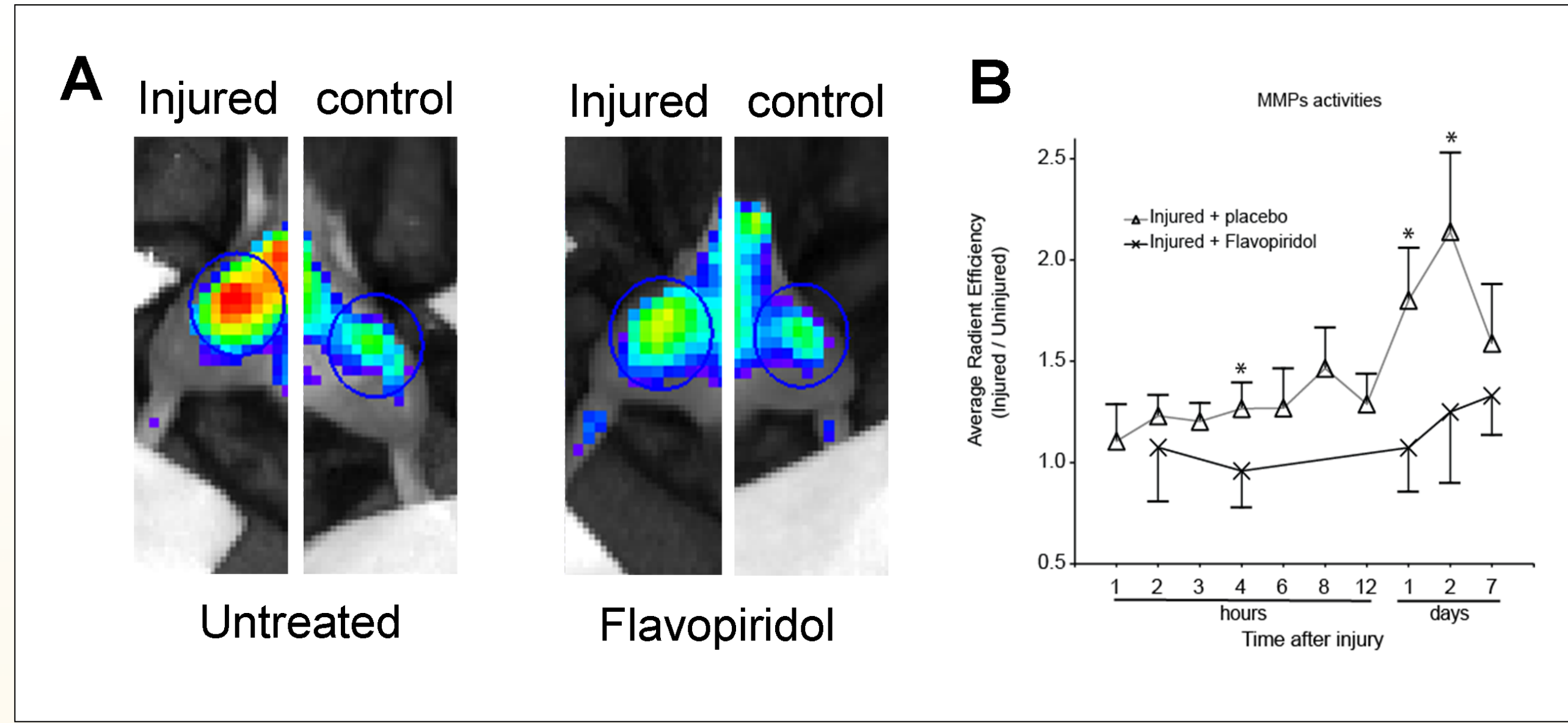

Fig 3. **Functional imaging of MMP activity in vivo.** C57BL/6 mice (n=8/time point) were pre-injected with the MMP-Sense 680 substrates (Perkin-Elmer) 24-hr prior. Their right knees were then injured, with the left knees as uninjured control. The mice were then immediately injected with 7.5 mg/Kg Flavopiridol or vehicle. At the indicated times while under anesthesia, MMP activities at the mouse knees were determined by in vivo fluorescence IVIS imaging system. **(A)** Representative fluorescence images of injured and uninjured knees. **(B)** For each mouse, fluorescence (MMP activity) was expressed as a ratio of the injured to uninjured knee.
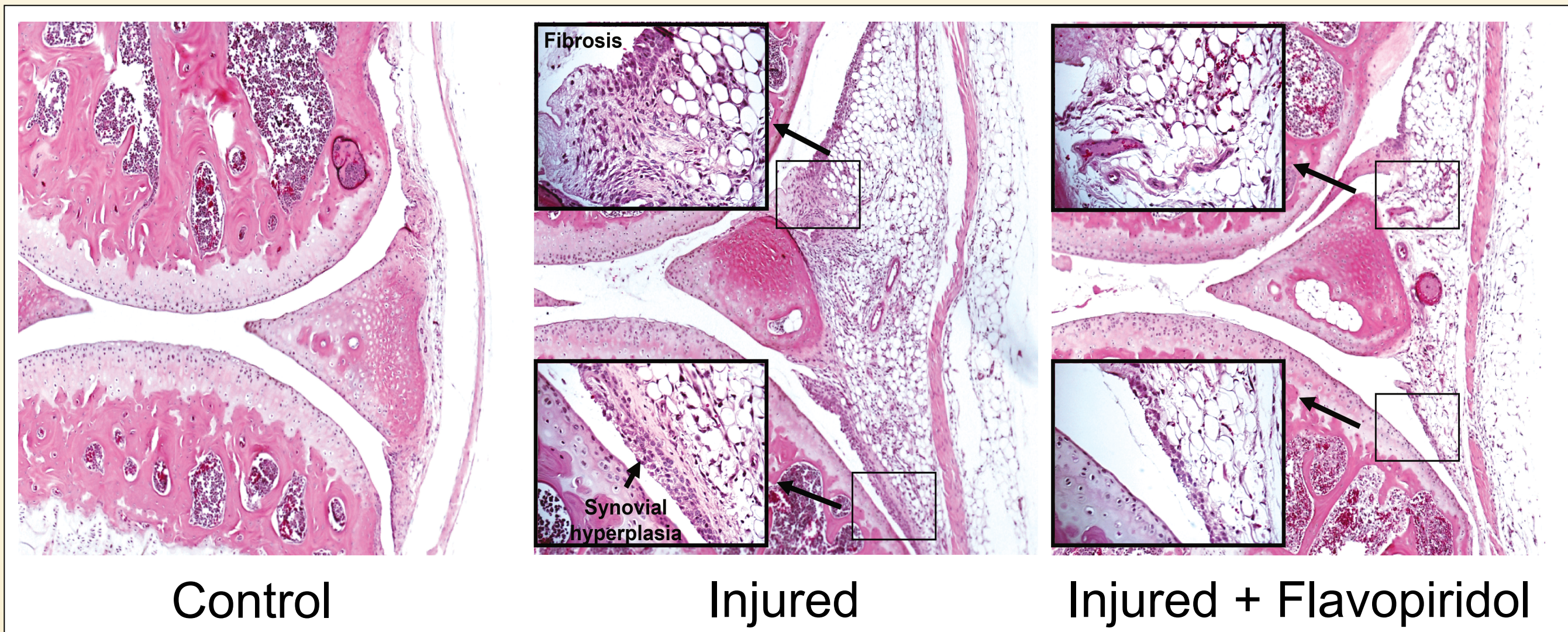

Fig. 4. Cdk9 inhibition reduced inflammation at the injured joints. Histological analysis of knees 3-days post-injury showed heavy signs of inflammation, fibrosis, synovial hyperplasia, pennas formation, and leukocyte infiltration. However, these clinical presentations were reduced by Flavopiridol treatment.
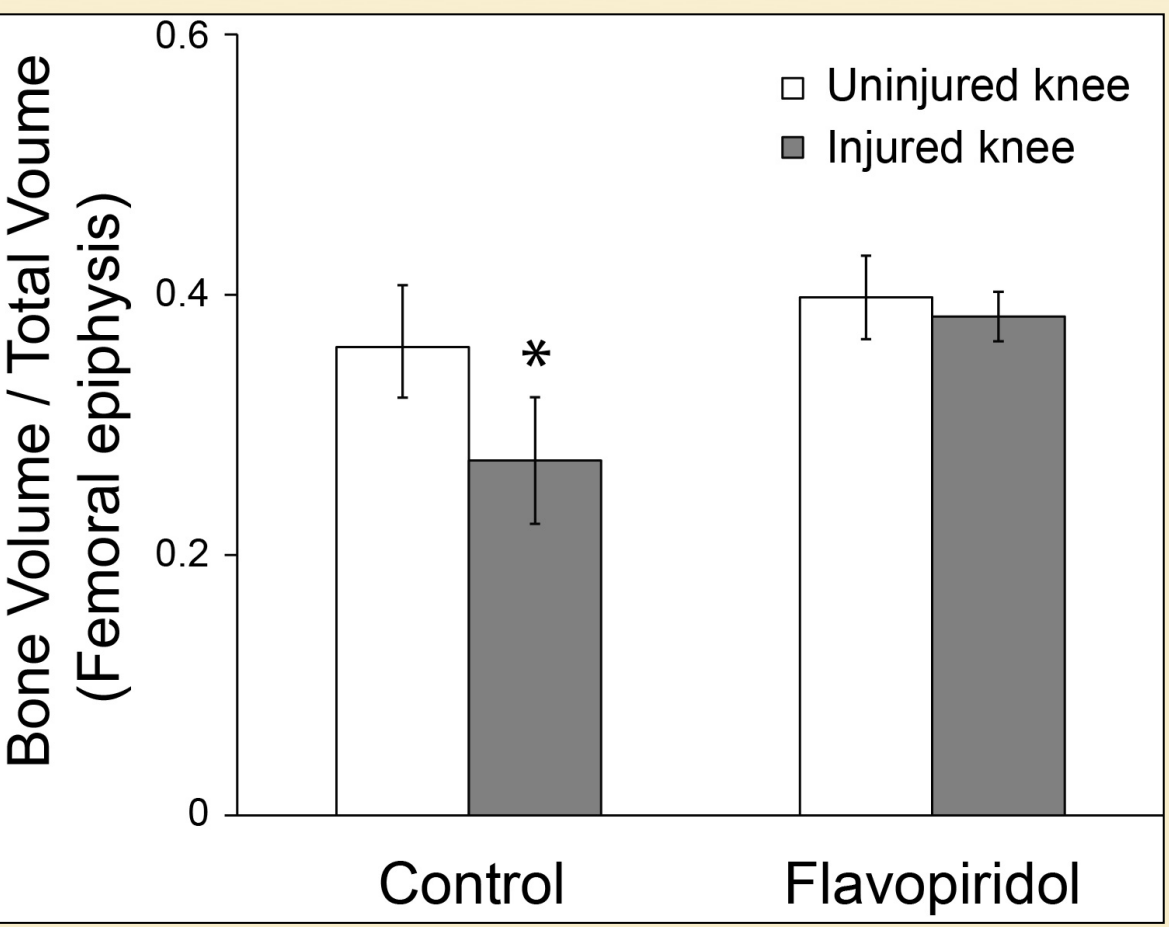

Fig. 5. CDK9 inhibition prevents bone loss after joint injury. The femoral epiphysis bone volumes were determined by μCT. Injury caused a significant bone loss in 3 days but this was prevented by Flavopiridol treatment.

Discussion

The acute inflammatory reaction to joint injury is largely dependent on CDK9 kinase activity. Inhibition of CDK9 activity after injury will:
- Reduce pro-inflammatory gene expression in explants and in-vivo
- Preserve the mechanical integrity of cartilage explants
- Reduce post-injury MMP activity in-vivo
- Reduce inflammation, fibrosis, synovial hyperplasia, and leukocyte infiltration
- Prevent post-traumatic loss of sub-chondral bone

Significance: PTOA is commonly associated with joint injuries in young active patients. Currently there is no clinical treatment available to prevent the development of PTOA. Our studies suggest that CDK9 inhibition shortly after injuries can prevent cartilage and bone loss, and may prevent or delay the onset of PTOA.

References

(1) Yik JHN, Hu Z, Kumari R, Christiansen BA, and Haudenschild DR. *Arthritis Rheumatology* 2014, ePublished

(2) Christiansen BA, Anderson MJ, Lee CA, Williams JC, Yik JNH, and Haudenschild DR. *Osteoarthritis Cartilage* 2012, **20**(7): 733-82.

Early Transient Induction of IL-6 in a Mouse Joint Injury Model

Jasper Yik, Zi' ang Hu, Blaine Christiansen, Dominik Haudenschild

Department of Orthopaedic Surgery, Lawrence J. Ellison Musculoskeletal Research Center, Sacramento CA 95817

UCDAVIS HEALTH SYSTEM

Introduction

Although the etiology of osteoarthritis (OA) is unknown, it is often associated with joint injuries. For example, ~50% of people with knee injuries, such as an anterior cruciate ligament (ACL) tear, develop post traumatic osteoarthritis (PTOA) within 10-20 years. The mechanical damage during joint trauma immediately causes cell death and physical damage to the surrounding tissues. This is followed by an acute cellular response, which occurs within a time-scale of minutes to hours. The acute response phase is characterized by the release of inflammatory mediators from the injured joint tissues, including IL-1, IL-6, TNFa, and iNOS. This causes the transcriptional activation of primary response genes (or inflammatory genes), and leads to increased production of matrix degrading enzymes such as MMPs, collagenases and aggrecanases. The enzymatic degradation of matrix contributes to OA via a cascade of destructive events. We believe that a window for therapeutic intervention exists shortly after injury, during which attenuating the acute cellular response will decrease the production of matrix degrading enzymes and thus decrease the likelihood of developing PTOA.

The acute cellular response within hours of knee injury has not been studied in detail in a mouse model. We have developed a non-invasive knee injury mouse model, in which the ACL is ruptured by a single mechanical compression. These mice consistently develop osteoarthritis in the injured knees within 2-3 months. The non-surgical nature of our model allows us to focus on the acute phase response that initiate the progression of osteoarthritis without the confounding effects of surgery. Using our mouse model, we have examined the short-term temporal expression of pro-inflammatory cytokines and their selected target genes. Our study will characterize the temporal changes in gene expression shortly after knee trauma and identify a window of opportunity for therapeutic intervention.

Methods

Non-invasive knee injury model

Under isoflurane anesthesia, 10-week old C57BL/6 mice were placed into the loading device, and the right leg subjected to a single axial compressive load to -12 N at 1mm/sec. The loading causes anterior subluxation of the tibia relative to the distal femur, demonstrated by the μCT image. Knee injury is evident by the release of compressive force during loading (red line on graph), with continued displacement of the loading actuator (black line). Avulsion fractures of the ACL are typical.

Total RNA was isolated from the injured knee joints shortly after injury, with the contralateral uninjured knee as control. The mRNA expression of pro-inflammatory cytokines and MMP13 was then determined by quantitative PCR and normalized to the 18s rRNA.


Non-Invasive Knee Injury Model

Results
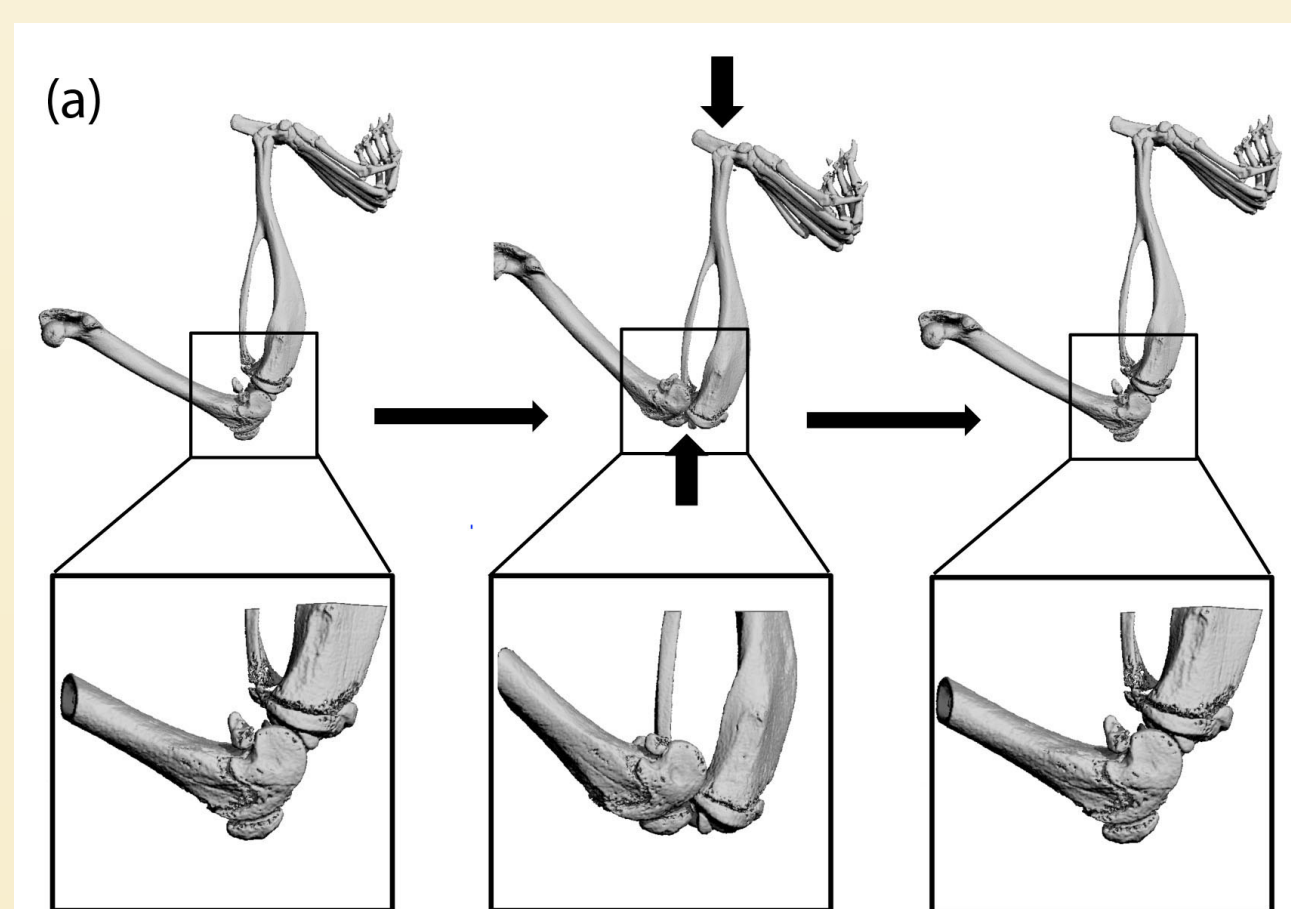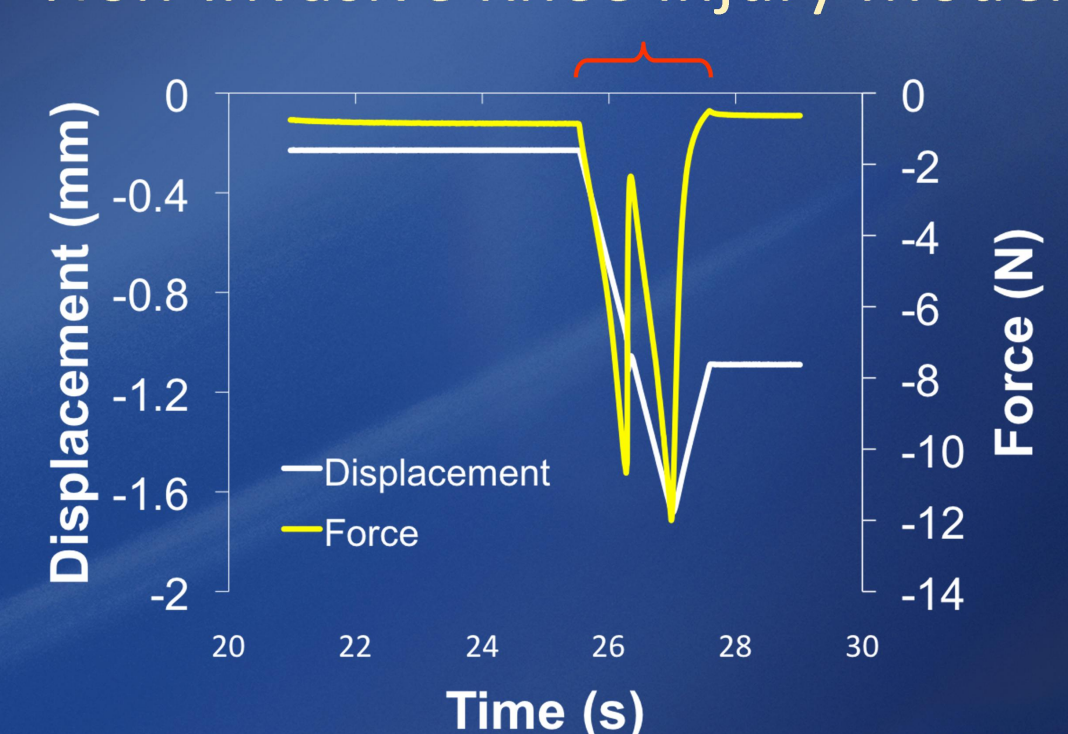
Gene expression analysis of total and partial knee

Two groups of mice were subjected to knee injury. For the first group, tissues were harvested from the entire joint capsule (whole knee), including the synovium, patella, ligaments and tendons, with most of the muscles removed (area within the dotted line). For the second group, only the tissues from the femeral to tibial growth plates were isolated (area within the red line). This partial knee region is composed of mainly articular cartilage and the subchondral bones, as well as the meniscus, ACL, PCL, and lateral ligaments. Total RNA were then isolated by the miRNeasy Kit (Qiagen) and reverse transcribed with First strand cDNA synthesis Kit (Invitrogen). The mRNA levels of the three most characterized pro-inflammatory cytokines, IL-1, IL-6, and TNF, as well as IL-6 receptor, MMP13, were determined by quantitative PCR, with gene-specific probes (ABI). Results were normalized to the 18s rRNA.
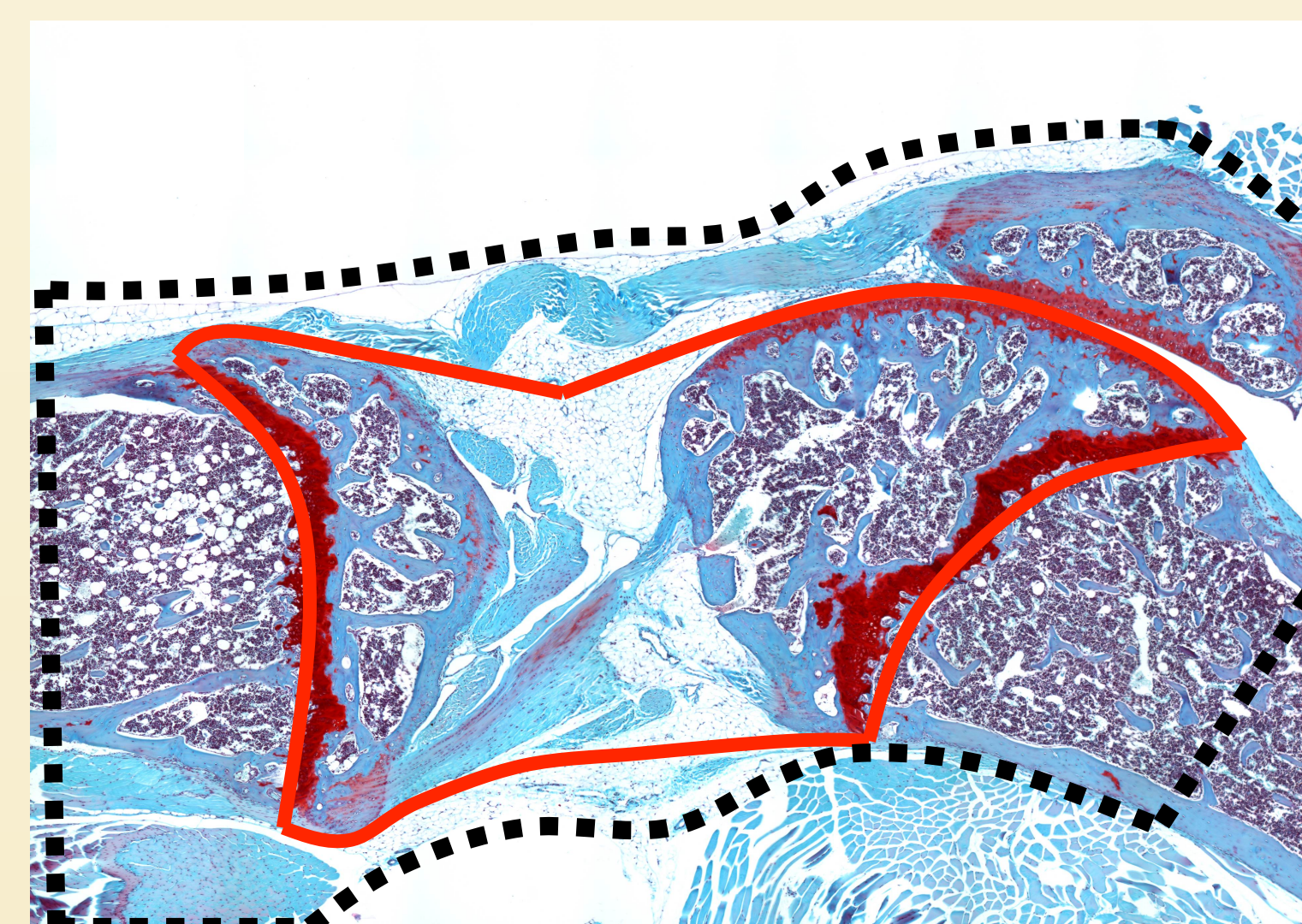

TNF expression does not change significantly after knee injury

Next, we determined the expression of TNF in the injured knee but found that TNF mRNA was not induced within 1-day post-injury (see below), and its level remained the same through a 7-day time course (not shown).
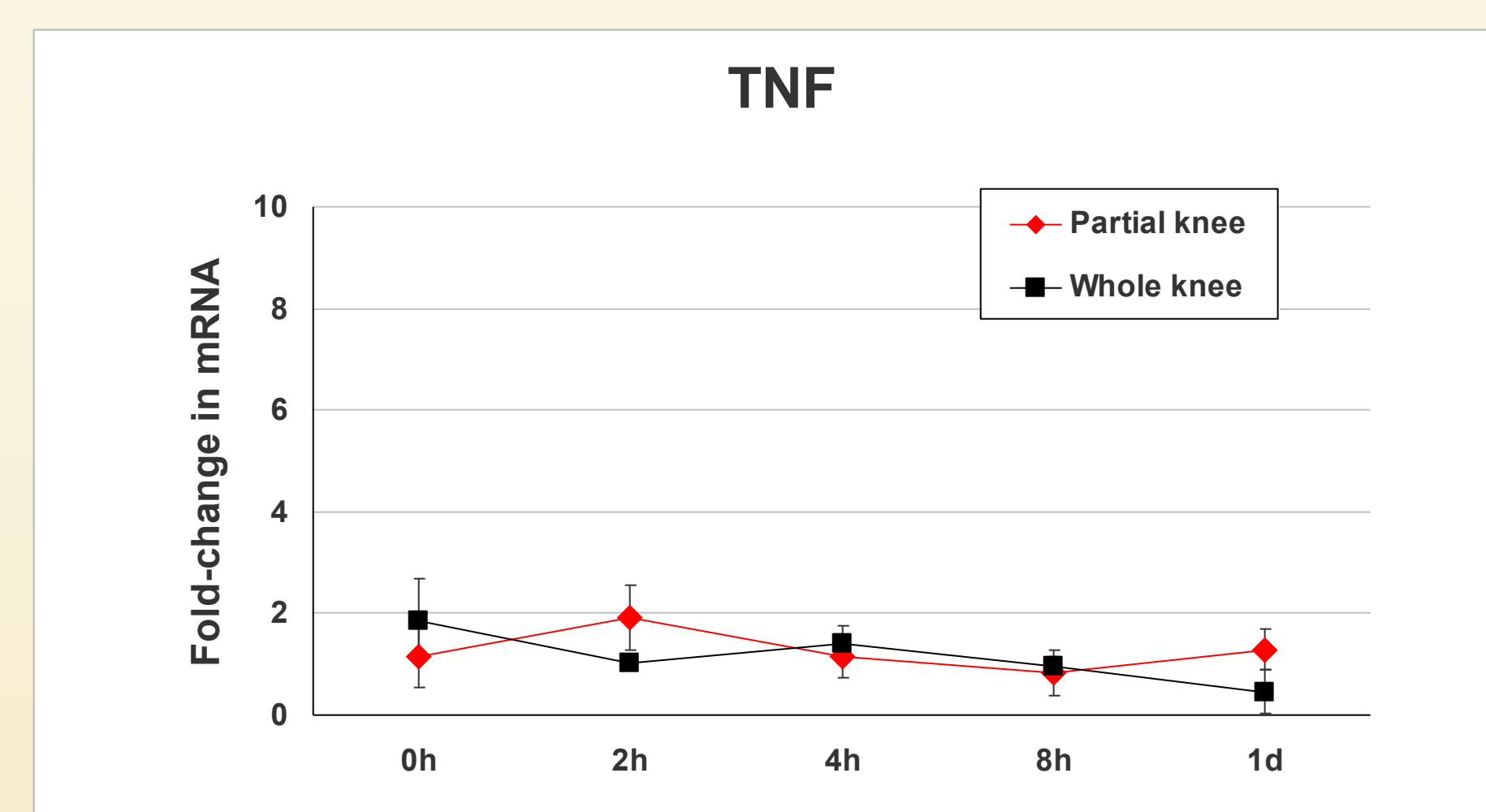

IL-6 mRNA expression is transiently induced at the origin of injury, and subsequently spread to the whole joint

Dramatic elevation (~40-fold) of IL-6 mRNA was first detected and peaked at 2-hour post-injury in the partial knee dissection. In contrast, IL-6 induction was delayed in the whole knee dissection, but the magnitude of peak induction was higher (~80-fold). This results indicated that IL-6 was first induced at the inner knee where the ACL injury occurred (partial knee), and later spread to the outer region of the knee. The expression of IL-6 receptor, however, did not change significantly through out the entire time course.
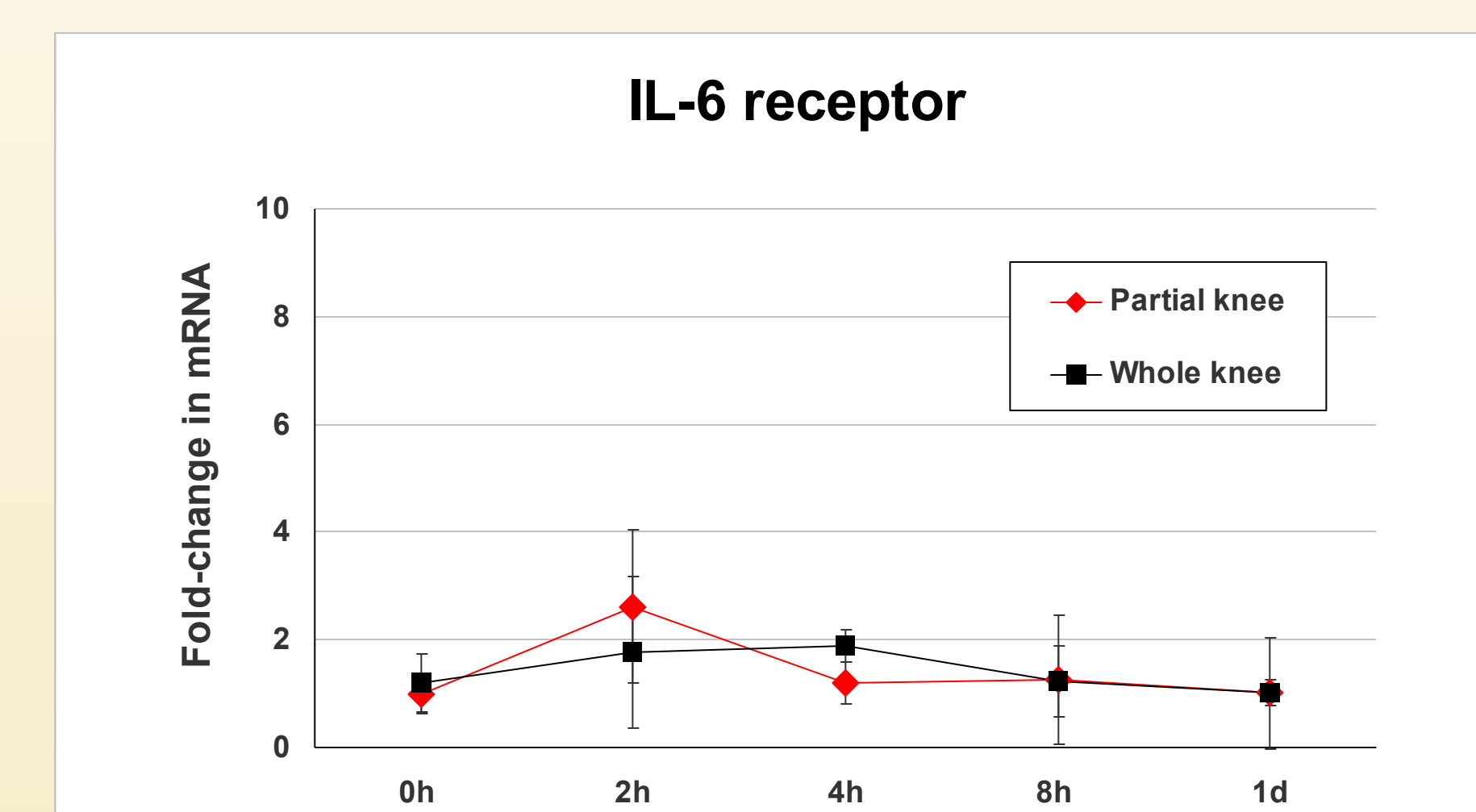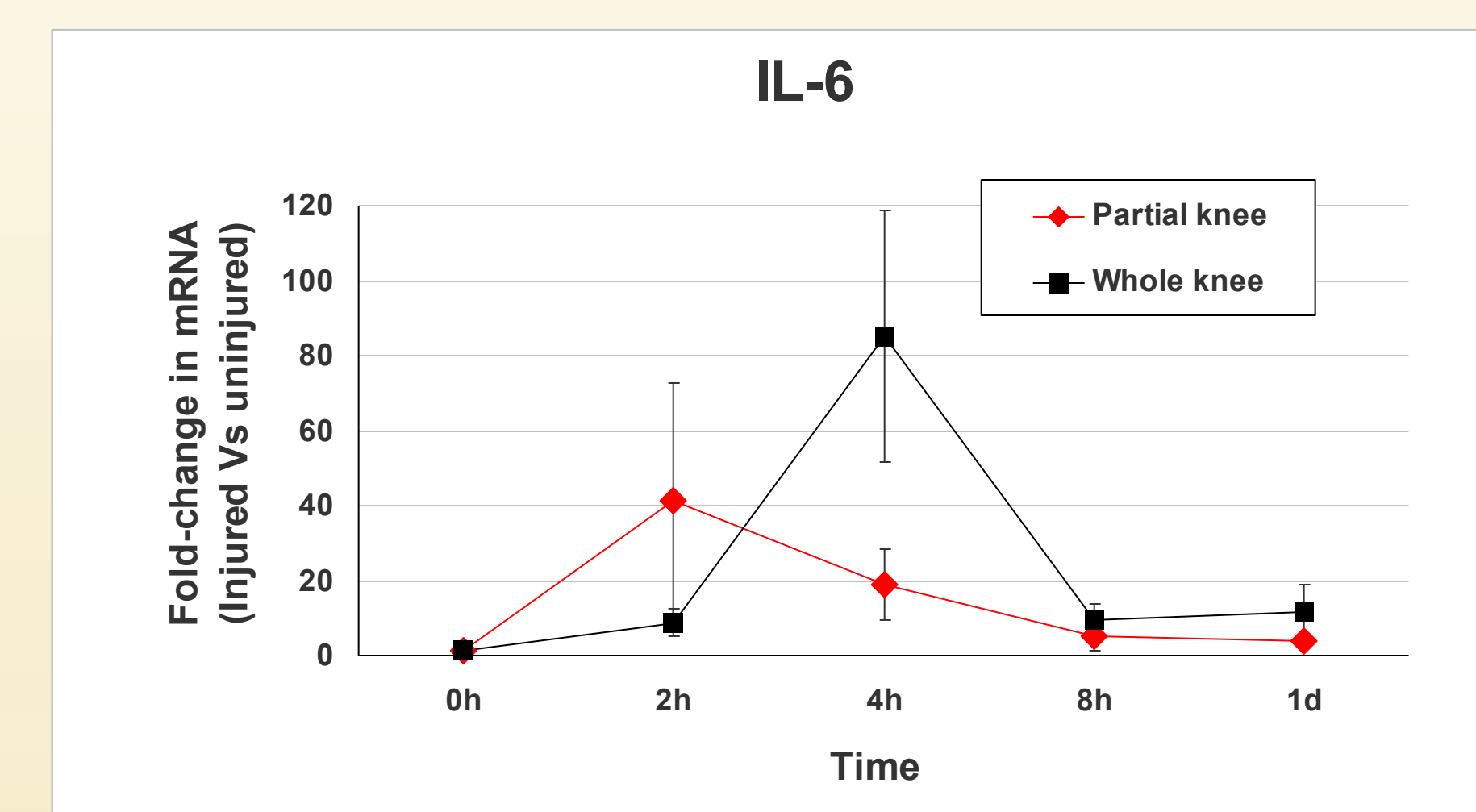

IL-1b mRNA induction is higher in whole knee compared to partial knee

IL-1b mRNA expression was slightly increased in partial knee at 2- and 4-hour post-injury, ~3.4- and 2.3-foldrespectively. In contrast, IL-1b induction was only ~2-fold at 2-hour, but was markedly upregulated by ~17-fold at 4 hour in the whole knee. Coincide with the peaked IL-1b induction in whole knee, its downstream target MMP13 was also increased ~4-fold at 4 hour.
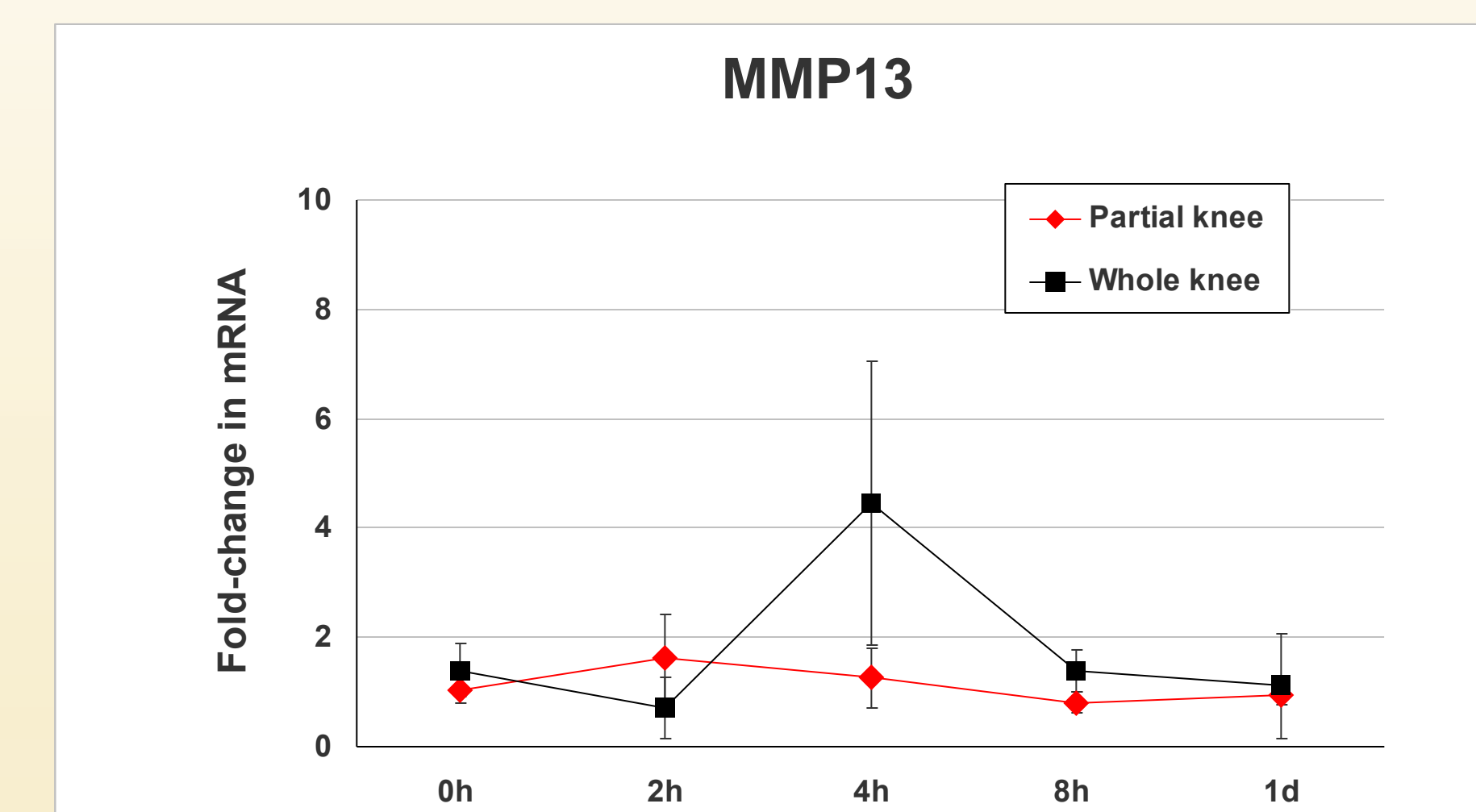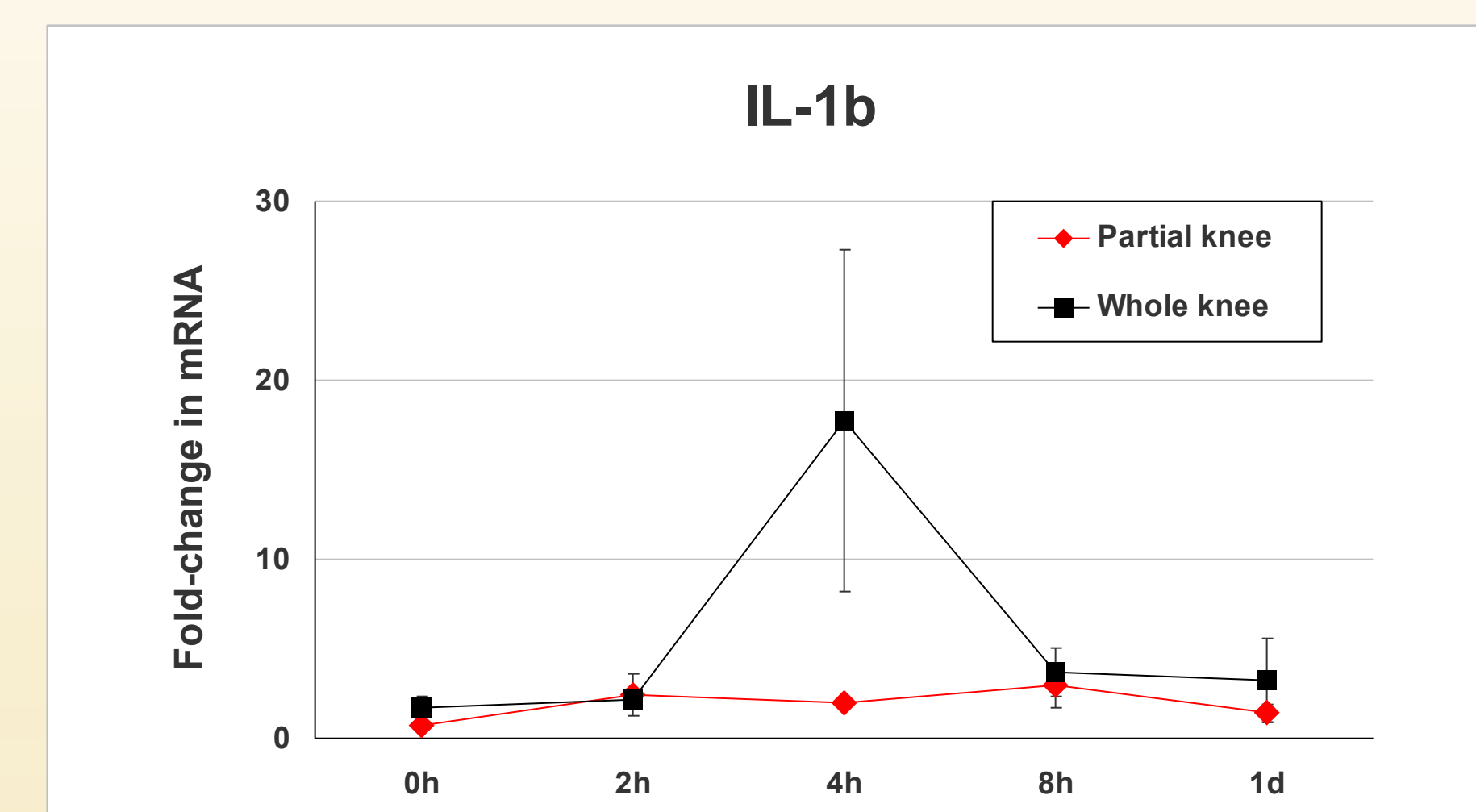
Involvement of IL-6 in cartilage degradation and bone remodeling and its implication in osteoarthritis

Activation of the IL-6 pathway may contribute to the development of osteoarthritis. Although the precise mechanism remains incompletely understood, IL-6 contributes to cartilage matrix degradation through activation of the NF-kB pathway, leading to upregulation of matrix-degradating enzymes that destroy cartilage. IL-6 also activates the JAK/STAT3 signaling pathways and enhances bone matrix remodeling, thus contributing to changes in the subchondral bone that may in turn affects the health of the cartilage.
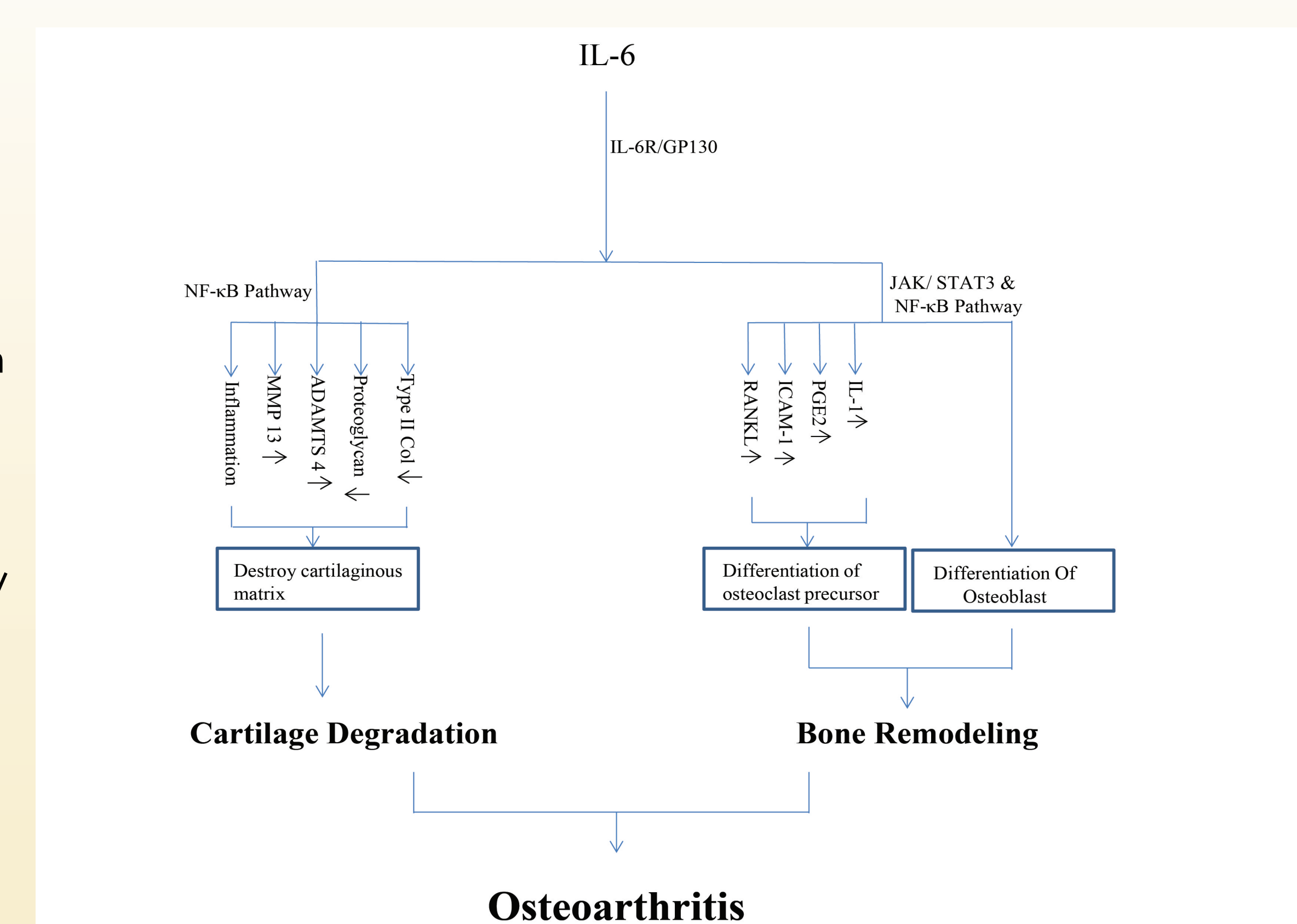
Conclusion

- IL-6 is transiently but markedly elevated in cartilage/subchondral bone tissues shortly after knee injury

- IL-6 may play an important role in the acute phase response to joint injury and the subsequent development of post-traumatic osteoarthritis

📠 **Print this Page for Your Records.**

Patrick B Satkunananthan
UC Davis Medical Center
4635 2nd Ave
Suite 2000
Sacramento CA 95817
Dear Patrick Satkunananthan:

Thank you for submitting your abstract **FLUORESCENCE REFLECTANCE IMAGING OF EARLY PROCESSES OF POST-TRAUMATIC OSTEOARTHRITIS IN MALE AND FEMALE MICE**, to the 2013 World Congress on Osteoarthritis, being held April 18 – 21, 2013 in Philadelphia, Pennsylvania at the Marriott Philadelphia DowntownOn behalf of the OARSI Program Committee, we are pleased to inform you that your abstract has been accepted as a poster presentation.

As part of the abstract submission process, it is understood that acceptance of your abstract by the program committee would constitute your participation as a presenter.

Please click on the CONFIRM button below. By clicking confirm, you are acknowledging receipt of this notification and your agreement to participate as a poster presenter.
Please respond no later than Friday, February 4, 2013.

Your poster number will be sent to you in the next six weeks.

The poster sessions are taking place at the following times:

Poster Session I
Friday, April 19, 2013
3:30 PM – 5:00 PM
Poster Session II
Saturday, April 20, 2013
3:30 PM – 5:00 PM

It is **important** for you to be present at your poster during these times to answer questions and discuss issues on your research with meeting attendees. (**Please note that you will receive specific presentation times when you receive your poster number)

POSTER FORMAT and SET-UP

Each poster will have a display area of two (2) meters tall by one (1) meter wide (6.5 feet tall by 3 feet wide) to display your materials. The overall area is reduced by a two-inch frame on all four sides.

PLEASE NOTE THAT THE SIZES FOR THE POSTERS ARE
TWO (2) METERS HIGH BY ONE (1) METER WIDE.

You may display your information in figures, tables, text, photographs, etc. Please prepare all illustrations neatly and legibly beforehand, in a size sufficient to read at a distance of three (3) feet. A series of typewritten sheets attached to the poster board is not acceptable. Materials will be available to fasten your material to the poster board.

   Poster set up is to convene on Thursday, April 18, 2013 from 8:00 AM – 5:00 PM
   Posters **MUST** remain on display until 5:00 PM on Saturday, April 20, 2013 at which time authors will be responsible for dismantling. Any posters remaining after 5:00 PM on Saturday will be removed by staff and OARSI cannot be

responsible for your poster.

For your convenience, please visit the OARSI 2012 Congress Website at http://2013.oarsi.org for registration and hotel information. On-line registration is available for the meeting. Please be sure to register prior to March 11, 2013 to receive the Pre-Congress rate.

Please note that all presenters are expected to cover their own travel and lodging and pay the registration fees. ALL presenters are required to register for the meeting.

If you have any questions, please feel free to contact me at the OARSI Meetings Department.

We look forward to meeting with you at what promises to be an exciting and informative program. For more information regarding the meeting and OARSI, please go to our website at http://2013.oarsi.org.

Sincerely,

Anthony Celenza, CMP
Senior Meeting Manager

Francisco J. Blanco, MD, PhD
Congress Chair

Rita Kandel, MD
Abstract Chair

Your Response: Confirm

OsteoArthritis Research Society International (OARSI)
15000 Commerce Parkway, Suite C
Mt. Laurel, NJ 08054, USA
Tel.: +1/856-439-1385
Fax: +1/856-439-0525
Email: **info@oarsi.org**

Leave OASIS Feedback

Purpose: Approximately 50% of individuals that experience anterior cruciate ligament (ACL) rupture develop post-traumatic osteoarthritis (PTOA) within 10-20 years, resulting in severe joint pain and stiffness. Although females are 4-6 times more likely than males to sustain an ACL injury during exercise or sports, males demonstrate an increased tendency to develop osteoarthritis following injury. ACL rupture initiates a surge of inflammatory cytokines, matrix metalloproteinases (MMPs), and other proteases, as well as cartilage degeneration and rapid bone turnover. It is possible that the magnitude or time course of these early biological responses may differ by sex, making males more likely to develop PTOA, however the quantification of these processes in males and females has not been performed. In this study, we used fluorescence reflectance imaging to quantify the time course of the early biological response to traumatic joint injury in male and female mice in vivo using highly sensitive activatable fluorescent agents that quantify protease activity, MMP activity, and osteoclastic bone resorption in injured and uninjured knees.

Methods: A total of 48 mice were subjected to non-invasive knee injury as previously described (Christiansen et al., Osteoarthritis and Cartilage, 2012). Three groups of 16 mice (8 male, 8 female) were imaged with either ProSense 680, MMPSense 680, or CatK 680 FAST (Perkin Elmer, Waltham, MA) in order to quantify protease activity, MMP activity, or osteoclastic bone resorption, respectively. Injections were administered 24-30 hours prior to imaging, on days 1, 3, 7, 14, 21, 28, and 56 after initial injury. At each time point of interest, mice were anesthetized with isoflurane, and imaged with the IVIS Spectrum system. Fluorescent signals were quantified by evaluating radiant efficiency of the signal within a uniform region of interest (ROI), anatomically selected around the knee on grayscale photograph. Radiant efficiency of the injured knee was normalized by that of the contralateral uninjured knee.

Results: For both male and female mice, protease activity (ProSense), MMP activity (MMPSense), and osteoclastic bone resorption (CatK) were significantly increased in the injured knee relative to the uninjured knee at nearly all time points. For example, Protease activity was significantly increased by day 1, reached a peak between 3 and 14 days, then decreased at later time points (Figure). Males and females displayed similar changes in injury response through the time periods observed, with males averaging a slightly higher normalized radiant efficiency at early time points, although this was not statistically different.

Conclusions: Using commercially available activatable fluorescent agents, we were able to quantify the time course of protease activity, MMP activity, and osteoclastic bone resorption in male and female mice following traumatic knee injury. However, contrary to our hypothesis, we were not able to observe a significant differential response between male and female mice. Our future studies will continue to explore potential mechanisms of the sex-based adaptation to joint injury that may contribute to the greater incidence of PTOA development in males. Our future studies will also continue to use fluorescence reflectance imaging as a method for measuring biological activity in vivo.
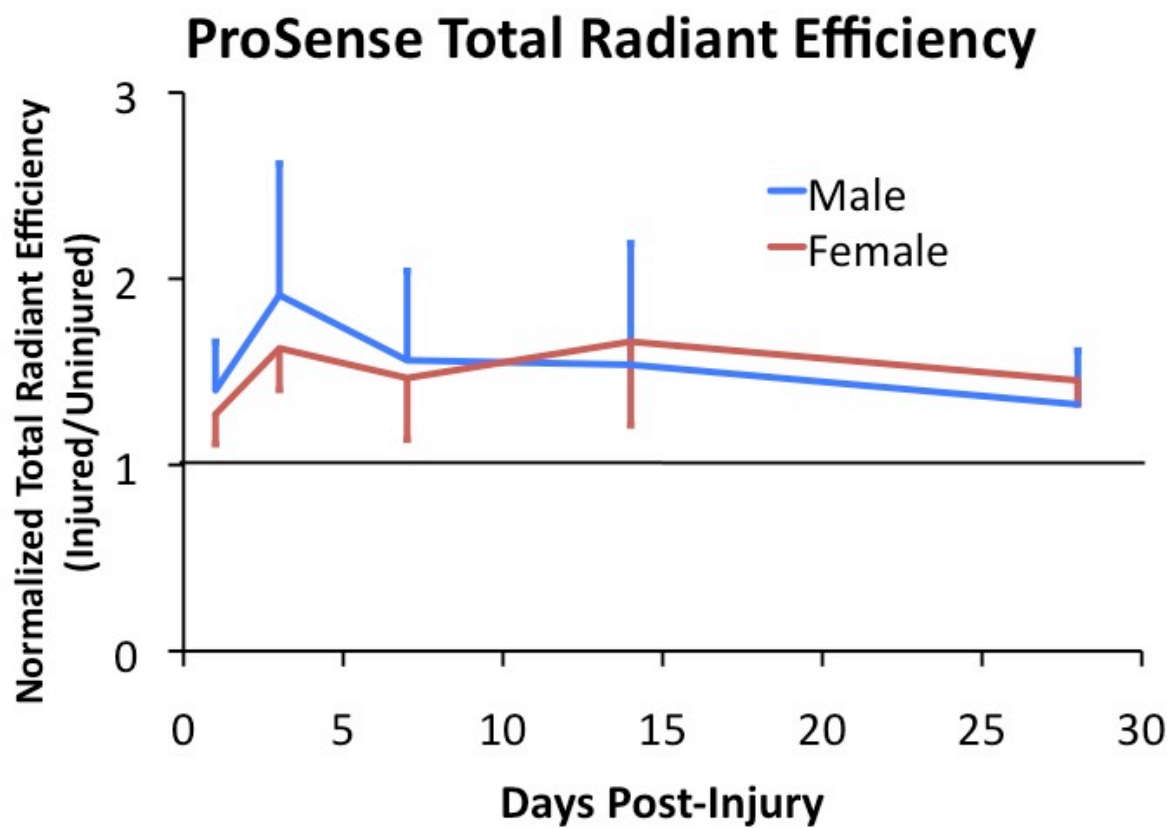
ProSense Total Radiant Efficiency

Comparison of Loading Rate-Dependent Injury Modes in a Murine Model of Post-Traumatic Osteoarthritis

Kevin A. Lockwood, Bryce T. Chu, Matthew J. Anderson, Dominik R. Haudenschild, Blaine A. Christiansen

Department of Orthopaedic Surgery, University of California-Davis Medical Center, 4635 2nd Ave, Suite 2000, Sacramento, California 95817

ABSTRACT: Post-traumatic osteoarthritis (PTOA) is a common long-term consequence of joint injuries such as anterior cruciate ligament (ACL) rupture. In this study we used a tibial compression overload mouse model to compare knee injury induced at low speed (1 mm/s), which creates an avulsion fracture, to injury induced at high speed (500 mm/s), which induces midsubstance tear of the ACL. Mice were sacrificed at 0 days, 10 days, 12 weeks, or 16 weeks post-injury, and joints were analyzed with micro-computed tomography, whole joint histology, and biomechanical laxity testing. Knee injury with both injury modes caused considerable trabecular bone loss by 10 days post-injury, with the Low Speed Injury group (avulsion) exhibiting a greater amount of bone loss than the High Speed Injury group (midsubstance tear). Immediately after injury, both injury modes resulted in greater than twofold increases in total AP joint laxity relative to control knees. By 12 and 16 weeks post-injury, total AP laxity was restored to uninjured control values, possibly due to knee stabilization via osteophyte formation. This model presents an opportunity to explore fundamental questions regarding the role of bone turnover in PTOA, and the findings of this study support a biomechanical mechanism of osteophyte formation following injury. © 2013 Orthopaedic Research Society. Published by Wiley Periodicals, Inc. J Orthop Res XX:XXX–XXX, 2013.

Keywords: mouse model; post-traumatic osteoarthritis; ACL injury; joint stability; osteophyte

Osteoarthritis (OA) is the most common joint disease, and the knee is the most commonly affected joint.[1] OA causes pain and stiffness in the joint, and severely limits mobility for those people who are affected. Current evidence indicates that after non-contact anterior cruciate ligament (ACL) injury, patients have an increased chance of developing post-traumatic osteoarthritis (PTOA) within 10–20 years after injury.[2,3]

Animal models are useful tools for studying PTOA, since the disease process can be studied in a more controlled environment on a dramatically condensed time line. There have been a number of mouse models developed for studying PTOA,[4–7] but many of these still have significant drawback such as invasive surgery or multiple bouts of mechanical loading. Our lab has developed a non-invasive mouse model that induces ACL rupture in mice in vivo by a single tibial compression overload.[8] This model closely mimics traumatic ACL rupture in humans without the costs and complications of surgery.

Our previous study using this mouse model had limitations, including ACL damage primarily by avulsion fractures rather than midsubstance tears, induction of only mild osteoarthritis by the end of the study (8 weeks post-injury), and little quantification of joint biomechanics.[8] Avulsion fracture is not a common injury mode in adults,[9] therefore a more clinically relevant mouse model would induce a midsubstance tear of the ACL rather than failure by an avulsion fracture. Based on the results from Crowninshield et al.[10] and Noyes et al.,[11] we hypothesized that increasing the loading rate during knee injury would cause midsubstance ACL tears and decrease the likelihood of an avulsion fracture.

In this study we used our non-invasive mouse injury model to compare biomechanical and structural changes in the joint following ACL injury either with avulsion fracture or with midsubstance tear. We examined short term (10 days) and long term (12–16 weeks) structural changes in subchondral bone and epiphyseal trabecular bone, osteophyte formation, articular cartilage degeneration, and biomechanical stability of injured vs. uninjured knees. We hypothesized that injury mode (avulsion vs. midsubstance tear) would not significantly affect structural bone changes, osteoarthritis development, or biomechanical stability.

METHODS

Animals

A total of 80 male C57BL/6N mice (10 weeks old at time of injury) were obtained from Harlan Sprague Dawley, Inc. (Indianapolis, IN). Mice underwent a 1-week acclimation period in a housing facility before injury. Mice were caged individually and were maintained and used in accordance with National Institutes of Health guidelines on the care and use of laboratory animals. All procedures were approved by our Institutional Animal Care and Use Committee.

Non-Invasive Knee Injury

ACL injury was induced as previously described.[8] Briefly, mice were anesthetized using isoflurane inhalation, then the right lower leg was positioned between two loading platens: an upper platen that held the flexed ankle at approximately 30 degrees of dorsiflexion and a lower platen that held the flexed knee. The platens were aligned vertically in an electromagnetic materials testing machine (Bose Electro-Force 3200, Eden Prairie, MN). A preload of 1 N was applied to the knee before a single dynamic axial compressive load was applied to a target displacement of −1.7 mm at a loading rate of either 1 or 500 mm/s. A target displacement was chosen rather than a target compressive load (as in our

previous study) to minimize overshoot at high loading rates. Compressive loads at ACL rupture were comparable for both 1 and 500 mm/s loading rates, and were similar to those observed in our previous study (8–12 N). After injury, mice were given a subcutaneous injection of buprenorphine (0.5 mg/kg body weight) for analgesia. Mice were allowed normal cage activity until sacrifice.

Characterization of Joint Injury

To determine the effect of tibial compression loading rate on injury mode (avulsion fracture vs. midsubstance tear), both knees of six mice were injured at loading rates of 1 or 500 mm/s ($n = 6$ knees per group). Immediately following injury, mice were sacrificed and injured knees were imaged with micro-computed tomography (µCT) as described below to detect the presence of bone fragments in the joint space indicative of avulsion fracture. To further characterize the injuries induced by High Speed or Low Speed tibial compression loading rate, both knees of 10 mice were injured using 1 mm/s ($n = 7$ knees) or 500 mm/s ($n = 7$ knees) loading rates, or left intact ($n = 6$ knees). Mice were sacrificed immediately after injury. Contrast enhanced µCT was performed on six knees ($n = 2$ per group). Knees were stained with phosphotungstic acid (PTA; 0.3% in 70% ethanol) for 1 week before being scanned with µCT (2 µm nominal voxel size, Micro Photonics, Inc., Allentown, PA). The remaining 14 knees ($n = 4$–5 per group) were decalcified, sectioned in the sagittal plane, and stained with hematoxylin and eosin (H&E) to assess joint structure.

Comparison of High Speed and Low Speed Injury Models

Study Design: A total of 64 mice were used for this study (Table 1). Half of the injured mice were injured with the 1 mm/s load rate (Low Speed injury; $n = 26$); the other half were injured with the 500 mm/s load rate (High Speed injury; $n = 26$). An additional 12 mice underwent sham injury (anesthetized and loaded with the 1 N preload only). Following injury, mice were immediately sacrificed ($n = 12$) or returned to normal cage activity for 10 days ($n = 22$), 12 weeks ($n = 15$), or 16 weeks ($n = 15$), at which point they were euthanized by CO_2 asphyxiation and both hind limbs were excised for analysis. The left limb served as an internal control for each mouse.

Micro-Computed Tomography of Distal Femoral Epiphysis, Tibial Subchondral Bone, and Osteophytosis

Injured and uninjured knees were imaged with micro-computed tomography (SCANCO µCT 35, Bassersdorf, Switzerland) to quantify trabecular bone structure in the distal femoral epiphysis, subchondral bone structure at the proximal tibia, and osteophyte formation around the joint. Dissected limbs were fixed in 4% paraformaldehyde for 24–

Table 1. Animal Numbers and Experimental Groups for "Comparison of High Speed and Low Speed Injury Models"

Time Point	Low Speed	High Speed	Sham
Day 0	6	6	
Day 10	8	8	6
Week 12	6	6	3
Week 16	6	6	3

48 h, then transferred to 70% ethanol. Knees were scanned according to the guidelines for micro-computed tomography (µCT) analysis of rodent bone structure[12] (energy = 55 kVp, intensity = 114 mA, 10 µm nominal voxel size, integration time = 900 ms). Trabecular bone in the distal femoral epiphysis was analyzed by manually drawing contours on 2D transverse slices. The distal femoral epiphysis was designated as the region of trabecular bone enclosed by the growth plate and subchondral cortical bone plate. We quantified trabecular bone volume per total volume (BV/TV), trabecular thickness (Tb.Th), trabecular number (Tb.N), and apparent bone mineral density (Apparent BMD; mg HA/cm³ TV) using the manufacturer's analysis tools. In our previous study[8] we observed comparable trabecular bone changes at the femoral epiphysis, tibial epiphysis, and tibial metaphysis following knee injury. The current study investigated only the femoral epiphysis, since it has the largest volume for analysis and therefore will yield the most consistent trabecular bone parameters. Subchondral bone of the proximal tibial plateau was analyzed for 12- and 16-week knees. The subchondral bone was segmented for 500 µm (50 slices) distal to the most proximal point of the tibia, excluding the trabecular bone compartment and any osteophytes growing from the tibia. We quantified cortical thickness (Ct.Th) and bone mineral density (BMD; mg HA/cm³ BV) of the subchondral bone using the manufacturer's analysis tools. We investigated only the tibial suchondral bone because analysis of the subchondral bone of the femoral condyles is technically challenging, as is highly dependent on the orientation of the femur in the µCT scan. Osteophyte volume was calculated for 12- and 16-week knees, and included all mineralized tissue in and around the joint space, excluding naturally ossified structures (patella, fabella, and anterior and posterior horns of the menisci).

Anterior–Posterior Joint Laxity

We quantified joint laxity of injured and uninjured mouse knees using a laxity tester based on previous designs.[13,14] This tester was designed to interface with a materials testing machine (Bose ElectroForce 3200). The protocol was similar to that described by Blankevoort et al.[14] for anterior–posterior (AP) laxity. Briefly, after fixation in brass tubes with polymethyl methacrylate (PMMA), the right and left knees of mice at day 0 ($n = 12$), week 12 ($n = 15$), and week 16 ($n = 15$) after injury were tested at 30°, 60°, and 90° of flexion. For each joint angle, knees underwent five loading cycles to a target force of ±1.5 N at a rate of 0.5 mm/s (Fig. 6). The force was applied normal to the longitudinal axis of the tibia. The femur was fixed during testing, but the tibia was allowed to translate and rotate about its longitudinal axis, giving the system three degrees of freedom of motion. Similar to Blankevoort et al., total AP joint laxity was computed based on the difference between displacement at +0.8 N and −0.8 N.

To assess whether fixation in 4% paraformaldehyde and 70% ethanol had an effect on joint laxity, day 0 limbs were tested fresh-frozen, and then retested after being fixed in 4% paraformaldehyde and preserved in 70% ethanol for 4 weeks. Fixed limbs were allowed to rehydrate in a bath of phosphate buffered saline (PBS) for 3 min before potting and testing. During testing, the limbs were continuously hydrated with PBS.

Long Term Whole Joint Histology

Knees were analyzed with whole joint histology to determine the extent of articular cartilage degeneration. Intact joints

were decalcified for 4 days in 10% buffered formic acid and then processed for standard paraffin embedding. For each limb, 6–7 sagittal sections (6 μm thickness) were cut across the entire joint separated by 250 μm. Slides were stained with Safranin-O and Fast Green to assess articular cartilage and other joint structures (meniscus, subchondral bone, osteophytes, etc.). Slides were blinded and graded by four independent readers using the semi-quantitative OARSI scale described by Glasson et al.[15] Grades were assigned to the medial and lateral tibial plateau, and medial and lateral femoral condyles.

Statistical Analysis

Trabecular bone μCT results for High Speed and Low Speed injury modes were compared at each time point by calculating the difference between injured and uninjured knees for each mouse (injured–uninjured) and using analysis of variance (ANOVA) to compare between groups. Joint laxity of uninjured control (UIC), 1, and 500 mm/s injury rate joints were compared at each time point using one-way ANOVA. Differences in joint laxity as a function of knee flexion angle were compared using repeated measures ANOVA. Histology OARSI scores of UIC, 1, and 500 mm/s injured knees were averaged between readers for each slide, then for all slides for each mouse, and were then compared using one-way ANOVA for each joint region (medial femur, medial tibia, lateral femur, lateral tibia). Significance was defined as $p < 0.05$ for all tests. Mean ± standard deviation is presented for all data.

RESULTS
Characterization of Joint Injury

Non-invasive injury of mice using tibial compression overload with increasing loading rates yielded observable differences in injury mode at the high speed loading rate (500 mm/s) compared to the low speed loading rate (1 mm/s). Using μCT imaging of injured mouse knees, we were able to observe bone fragments indicative of avulsion fracture for all mice injured at 1 mm/s, but we observed no bone fragments at a loading rate of 500 mm/s. We concluded that "High Speed injury" at 500 mm/s caused midsubstance disruption of the ligament, while "Low Speed injury" at 1 mm/s caused a combination injury involving ligament disruption with avulsion fracture. Contrast-enhanced μCT and whole joint histology showed disruption of the ACL for both 1 and 500 mm/s injury rates, with no obvious damage to the posterior collateral ligament, menisci, or other structures of the joint (Fig. 1). Consistent with our hypothesis, Low Speed injury (1 mm/s) caused disruption of the ACL with an avulsion fracture from the posterior femur. High Speed injury (500 mm/s) resulted in disruption of the ACL only, with no evidence of avulsion fracture.

Comparison of High Speed and Low Speed Injury Models

Micro-Computed Tomography of Distal Femoral Epiphysis, Tibial Subchondral Bone, and Osteophytosis

Both injury modes initiated a rapid loss of epiphyseal trabecular bone in the distal femur by 10 days post-injury, and long-term joint degeneration and osteophytosis by 12 and 16 weeks post-injury. At all time points, knees injured with either the High Speed or Low Speed loading rates had significantly reduced trabecular BV/TV at the femoral epiphysis compared to uninjured contralateral knees and UIC mice (Fig. 2). At 10 days post-injury, knees injured using the Low Speed loading rate had significantly greater
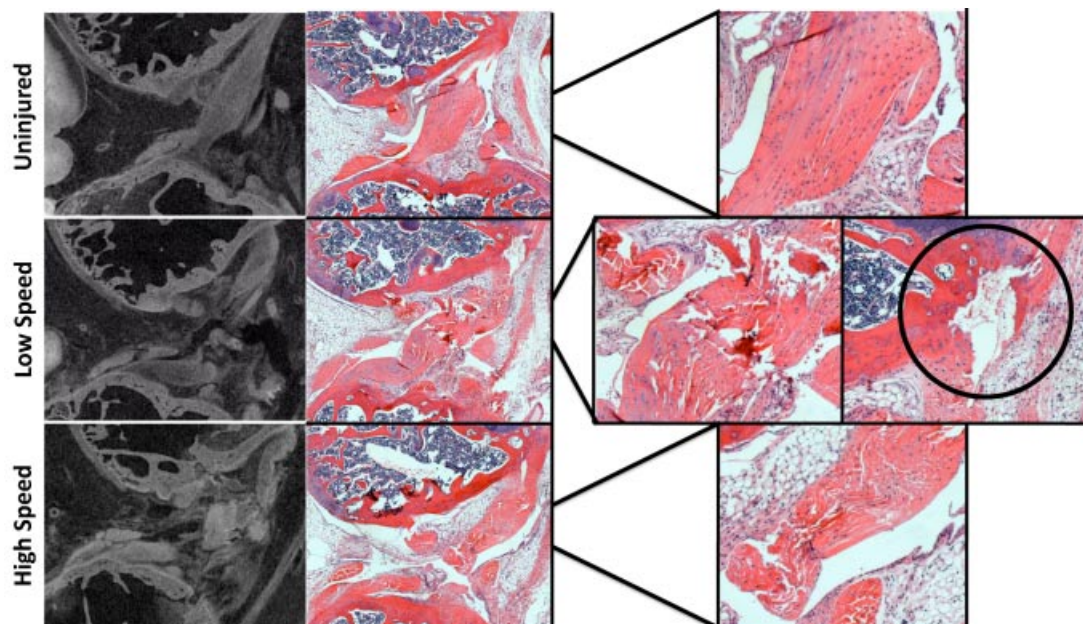
Figure 1. Imaging of injured and uninjured knee joints. Contrast-enhanced μCT images (left column) show disruption of the ACL in both High Speed and Low Speed injuries. Hemotoxylin and Eosin sections of intact, High Speed, and Low Speed injury modes (middle and right columns) show disruption of the ACL with both injury modes compared to uninjured ligament. Low Speed injury (1 mm/s) caused avulsion of the ACL from the posterior femur (circle). No avulsion was detected in the High Speed (500 mm/s) injury group.

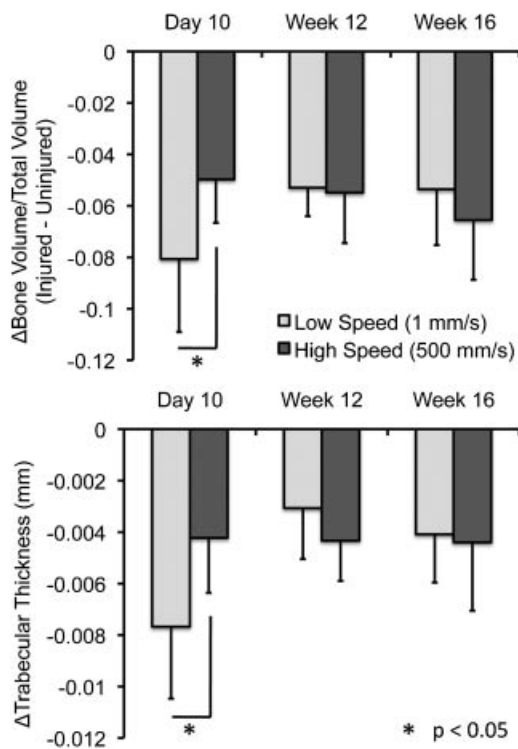**Figure 2.** Difference in bone volume fraction (BV/TV) and trabecular thickness (Tb.Th) of the distal femoral epiphyses for Low Speed (1 mm/s) and High Speed (500 mm/s) injury groups. Values are the average difference between injured and contralateral control legs for each mouse. Injured versus uninjured values were significantly different for all groups and all time points ($p < 0.05$). Mice injured at Low Speed, which induced avulsion from the distal femur, exhibited greater trabecular bone loss at 10 days post-injury. After 12–16 weeks, injured knees still had significantly reduced bone volume and trabecular thickness compared to uninjured knees, although there were no differences between High Speed and Low Speed injuries in trabecular structure at these time points.

loss of trabecular BV/TV compared to those injured with the High Speed loading rate (-31% vs. -20%, respectively). By 12 and 16 weeks post-injury, there were no differences in trabecular BV/TV between the High Speed and Low Speed injury modes, although BV/TV of injured knees remained significantly lower than contralateral knees ($p < 0.05$). At 12 weeks post-injury, BV/TV of High Speed and Low Speed injured knees was 20.9% and 19.6% lower than contralateral knees, respectively, while at 16 weeks, BV/TV of injured knees was 22.9% and 21.5% lower, respectively. Trabecular thickness (Tb.Th) and apparent BMD of the femoral epiphysis followed a similar pattern, with the Low Speed injury rate exhibiting a significantly lower thickness and apparent BMD than the High Speed injury rate at 10 days. At 12 and 16 weeks there were no significant differences between injury modes, but injured limbs had reduced Tb.Th and BMD compared to uninjured contralateral limbs.

Analysis of subchondral bone at the proximal tibia revealed significant thickening of the subchondral bone plate in injured knees by 12 and 16 weeks post-injury (Fig. 3). Cortical thickness was 20–26% larger for injured knees compared to contralateral knees for both injury modes and both time points ($p < 0.05$). However, we observed no significant differences in cortical thickness increase between time points or between injury modes. BMD of the subchondral bone plate was significantly higher for Low Speed injured knees compared to contralateral knees at week 12 only (908.7 vs. 891.7 mg HA/cm^3; $p = 0.001$). No significant differences in subchondral bone BMD were observed for High Speed injured knees or for any knees at 16 weeks post-injury.

Injured knees exhibited significant osteophytosis using both the High Speed and Low Speed injury modes by 12 and 16 weeks post-injury (Figs. 4–6). The pattern of osteophyte formation was consistent for all mice at 12 and 16 weeks, regardless of injury mode. Specifically, there was considerable osteophyte formation on the anterior-medial aspect of the distal femur, the menisci (particularly the medial meniscus) exhibited hypertrophy and osteophyte formation, primarily extending in an anteromedial direction from the joint (Fig. 5). The posterior medial tibial plateau exhibited bone formation in the posterior direction, and extreme erosion of the tibial plateau was observable with μCT, exposing the underlying subchondral bone.

Both injury models exhibited increased osteophyte volume from 12 to 16 weeks, although this increase was only significant for the Low Speed injury group (Fig. 6). The High Speed injury group exhibited higher osteophyte volume compared to the low speed injury group at both time points; this difference was statistically significant at 12 weeks ($p = 0.04$). We were able to observe preliminary signs of osteophyte formation on transverse μCT images of injured joints as early as 10 days post-injury, particularly on the anteromedial aspect of the distal femur (Fig. 5).

Anterior–Posterior Joint Laxity

We observed a greater than twofold increases in AP joint laxity immediately following joint injury with both injury modes (Fig. 7). We observed no significant difference in joint laxity between flexion angles for any group at any time point. By 12 and 16 weeks post-injury, AP joint laxity for both injured groups was reduced to control values. During AP laxity testing of week 16 legs, one control leg was broken during potting. Additionally, injured knees of week 16 mice had severely diminished range of motion and were difficult to extend to 30°. As a result, three of the 1 mm/s and two of the 500 mm/s week 16 knees were also fractured. Thirty-degree extension was tested last to ensure that data was collected for 60° and 90° joint angles.

No change in joint laxity was observed for day 0 uninjured joints after fixation in 4% paraformaldehyde and preservation in 70% ethanol for 4 weeks (compared to fresh-frozen joints), but injured joints exhibited significantly increased joint laxity after fixation (+18% AP joint laxity). Subsequently, joint laxity
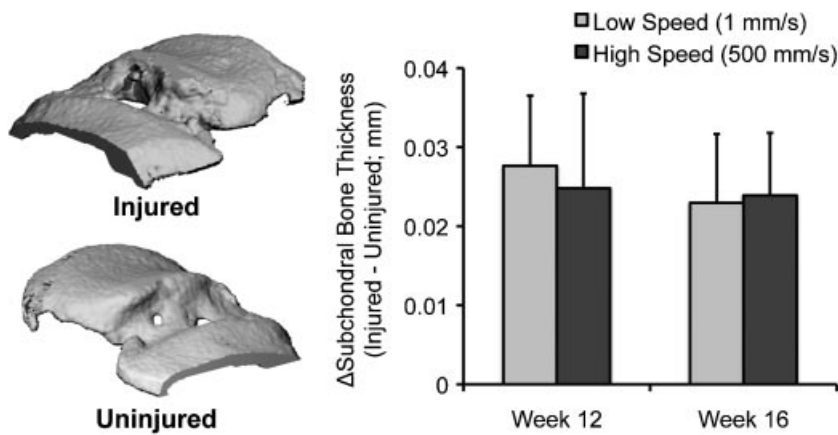
Figure 3. Left: Micro-computed tomography reconstructions of the subchondral bone plate of the tibial plateau of injured and uninjured knees, with a medial cut for visualization of subchondral bone thickness. Right: Difference in subchondral bone thickness of the proximal tibial plateau for Low Speed (1 mm/s) and High Speed (500 mm/s) injury groups. Values are the average difference between injured and contralateral control legs for each mouse. Injured versus uninjured values were significantly different for all groups and all time points ($p < 0.05$). No significant differences were observed between injury modes or time points.

values of day 0 preserved knees were used for all comparisons between day 0, week 12, and week 16 data.

Long Term Whole Joint Histology

Whole joint histology showed extreme degeneration and OA for both injury modes at 12 and 16 weeks post-injury (Fig. 8). OARSI scores were significantly higher than UIC joints at 12 and 16 weeks for both injury modes, however there were no significant differences between High Speed and Low Speed injured joints (Fig. 9). Injured joints exhibited extreme erosion of cartilage on both the medial and lateral aspects of the tibia and femur. Many injured joints had bone-bone contact and even erosion of subchondral bone, sometimes extending as far as the growth plate. There was extreme fibrosis within the joint space and osteophytes present on the tibia and femur. The menisci on both sides were hypertrophied and degenerated. Inspection of individual sections showed the most severe degeneration on the posterior aspect of the tibial plateau of injured joints, while the anterior aspect appeared comparable to UICs. At 16 weeks the UIC joints were given an average OARSI score of approximately 2, indicating mild OA occurring naturally in the mice by 26 weeks of age.
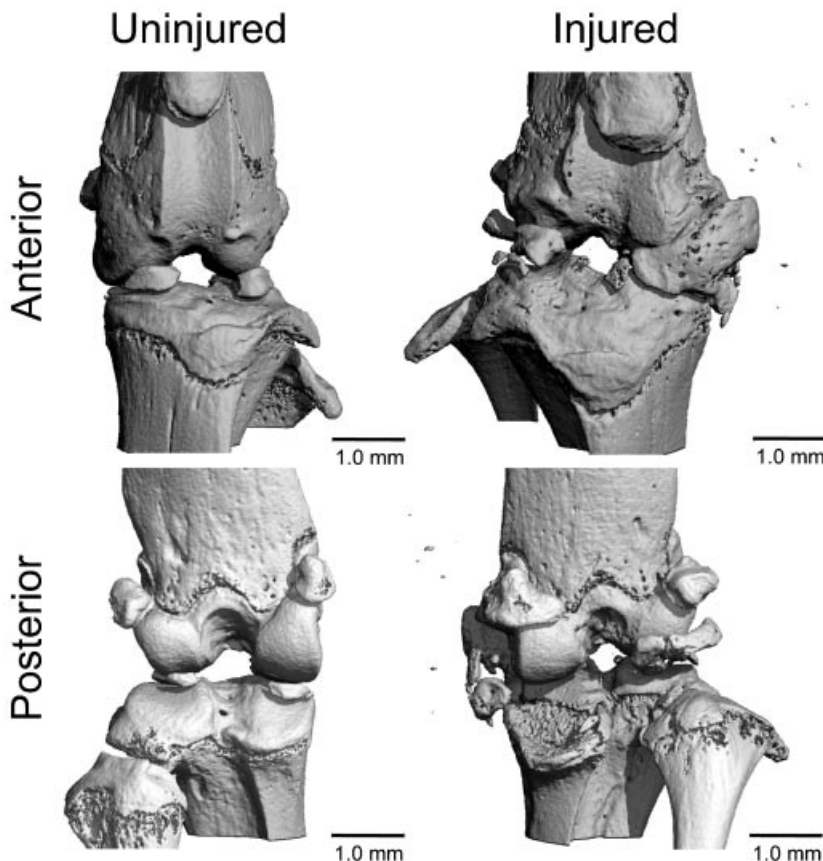

Figure 4. μCT images of injured and uninjured mouse knees at 12 weeks post-injury (Low Speed injury). Substantial osteophytosis and joint degeneration were observed in all injured knees. In particular, osteophytes were observed on the anteriomedial aspect of the distal femur, the posteromedial aspect of the proximal tibia, and the medial meniscus.
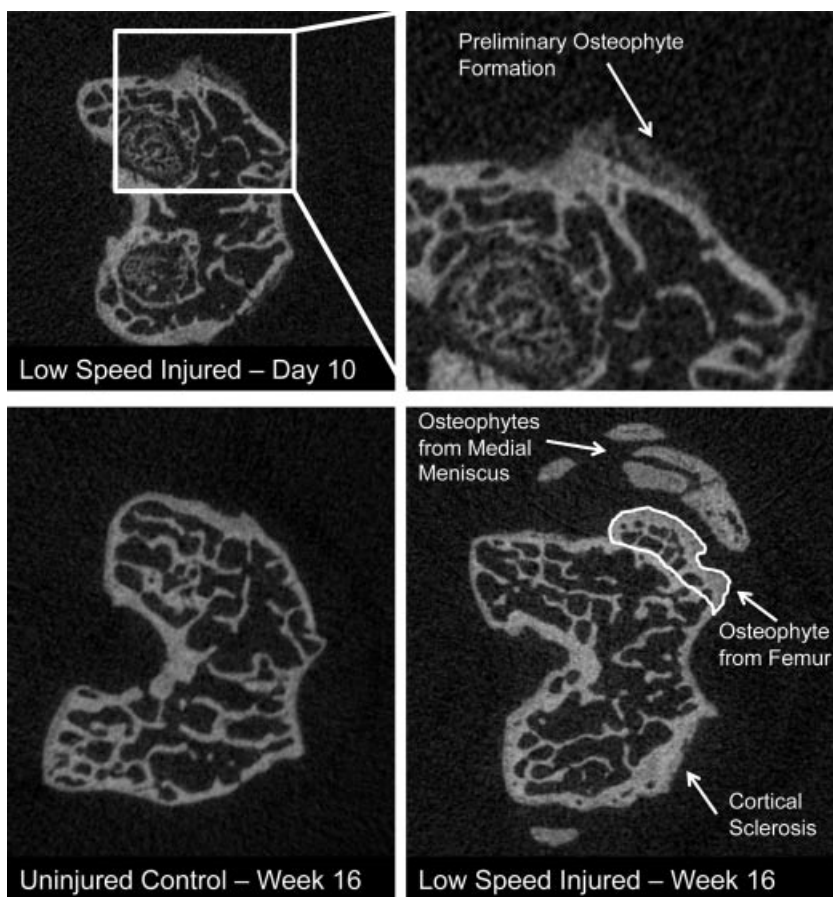
Figure 5. Transverse μCT slices of the distal femur. Top: Femoral epiphysis of an injured joint 10 days postinjury, with expanded image showing early osteophytosis from the anterio-medial femur. Bottom: Uninjured (left) and injured (right) femoral epiphysis at 16 weeks showing considerable osteophyte formation from the anteriomedial femur and medial meniscus, as well as sclerosis of cortical plate on the lateral condyle.

DISCUSSION

In this study we used a non-invasive injury model in mice to compare two similar but distinctly different injury modes, and assess potential differences in PTOA development. Using different tibial compression loading rates, we were able to produce two unique injury modes in the knees of mice: ACL rupture with avulsion fracture ("Low Speed injury", 1 mm/s loading rate) or midsubstance ACL rupture ("High Speed injury", 500 mm/s loading rate). Consistent with our hypothesis, we found that the two injury modes were not significantly different from each other with respect to long-term changes in bone structure, joint laxity, and cartilage degeneration. However, we observed a greater loss of trabecular bone in the distal femoral epiphysis at 10 days post-injury in the Low Speed injury model compared to High Speed injury. This difference is likely due to direct bone damage caused by avulsion of the ACL in the Low Speed injury group. We also observed significant differences in osteophyte formation, with High Speed injured knees developing greater osteophyte volume. Altogether, these results suggest that ACL injury mode in mice is a minor contributing factor to the subsequent joint degeneration that follows traumatic joint injury after 12–16 weeks.

The role of subchondral bone in progression of OA has been an active topic of discussion,[16–18] with authors hypothesizing that cartilage health is influenced by the structure of the underlying subchondral bone. However, early changes in subchondral bone and epiphyseal trabecular bone are not well defined in human subjects, but rather established (severe) OA is
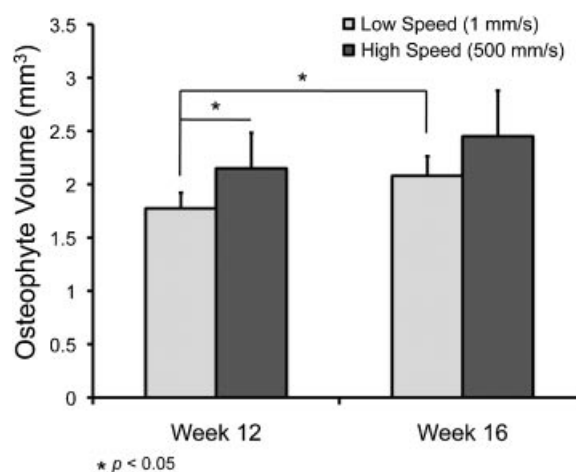
Figure 6. Osteophyte volume of injured joints. Non-native bone formation was quantified for Low Speed (1 mm/s) and High Speed (500 mm/s) injured joints at 12 and 16 weeks post-injury. High Speed injured joints exhibited greater osteophyte volume than Low Speed injured joints at 12 weeks postinjury. Osteophyte volume increased from 12 to 16 weeks for both groups, but this increase was only significant for Low Speed injured mice ($p < 0.05$).
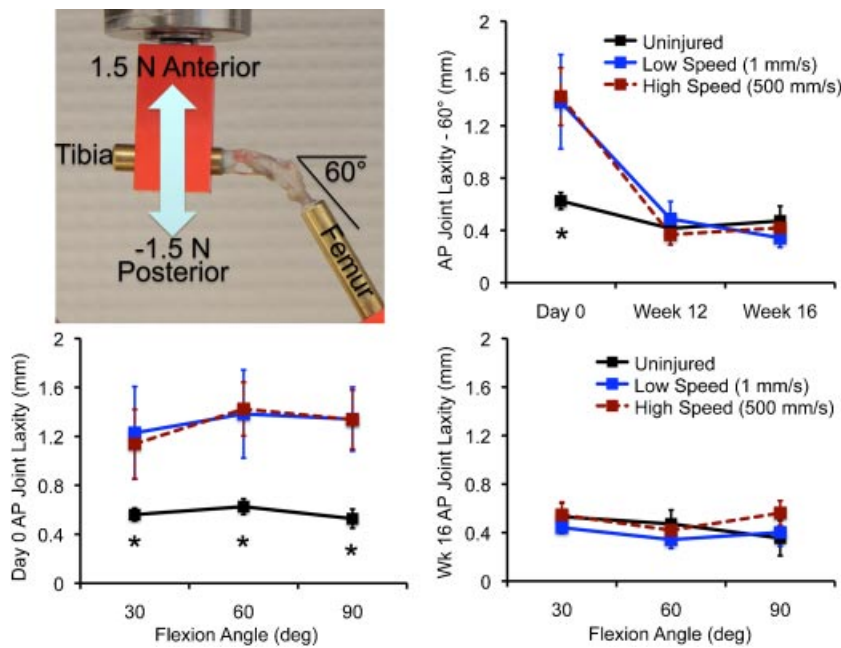
Figure 7. Top left: Joint laxity test setup for 60° of flexion. Top right: Total anterior–posterior joint laxity at 60° for day 0, week 12, and week 16 knees. $^*p < 0.05$ between injured and uninjured values. Injured joints had a greater than twofold increase in joint laxity at day 0, but joint stability was returned to control values by 12 and 16 weeks post-injury. Bottom: Total anterior–posterior joint laxity at day 0 (left) and week 16 (right) at 30°, 60°, and 90° of knee flexion. $^*p < 0.05$ between injured and uninjured values. There were no significant differences between joint angles, or between injury modes (High Speed vs. Low Speed injury).

typically studied.[19] A few recent studies have investigated epiphyseal trabecular bone changes in the knees of osteoarthritic subjects using MRI imaging,[20,21] and have observed decreased trabecular bone parameters (loss of trabecular bone) in osteoarthritic knees, particularly in the lateral compartment. This is consistent with the current study and our previous study[8] that showed trabecular bone loss from both the medial and lateral compartments in mice, although our previous study found similar magnitudes of trabecular bone loss from the medial and lateral compartments. Subchondral bone sclerosis and osteophyte formation are also common findings in humans with OA.[22] This is consistent with the current study, in which we observed thickening of the tibial subchondral bone plate, and considerable osteophyte formation around the joint by 12 and 16 weeks post-injury. The relative-

ly large scale of osteophytes observed in this study is not typical for OA in humans, although this may be due to the fact that bone features do not scale linearly with body size between mice and humans. For example, body mass in humans is approximately 2,000–4,000 times greater than that of mice, while trabecular thickness in humans is approximately 4–7 times greater (100–350 μm in humans vs. 25–50 μm in mice). Altogether, the subchondral and trabecular bone changes observed in this mouse model of PTOA are generally consistent with the bone changes observed in human OA.

By both 12 and 16 weeks post-injury we observed severe OA in injured knees. This is in contrast to our previous study, in which joints exhibited only mild OA by 8 weeks post-injury, with loss of Safranin-O staining, minor fissuring, and cell death in the superficial
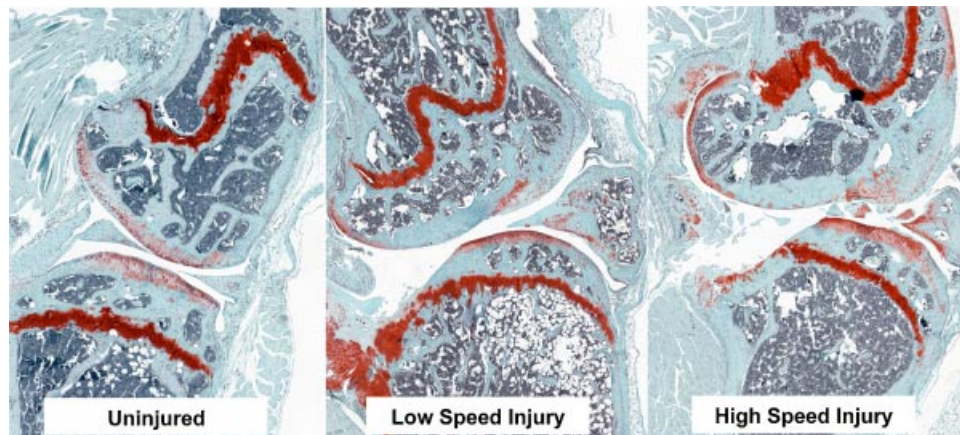

Figure 8. Whole joint histology at 12 weeks. Sagittal sections of the medial condyle stained with Safranin-O and Fast Green. By 12 weeks post-injury we observed significant degeneration of both the tibia and femur. In particular, the posterior aspect of the medial tibia has severe degeneration of cartilage and bone erosion, often extending as far as the growth plate.
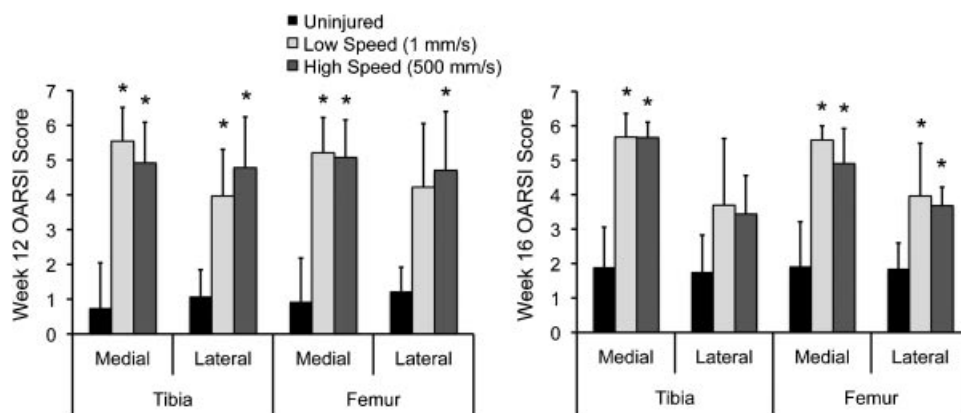
Figure 9. OARSI scores for whole joint histology at 12 and 16 weeks. We observed severe osteoarthritis of both the tibia and femur at both time points, often with degeneration of articular cartilage extending to the subchondral bone (* indicates significant difference from uninjured control. No statistically significant differences were observed in the OARSI score of knees injured with the High Speed versus Low Speed injury mode).

zone.[8] In the current study we found that by only 4 weeks later (12 weeks post injury), injured joints exhibited severe OA with total loss of cartilage tissue. In many joints there was bone on bone contact, extreme fibrosis, and severe meniscal degeneration visible by 12 weeks post-injury, often to a degree that is unnecessary for studies of arthritis development. The severe posterior bone erosion we observed on the tibial plateau, particularly on medial side, is not typical of ACL injury-induced PTOA in other animal species or in humans, although similar erosion has been described with surgical transection of the ACL in mice.[4] This posterior degeneration may therefore be specific to mouse models of ACL-induced PTOA irrespective of how the ACL is ruptured (with or without surgery). In this way, ACL injury in mice may be limited for translation to human injuries. For future studies with this model, we anticipate that an 8–10 weeks end point should be sufficient to show moderate to severe OA, and would be sufficient to detect any improvement in OA development due to treatment. In contrast, the DMM and ACLT models utilized by Glasson et al.[4] were able to induce moderate-to-severe OA by 4 weeks post-injury.

Changes in AP joint laxity of injured knees in this study were similar to values obtained from previous studies using C57BL/6 mice with healthy knees. At $\pm 0.8\,N$ in healthy ACL intact joints, Blankevoort et al.[14] measured $0.43 \pm 0.16\,mm$ and Wang et al.[13] measured $0.50 \pm 0.09\,mm$, compared to $0.57 \pm 0.08\,mm$ in our study. The increased joint laxity measured in this study is likely due to the additional degree of freedom in our test fixture, which allowed rotation of the tibia about its longitudinal axis. The previous studies only allowed two degrees of freedom of motion.

In this study we observed consistent and repeatable patterns of osteophytosis around the joint capsule by 12 and 16 weeks post injury for both injury modes. In particular, we observed osteophytes forming from the anteriomedial femur, the posteromedial tibia, and the

medial meniscus. It is possible that osteophyte formation around the joint may have contributed to the reduction in joint laxity from day 0 values. The stabilizing effect of osteophytes in osteoarthritic joints was previously studied by Pottenger et al.[23] in humans undergoing total knee arthroplasty (TKA) by measuring varus-valgus (VV) laxity before and after removal of osteophytes. They observed an increase in VV joint laxity from 11.0° to 14.7° after osteophyte removal, showing that osteophytes helped stabilize the joint. These results support the hypothesis that osteophytes form as a response to joint instability. The drawback to restoring joint stability by osteophyte formation is severe reduction in joint range of motion, which was observed in the current study. Twelve- and sixteen-week knees were extremely stiff and resisted extension to 30°. This was supported by a study in humans undergoing TKA, in which residual posterior femoral condyle osteophytes were associated with reduced knee flexion after surgery. Removal of the osteophytes avoided impingement with the implant and allowed more flexion to occur.[24] Unfortunately, our study did not investigate AP joint laxity at intermediate time points between 0 and 12 weeks post-injury. Future analyses could investigate the time course of "re-stabilization" of the joint after ACL rupture, and could confirm the proposed correlation with osteophyte formation.

Future studies using this model should include additional biomechanical analyses to further characterize relationships between joint injury and OA progression. Gait analysis of injured mice could address questions concerning voluntary mechanical loading after injury and whether mice change limb-loading patterns. If the mice are unweighting the injured limb, then loss of bone volume may be partly explained due to disuse. Additionally, future studies could investigate the activity level of mice following joint injury. It is possible that voluntary cage activity is reduced, which would result in further mechanical loading-

related bone atrophy. The opposite is also likely true; increased cage activity or exercise (including fighting) could exacerbate PTOA progression following injury.

This study advances our previous study by analyzing multiple injury modes, quantifying biomechanical changes in the joint, and analyzing time points at which severe OA is present. However, there are still limitations that must be acknowledged. In particular, while anatomical structures between human and mice are similar, the bipedal gait of humans is very different from that of mice, and may result in divergent laxity changes, loading patterns, and locations of degeneration. Additionally, the severe osteophyte formation that we observe with this model is not typical for human joints, although it is comparable to other widely used mouse models,[25] and may be largely explained by the dramatic size difference between mouse and human joints. Finally, these studies used 10-week-old mice with open growth plates (the growth plates in mouse long bones typically remain open throughout the lifetime of the animal). This is a ubiquitous limitation of using mice for studies of bone, and may have contributed to the skeletal adaptation observed in this study. While this model may not be able to overcome all of these limitations, it still has several advantages over other existing mouse models of PTOA, and may be uniquely useful for investigating OA progression in humans.

In conclusion, in this study we found that ACL injury mode does not affect the long term bone changes or OA severity in mice, although it does affect short term trabecular bone turnover, with injury involving direct bone damage (avulsion) exhibiting greater short term trabecular bone loss. We also found that ACL injury dramatically increased AP joint laxity in mice immediately following injury, but joint stability is restored by 12 weeks post-injury, possibly due to extensive osteophyte formation around the joint. These studies further characterize the non-invasive knee injury mouse model developed in our lab, and begin to describe mechanical loading changes initiated by joint injury. The model presented provides an opportunity to explore fundamental questions regarding the role of bone turnover in PTOA progression, and findings from this model may point to bone turnover as a potential target for therapies aimed at slowing or preventing PTOA.

ACKNOWLEDGEMENTS

REFERENCES

1. Felson DT. 1988. Epidemiology of hip and knee osteoarthritis. Epidemiol Rev 10:1–28.
2. Lohmander LS, Englund PM, Dahl LL, et al. 2007. The long-term consequence of anterior cruciate ligament and meniscus injuries: osteoarthritis. Am J Sports Med 35:1756–1769.
3. Oiestad BE, Engebretsen L, Storheim K, et al. 2009. Knee osteoarthritis after anterior cruciate ligament injury: a systematic review. Am J Sports Med 37:1434–1443.
4. Glasson SS, Blanchet TJ, Morris EA. 2007. The surgical destabilization of the medial meniscus (DMM) model of osteoarthritis in the 129/SvEv mouse. Osteoarthritis Cartilage 15:1061–1069.
5. Furman BD, Strand J, Hembree WC, et al. 2007. Joint degeneration following closed intraarticular fracture in the mouse knee: a model of posttraumatic arthritis. J Orthop Res 25:578–592.
6. van Beuningen HM, Glansbeek HL, van der Kraan PM, et al. 2000. Osteoarthritis-like changes in the murine knee joint resulting from intra-articular transforming growth factor-beta injections. Osteoarthritis Cartilage 8:25–33.
7. Poulet B, Hamilton RW, Shefelbine S, et al. 2011. Characterising a novel and adjustable non-invasive murine knee joint loading model. Arthritis Rheum 63:137–147.
8. Christiansen BA, Anderson MJ, Lee CA, et al. 2012. Musculoskeletal changes following non-invasive knee injury using a novel mouse model of post-traumatic osteoarthritis. Osteoarthritis Cartilage 20:773–782.
9. Gottsegen CJ, Eyer BA, White EA, et al. 2008. Avulsion fractures of the knee: imaging findings and clinical significance. Radiographics 28:1755–1770.
10. Crowninshield RD, Pope MH. 1976. The strength and failure characteristics of rat medial collateral ligaments. J Trauma 16:99–105.
11. Noyes FR, DeLucas JL, Torvik PJ. 1976. Biomechanics of anterior cruciate ligament failure: an analysis of strain-rate sensitivity and mechanisms of failure in primates. J Bone Joint Surg Am 56:236–253.
12. Bouxsein ML, Boyd SK, Christiansen BA, et al. 2010. Guidelines for assessment of bone microstructure in rodents using micro-computed tomography. J Bone Miner Res Off J Am Soc Bone Miner Res 25:1468–1486.
13. Wang VM, Banack TM, Tsai CW, et al. 2006. Variability in tendon and knee joint biomechanics among inbred mouse strains. J Orthop Res Off Publ Orthop Res Soc 24:1200–1207.
14. Blankevoort L, van Osch JVM, Janssen B, et al. 1996. In vitro laxity-testers for knee joints of mice. J Biomechanics 29:799–806.
15. Glasson SS, Chambers MG, Van Den Berg WB, et al. 2010. The OARSI histopathology initiative—Recommendations for histological assessments of osteoarthritis in the mouse. Osteoarthritis Cartilage 18:S17–S23.
16. Mansell JP, Tarlton JF, Bailey AJ. 1997. Biochemical evidence for altered subchondral bone collagen metabolism in osteoarthritis of the hip. Br J Rheumatol 36:16–19.
17. Hayami T, Pickarski M, Zhuo Y, et al. 2006. Characterization of articular cartilage and subchondral bone changes in the rat anterior cruciate ligament transection and meniscectomized models of osteoarthritis. Bone 38:234–243.
18. Radin EL, Rose RM. 1986. Role of subchondral bone in the initiation and progression of cartilage damage. Clin Orthop Relat Res 213:34–40.
19. Mastbergen SC, Lafeber FP. 2011. Changes in subchondral bone early in the development of osteoarthritis. Arthritis Rheum 63:2561–2563.
20. Chiba K, Uetani M, Kido Y, et al. 2011. Osteoporotic changes of subchondral trabecular bone in osteoarthritis of the knee: a 3-T MRI study. Osteoporos Int 23:589–597.
21. Bolbos RI, Zuo J, Banerjee S, et al. 2008. Relationship between trabecular bone structure and articular cartilage

morphology and relaxation times in early OA of the knee joint using parallel MRI at 3 T. Osteoarthritis Cartilage 16:1150–1159.

22. Jacobson JA, Girish G, Jiang Y, et al. 2008. Radiographic evaluation of arthritis: degenerative joint disease and variations. Radiology 248:737–747.

23. Pottenger LA, Phillips FM, Draganich LF. 1990. The effect of marginal osteophytes on reduction of varus–valgus instability in osteoarthritic knees. Arthritis Rheum 33:853–858.

24. Yau WP, Chiu KY, Tang WM, et al. 2005. Residual posterior femoral condyle osteophyte affects the flexion range after total knee replacement. Int Orthop 29:375–379.

25. Moodie JP, Stok KS, Muller R, et al. 2011. Multimodal imaging demonstrates concomitant changes in bone and cartilage after destabilisation of the medial meniscus and increased joint laxity. Osteoarthritis Cartilage 19:163–170.

Appendix 5 Page 60

UNIVERSITY OF CALIFORNIA, DAVIS

Department of Orthopaedic Surgery
Orthopaedic Research Laboratory

Dominik R. Haudenschild, PhD
Research Building 1 Suite 2000
4635 Second Avenue
Sacramento, CA 95817
Office: (916) 734-5015
Cell: (530) 746-8866
www.ucdmc.ucdavis.edu/orthopaedics

Dr. Stefan Lohmander
Editor-in-Chief,
Osteoarthritis and Cartilage

Dear Dr. Stefan Lohmander,

My co-authors and I would like to submit an original manuscript entitled "**In-vitro and In-vivo Imaging of MMP Activity in Cartilage and Joint Injury**", which we prepared for publication in the special themed issue of "**Imaging in Osteoarthritis**" in the journal "**Osteoarthritis and Cartilage**".

In this manuscript we use functional imaging of MMP activity in cartilage explants subjected to mechanical impact or cytokine treatment, and in vivo in a mouse model of acute knee joint injury. We further characterize the sensitivity and reaction kinetics of the in-vivo imaging probe to various different OA-related MMP enzymes in-vitro. The development of a non-invasive assay to measure the degradative activity in joints and cartilage explants is an important contribution to the field of OA research, complementing existing imaging technologies that show the resulting structural changes.

The manuscript has been read and approved for submission by all authors. All persons listed as authors have contributed to preparing the manuscript and no person other than the authors listed have contributed significantly to its preparation. The contents of this manuscript are our original work and have not been published, in whole or in part, prior to or simultaneous with our submission of the manuscript to Osteoarthritis and Cartilage. All authors have no conflict of interest to report.

We thank you in advance for consideration of this manuscript.

Sincerely yours,

Dominik R. Haudenschild

Elsevier Editorial System(tm) for Osteoarthritis and Cartilage
Manuscript Draft

Corresponding Author: Dr. Dominik R Haudenschild, Ph.D.

Corresponding Author's Institution: University of California Davis

First Author: Tomoaki Fukui, M.D., Ph.D

Order of Authors: Tomoaki Fukui, M.D., Ph.D; Elizabeth Tenborg; Jasper H Yik , Ph.D.; Dominik R Haudenschild, Ph.D.

Abstract: Objective: The matrix metalloproteinase (MMP) family of proteins are principal enzymes in cartilage degradation during osteoarthritis (OA). Non-destructive detection of MMP activity could be useful in studies of OA pathogenesis, progression, and to evaluate intervention strategies. MMPSense750 is an in-vivo fluorimetric imaging probe with the potential to continuously and non-invasively trace real time MMP activities, but its use in OA-related research has not been reported. The objective of the current study is to investigate the use of MMPSense750 in OA imaging, using chondrocytes and cartilage explants in an in-vitro setting, and a mouse knee injury model for in-vivo imaging.
Design: We first determined the appropriate MMPSense concentration, assay time, and linear range using various concentrations of recombinant MMP-3, -9 and -13. Next we tested whether we could quantifiably image MMP activity in cytokine-treated chondrocytes, and bovine cartilage explants subjected to either mechanical injury or cytokine treatment in-vitro. Finally, we performed in-vivo imaging of a mouse model of post-traumatic OA to compare MMP activity in the injured versus contralateral knee.
Results: The best time to measure fluorescence intensity was highly dependent on the type of MMP enzyme. In cartilage explants, mechanical impact or cytokine treatment increased the fluorescent signal indicating elevated MMP activity. Injured knees of mice showed significantly higher fluorescent signal than uninjured knees 48 hours after injury.
Conclusions: MMPSense750 is a convenient tool to detect MMP activities for in-vitro study with cartilage, as well as in-vivo studies of knee injury, offering insight into the degradative processes within the joint.

In-vitro **and *in-vivo* imaging of MMP activity in cartilage and joint injury**

Tomoaki Fukui (n.f.n.l.tf@gmail.com), Elizabeth Tenborg (etenborg@gmail.com), Jasper H.
N. Yik (jyik@ucdavis.edu), *Dominik R. Haudenschild
(Dominik.Haudenschild@ucdmc.ucdavis.edu)

Lawrence J. Ellison Musculoskeletal Research Center, Department of Orthopaedic Surgery,
University of California Davis Medical Center, 4635 Second Avenue Suite 2000, Sacramento
CA 95817, USA

*Corresponding author:
Dominik R. Haudenschild
Lawrence J. Ellison Musculoskeletal Research Center, Department of Orthopaedic Surgery,
University of California Davis Medical Center, 4635 Second Avenue Suite 2000, Sacramento
CA 95817, USA
Tel: +1-916-734-5015
Fax: + 1-916-734-5750.
Dominik.Haudenschild@ucdmc.ucdavis.edu

Running title: *In-vitro* and *in-vivo* imaging of MMPs Activity

Abstract

Objective: The matrix metalloproteinase (MMP) family of proteins are principal enzymes in cartilage degradation during osteoarthritis (OA). Non-destructive detection of MMP activity could be useful in studies of OA pathogenesis, progression, and to evaluate intervention strategies. MMPSense750 is an *in-vivo* fluorimetric imaging probe with the potential to continuously and non-invasively trace real time MMP activities, but its use in OA-related research has not been reported. The objective of the current study is to investigate the use of MMPSense750 in OA imaging, using chondrocytes and cartilage explants in an *in-vitro* setting, and a mouse knee injury model for *in-vivo* imaging.

Design: We first determined the appropriate MMPSense concentration, assay time, and linear range using various concentrations of recombinant MMP-3, -9 and -13. Next we tested whether we could quantifiably image MMP activity in cytokine-treated chondrocytes, and bovine cartilage explants subjected to either mechanical injury or cytokine treatment *in-vitro*. Finally, we performed *in-vivo* imaging of a mouse model of post-traumatic OA to compare MMP activity in the injured versus contralateral knee.

Results: The best time to measure fluorescence intensity was highly dependent on the type of MMP enzyme. In cartilage explants, mechanical impact or cytokine treatment increased the fluorescent signal indicating elevated MMP activity. Injured knees of mice showed significantly higher fluorescent signal than uninjured knees 48 hours after injury.

Conclusions: MMPSense750 is a convenient tool to detect MMP activities for *in-vitro* study with cartilage, as well as *in-vivo* studies of knee injury, offering insight into the degradative processes within the joint.

Keywords: MMP activity, cartilage, mechanical injury, osteoarthritis, *in-vivo* imaging, fluorescent, MMPSense750

Introduction

Osteoarthritis (OA) is a degenerative disease of the articular joints characterized by cartilage degradation. The number of OA patients continues to increase, estimated at nearly 27 million in the United States[1], and at this time there is no effective treatment to prevent OA or restore joints after the onset of OA. Although OA pathogenesis is incompletely understood, it is generally accepted that the cartilage degradation is mediated by both mechanical forces and enzymatic activities.

Matrix metalloproteinases (MMPs) are a family of zinc-dependent degradative proteinases with principal roles in cartilage degradation that occurs during OA. MMP-mediated degradation of type II collagen fibrils is considered one of the first irreversible steps in OA pathogenesis (reviewed in [2]), and the presence of MMPs correlates with OA symptoms including joint effusion and pain[3, 4]. Therefore, quantitative and non-destructive detection of MMP activity could potentially be a powerful tool to study OA pathogenesis and evaluate therapeutic strategies.

Most studies investigating OA evaluate MMPs levels *in-vivo* or *in-vitro* with techniques such as ELISA[5-7] or Western Blotting,[7-9] and RT-PCR[10, 11] to estimate protein levels and mRNA expression[10, 11], respectively. However, these assays do not directly measure MMP activity and are not suitable for *in-vivo* use. MMP activity is generally measured using zymography[7, 11, 12], or more recently, fluorimetric MMP assays[7, 13]. While these techniques are broadly used and well established, known limitations of these assays include the necessary destruction and homogenization of the source tissues, and therefore the inability for repeated measurements on the same samples. As such, these assays of MMP activity are generally not suited for *in-vivo* imaging. In contrast, most of the imaging methods used in clinical situation for diagnosis or evaluation of OA are morphologic assessments like radiography[14], computed tomography (CT)[15], or MRI[14-16], which cannot

investigate the intensity of symptoms objectively. The development of a novel method to visualize MMP activities *in-vivo* hence may offer new insight into OA progression and treatment efficacy.

An *in-vivo* fluorimetric probe was recently developed that allows non-destructive imaging of activity from a broad spectrum of MMPs (MMPSense™ 750 FAST PerkinElmer, Inc., Boston, MA). It is a near-infrared fluorescent probe with a peak excitation at approximately 745nm and emission at 800nm. It is a peptide substrate that enables the detection of MMPs activities (i.e. MMP-2, -3, -7, -9, -12 and -13) by exhibiting fluorescent signal when cleaved by MMPs[17, 18]. Bioimaging with this reagent has the potential to continuously trace real time MMP activities non-invasively. It was reported that this probe can detect tumor progression[18] or ischemia reperfusion[17] *in-vivo*. However, though only one paper used MMPSense680 to assess the effect of circulating cells on MMP activities in rheumatoid arthritis[19], there is no previous report investigating the usability of MMPSense750 for the assessment of MMP activity in chondrocytes, in cartilage, or during OA progression.

The objective of the present study is to investigate the potential of MMPSense750 for research in OA, using *in-vitro* cultures of chondrocytes and cartilage explants, as well as an *in-vivo* mouse model of acute knee injury.

Methods

Assessment for optimal concentration of MMPSense750

We first wanted to determine the appropriate MMPSense750 concentration for *in-vitro* studies using purified recombinant MMPs. MMP-3, -9, and -13 were chosen based on their established importance in OA[20-22]. To achieve comparable results between the different enzymes, the amount of active enzyme in each assay was normalized using the

specific activity (Units of enzyme activity per weight) provided by the manufacturer. MMPSense750 was added to media containing the active proteases, the reactions were incubated at 37 °C, and the resulting fluorescent signal was measured at different time points.

Recombinant human MMP-9 and MMP-13 (Enzo Life Sciences, Farmingdale, USA) had identical unit definitions and assay buffers. The assay buffer consisted of 50mM HEPES, 10mM $CaCl_2$ and 0.05% Brij-35 at pH 7.5[23]. One Unit is defined by the manufacturer as the amount of enzyme that hydrolyzes 100pmol substrate (Ac-Pro-Leu-Gly-S-Leu-Leu-Gly-OEt) per minute at 37°C. The specific activity of the lots available to us were 66U/μg for MMP-9 and 51.5U/μg for MMP-13. These enzymes were used at 0.001, 0.01, 0.1, 1 and 10U per assay.

Recombinant human MMP-3 (Enzo Life Sciences, Farmingdale, USA) was reconstituted in assay buffer consisting of 50 mM sodium acetate, 10mM $CaCl_2$, 150mM NaCl and 0.05% Brij-35 at pH 6.0[2]. One Unit is defined by the manufacturer as the amount of enzyme that hydrolyzes 1μmol substrate (Mca-Arg-Pro-Lys-Pro-Val-Glu-Nva-Trp-Arg-Lys(DNP)-NH2) per minute at 37°C at pH 7.0. The lot available to us was 900mU/mg, we used 0.1, 1, 10 and 100mU per assay. Note the different unit definitions for MMP-3 compared to MMP-9 and -13. An equivalent substrate hydrolysis rate of 1nmol/minute requires 1mU of MMP-3 and 10U of MMP-9 and -13.

MMPSense750 was reconstituted in 1200μl sterile phosphate-buffered saline (Invitrogen) per vial of 24nmol as recommended, then added into the MMP solutions at 0.2, 0.7 and 2.0μM final concentration. Assays were performed in black 96-well plates, and imaging was performed on an IVIS-Spectrum imaging station using the appropriate filter sets. The time points were 0, 15, 30 and 60 minutes, 24, 48 and 72 hours after adding

MMPSense750. In between imaging time points, the plates were returned to a humidified 37°C incubator.

Cartilage Explants

Cartilage explants were harvested from the weight bearing area of femoral articular surfaces of bovine stifle knee joints purchased from a local slaughterhouse (Petaluma, CA). A 6mm dermal biopsy punch was used to isolate cartilage cylinders, which were then cut to 2mm height from the articular surface using a custom jig. Explants were cultured for 3 days in DMEM with 10% FBS and 1% penicillin-streptomycin (all from Invitrogen, Carlsbad, CA) at 37°C and 5% CO_2. Six joints were used, and 1 or 2 explants from each joint was randomly assigned to one of three treatment groups; IL-1β, mechanical injury, or control. There was no significant difference between the cartilage weights of each group for the IL-1β treatment (IL-1β: 62.4±4.4g, Ctrl: 65.1±4.1g, p=0.1767) or for the mechanical injury (Mech. Inj.: 63.9±4.9g, Ctrl: 65.1±4.1g, P=0.5604). The IL-1β group was treated with 10ng/ml IL-1β (R&D Systems, Minneapolis, MN). Media was replenished at day 3, with the IL-1β group also receiving fresh cytokine. At each time point (3 and 6 days of treatment), media from 10 explants from 6 donors were assayed for each treatment group. To quantify MMP activity in the culture media, 90μl of media were mixed with 10μl of MMPSense750 (0.7μM final concentration) and imaged as described above after 60 minutes and 24 hours.

Mechanical Injury

The explants in the mechanical injury group were mechanically compressed with an Instron 8511.20 digital servo-hydraulic mechanical testing device operated using displacement control. The explant was placed into the center of a custom-designed stainless steel well, and the thickness measured within 1μm precision by lowering a stainless steel

cylinder until it contacted the sample. A compressive preload of ~0.5N was applied, and then the explant was loaded to 30% strain at a strain rate of 100%/s, held at 30% strain for 100ms, then unloaded. Following compression, all loaded explants were transferred to fresh culture medium and returned to an incubator at 37 °C and 5% CO_2 until the termination of the experiment. In the control group, the explants were given a preload of ~0.5N and then returned to the culture media.

MMPSense Imaging of Explants

The culture media were collected from the explants at 3 days and 6 days after the mechanical injuries or IL-1β stimulation, and MMPSense750 was added to 0.7µM in an opaque 96-well plate. Imaging was performed at 60 minutes and 24 hours after adding MMPSense750, as described below. In a separate set of explants, MMPSense probe was added to the injured explants after 48 hours, and the cartilage explants imaged at day 3 after 24 hours exposure to the imaging probe.

Animal model of Joint Injury

Eight adult male BALB/cByJ mice (9-week-old at time of injury) were obtained from Jackson Laboratory (Bar Harbor, Maine). All animals were maintained and used in accordance with National Institutes of Health guidelines on the care and use of laboratory animals. This study was approved by our Institutional Animal Care and Use Committee (IACUC). The right knees of the mice were injured with a single mechanical compression as previously described in our PTOA model[24]. Briefly, the tibial compression system consists of two custom-built loading platens; the bottom platen that holds the knee flexed, and the top platen that holds the heel. The platens were aligned vertically and positioned within an electromagnetic materials testing machine (Bose ElectroForce 3200) (Eden Prairie, MN).

Mice were anesthetized using isoflurane inhalation, then the right leg of each mouse was subjected to a single dynamic axial compressive load (1mm/s loading rate) to a target compressive load of 12N. This loading method causes a transient anterior subluxation of the tibia, which injures the anterior cruciate ligament and leads to PTOA at 8 weeks later. The contralateral knees were used as uninjured control.

All mice received an intravenous injection of 2nmol of MMPSense750 via the orbital sinus at 24-hours post-injury, and IVIS imaging was performed 24 hours after the injection (48 hours post-injury). Mice were euthanized immediately after the imaging and both knees were dissected for isolation of total RNA and analysis of mRNA expression.

Quantitative real-time RT-PCR

Total RNA was extracted from injured and uninjured knees of 8 mice using the miRNeasy Mini Kit (Qiagen Valencia, CA) and reverse transcribed by the QuantiTect Reverse Transcription Kit (Qiagen). 2μl of cDNA was used for quantitative RT-PCR (in a final volume of 10μl) performed in triplicate in a 7900HT RT-PCR system with gene-specific probes according to the manufacturer's conditions. Results were normalized to 18s rRNA and calculated as fold-change in mRNA expression relative to the untreated control, using the $2^{-\Delta\Delta CT}$ method. The probes used are as follow: MMP-3 (Genbank: NM_133523; Primer 1: 5'-CTGTGGAGGACTTGTAGACTG-3', Primer 2: 5'-CTATTCCTGGTTGCTGCTCAT-3', Probe: 5'-/56-FAM/AGCATTGGC/ZEN/TGAGTGAAAGAGACCC/3IABkFQ/-3') (from Integrated DNA Technologies (IDT), Coralville IA); ; MMP-9 (Primer 1: 5'-CTGGAACTCACACGACATCTT-3', Primer 2: 5'-TCCACCYYGTTCACCTCATTT-3', Probe: 5'-/56-FAM/ACTCACACG/ZEN/CCAGAAGAATTTGCC/3IABkFQ/-3') (from IDT); MMP-13 (Primer 1: 5'-AGACTGGTAATGGCATCAAGG -3', Primer 2: 5'-GCCATTTCATGCTTCCTGATG -3', Probe:

5'-/56-FAM/AGGGCTGGG/ZEN/TCACACTTCTCTG/3IABkFQ/-3') (from IDT); 18s rRNA

(Catalog# 4319413E, Applied Biosystems).

<u>IVIS imaging</u>

An IVIS Spectrum imaging system (Perkin Elmer) was utilized to monitor

fluorescent signal of MMPSense750. For imaging of media cultured with cartilage explants,

the samples were placed in black plates. For *in-vivo* imaging of mice, the hairs from the

lower trunk and both legs were removed using Nair, and then imaging was performed

under general anesthesia by isoflurane inhalation. The excitation and emission

wavelengths were set to 745 and 800nm, respectively. The fluorescence intensities were

analyzed by Living Image software 4.2(Perkin Elmer). Grid type and circle type of regions of

interest (ROI) were set for plates and mice, respectively. Average radiant efficiency

$[p/s/cm^2/sr]$ / $[\mu W/cm^2]$ in the ROI was measured as an index of intensity of fluorescent

signal. For the experiment with MMP enzymes, normalized average radiant efficiency was

calculated by subtracting the value of average radiant efficiency with 0(m)U of MMPs from

that with each concentration of MMPs and used for the assessment. For the purpose of

clarity, we use the term "fluorescence intensity" to indicate normalized average radiant

efficiency in the ROI.

<u>Statistical analysis</u>

The results were statistically analyzed using a software package (GraphPad Prism;

MDF Software, Inc.). Values of all measurements were expressed as the mean with error

bars representing the 95% confidence interval. Correlation between MMP concentration

and MMPSense signal was evaluated with Pearson correlation coefficient. Differences of

MMPSense signal with MMP enzymes and *in-vivo* study were analyzed by paired t tests.

Comparison of MMPSense signal between different concentrations of MMPs, comparison of MMPSense signal with cartilage explants and comparison between cartilage explant weights among groups were analyzed by unpaired t test. Comparison of mRNA expression was analyzed by Wilcoxon signed rank test.

Results

Determination of the optimal MMPSense750 concentration for *in-vitro* experiment

We first used purified recombinant active MMPs to determine the assay's sensitivity and linear range, by varying the MMPSense probe concentration, MMP activities, and assay times. We used MMPSense750 at three different concentrations, 0.2, 0.7, and 2.0μM. At each concentration of MMPSense we added active MMP-3, -9 and -13, ranging from 0.0001 to 100U. The resulting fluorescence was imaged at multiple time points (0, 15, 30, 60 minutes, 24, 48, 72 hours after adding MMPSense750).

To analyze this data we first examined how well the normalized fluorescent signal correlated to the MMP activity at each time point. Pearson's correlation coefficients (R) were calculated for each combination of MMPSense and time, with an R^2 value above 0.8 considered a strong correlation and highlighted with shading (Figure 1). For all MMPs, the best correlation between MMP activity and fluorescent signal occurred at the higher concentrations of MMPSense probe, 2.0 or 0.7μM. Perhaps more surprisingly the best time to measure fluorescence intensity was highly dependent on the types of MMP enzyme. For MMP-13, high correlations were observed as early as 15 minutes, while MMP-3 started to become significant after 60 minutes, and MMP-9 not until after 24 hours. At the later time points (24, 48, 72 hours) the MMP activity and fluorescent signal were highly correlated for all three MMP enzymes.

We next estimated the detection limit of the assay at each concentration of MMPSense750 over time. For this, we statistically analyzed the differences between fluorescent intensity for each concentration increase of MMP, as indicated by the p-values between points in the graphs (Figure 2). The intermediate concentrations of MMP generated significantly different fluorescence signal in all conditions, but there were variations in the lower and upper detection limits. The lower detection limit, for MMP-13 a significant difference between 1 and 10U at 60 minutes was detected by 2µM of MMPSense but not by 0.7µM, but between 0.01 and 0.1U was detected by 0.7µM of MMPSense but not by 2µM. For MMP-9 a significant difference between 0.1 and 1U at 24 hours were detected by 0.7µM of MMPSense750 but not by 2µM. Differences of MMP-3 and MMP-13 were detectable at 60 minutes, but the differences in MMP-9 concentration were not significant until 24 hours after the addition of MMPSense probe.

With respect to the upper detection limit, we examined the fluorescent signal over time for each enzyme and the higher MMPSense probe concentrations (Figure 3). While higher concentrations of MMPSense yielded greater absolute fluorescence signals, the statistical analysis showed no benefit of the 2µM compared to 0.7µM MMPSense probe. Significant difference between 10 and 100mU of MMP-3 was detected at and after 30 or 60 minutes, 1 and 10U of MMP-9 at and after 24 hours and 10 and 100U of MMP-13 at and after 15 minutes. For MMP-3 and -13, the maximum fluorescence signal was obtained after 24 hours, suggesting perhaps that the enzymatic activity was depleted.

Taken together, these results indicate that 0.7µM of MMPSense750 at a 24 hour time point would yield the best assay, which could measure the activities of all three MMPs over the greatest range of concentrations. Time points shorter than one hour would selectively measure MMP-13 activity.

MMP Activity in IL-1β-treated Cartilage Explants

Having established a set of assay parameters using active recombinant MMPs, we next studied MMP activity in cartilage explants subjected to catabolic cytokine treatment. We chose IL-1β, since this is an important cytokine involved in the initiation and progression of OA. Bovine cartilage explants were cultured in control media or identical media supplemented with 10ng/ml of IL-1β. Media was collected after 3 and 6 days, and MMP activity in the media was assayed after 60 minutes and 24 hours subsequent to the addition of MMPsence750.

Three days of IL-1β treatment caused a significant increase in fluorescence intensity, indicating elevated MMP activity in the cartilage explant (Figure 4). Specifically, the fluorescence signal in culture media of the IL-1β group at day 3 was significantly greater than that of the control group both at 60 minutes and 24 hours after adding MMPSense750. At day 6, fluorescence intensity in the IL-1β-treated group was significantly greater than in the control group at 24 hours (but not 60 minutes) after adding MMPSense750.

MMP activity in mechanically injured cartilage explants

To assess MMPs activities produced by cartilage explants after mechanical injury, we rapidly applied a single 30% compressive strain onto the cartilage explants (100% strain/sec). Media was collected and assayed for MMP activity as described above for IL-1β-treated cartilage explants.

Mechanical injury caused a significant increase in fluorescence intensity, indicating elevated MMP activity in the culture media of cartilage explants (Figure 5). As observed with the IL-1β treatment, the fluorescence of the mechanical injury group at day 3 was significantly greater than that of the control group at both 60 minutes and 24 hours after

adding MMPSense750. At day 6, the trends are similar to the IL-1β treatment, with greater

fluorescence at the 24 hour, although this did not reach statistical significance.

MMP activity *in-vivo* after knee injury

We next determined whether we could image MMP activity in mouse knees after

injury, using our non-surgical joint injury model. To assess MMP activities in knee joints,

the mice were injured, then injected with MMPSense750 at 24 hours after injury, and

imaged at 24 hours after the injection. Injury caused a substantial increase in the

fluorescence intensity in the injured right knee relative to the uninjured left knee of the

same animal, indicating that injury increased the local MMP activity (Figure 6). We further

measured the mRNA expression of MMP-3, -9, and -13 immediately after the imaging was

completed. The results showed elevated mRNA expression of MMP-3 in the injured knee at

this time point (48 hours after injury), while the expression of MMP-9 and -13 were not

statistically different in the injured and contralateral limb at this time point (Figure 7).

In summary, using the MMPSense imaging reagent we have established assay

parameters to quantify the activity of multiple recombinant MMPs. Using these assay

parameters we used non-invasive imaging to demonstrate increased MMP activity secreted

by cartilage explants subjected to an inflammatory cytokine or mechanical injury, and

increased MMP activity in mouse knees 48 hours after injury.

Discussion

Imaging technologies used in OA primarily measure structural morphology rather

than the biological processes that contribute to joint degradation. In the present study, we

tested whether an *in-vivo* imaging reagent sensitive to MMP activity could be adapted for studying OA in cartilage explants subjected to cytokine treatment or mechanical injury, as well as for *in-vivo* imaging of MMP activity in injured mouse knee joints. The results demonstrate that the MMPSense750 reagent is useful for *in-vitro* studies of cartilage explants, provide insight into the parameters to consider when interpreting the data, and show a good response of the assay in a mouse model of joint injury.

The relationship between the activity of MMP-3, -9 and -13 and the fluorescent signal from MMPSense750 was investigated. With all MMPs tested, the fluorescent signal increased as the MMP activity increased. The activity of each enzyme was normalized, such that equivalent rates of substrate hydrolysis should occur in each assay. Interestingly, the reaction kinetics of the enzymes were different for the three MMPs tested. For example, recombinant MMP-13 caused a rapid increase in fluorescence within 15 minutes even at low enzyme concentrations, and longer incubations past 24 hours decreased the assay linearity. In contrast, MMP-9 required at least 24 hours to show a dose-dependent increase in substrate activation, and longer incubations out to 3 days improved the assay linearity. MMP-3 was intermediate, showing linear response after 1 hour out to 2 days, but decreasing at 3 days. The experiments were all performed within the reported tissue half-life of 72 hours for this reagent. MMPSense produces fluorescent signal upon MMP-mediated hydrolysis, and the discrepancy of the detection time between MMPs may suggest the kinetics of cleavage would differ between MMPs. We examined MMP-3, -9 and -13 in the current study, but according to the manufacturer MMPSense750 can also detect the activities of MMP-2, -7, and -12. In summary, it is important to recognize that a fluorescent signal indicates activities from multiple MMPs with differing sensitivities and reaction kinetics. Based on our results with recombinant MMP-3, -9, and -13, we selected *in-vitro*

assay parameters of 0.7μM MMPSense, and imaging at 60 minutes and 24 hours after adding MMPSense to adequately cover the activities of all three MMPs.

In cartilage explants, we detected increased MMP activity when the explants were treated with the catabolic cytokine IL-1β or subjected to mechanical injury. It is well known that IL-1β stimulates articular chondrocytes to produce MMPs[25, 26] and mechanical injury was reported to cause increased gene expression of MMPs in cartilage explants or articular chondrocytes [27, 28]. The current result supports this data and provides a novel non-destructive method to quantify the MMP activity. At day 6, significantly higher fluorescence was detected in the IL-1β group when compared with the control group, while there was no significant difference between the mechanical injury group and the control group at both 60 minutes and 24 hours after adding MMPSense. A possible reason for this difference could be the continuous presence of IL-1β during the 6 days, compared to a single mechanical injury at day 0.

The MMP activity in these cartilage experiments was measured from the culture media, and thus represents secreted MMP. We also tested whether we could use the MMPSense reagent to directly image the MMP activity within the matrix of the cartilage explants. However, these experiments were unsuccessful in that virtually no signal could be detected in any of the cartilage explants, and there was no difference between control explants and IL-1β-treated or injured explants. The excitation and emission wavelengths of this probe should both pass through the 2mm cartilage explant, but it is possible that the MMPSense reagent itself did not penetrate the cartilage matrix sufficiently within the 24 hours, although we did not test this directly. Alternate explanations could be that insufficient MMP activity was retained within the cartilage to produce a detectable signal.

We also tested MMPSense in monolayer human chondrocytes stimulated with IL-1β, lipopolysaccharide or TNF-α to elevate the expression of MMP-3, -9, and -13. However, we

were unable to measure an increase in fluorescent signal in monolayer culture, perhaps because MMP activity secreted by monolayer chondrocytes was below the MMPSense750 detection limit even with cytokine or lipopolysaccharide stimulation.

   In the *in-vivo* mouse model, injured knees showed significantly higher signals of MMPSense750 than the contralateral uninjured knees, indicating that injury elevated the MMP activities after 48 hours.   This provides a novel real-time non-destructive imaging method to quantify knee injury response and the progression of cartilage degradation and OA based on MMP activity. Interestingly, when we examined MMP mRNA expression at 48 hours after injury, we found that only MMP-3 was still elevated. In a separate study, we found that mRNA up-regulation of MMPs after injury peaked at 4 hours after injury and returned to baseline after 24 ours using the same animal model (data not shown). MMPs are secreted as inactive pro-enzymes that are later activated in the extracellular matrix, which may explain the apparent discrepancy between the mRNA expression and the protease activity.

   Joint injury clearly elevated MMP activity in the mouse model. In fact, in this study of white BALB/cByJ mice, the increase in signal intensity was more reproducible between individual mice than in similar experiments on black C57Bl/6 mice (data not shown), perhaps because the black mice often responded to hair removal by increased skin pigmentation. A limitation of the imaging technology is that we did not have sufficient resolution to determine the tissue source of MMP activity. It is likely that MMPs are active in multiple tissues, including cartilage, bone, and synovium. In our explant experiments we were able to detect MMP activity secreted by cartilage, but not within the cartilage itself. Based on these observations we expect that the *in-vivo* source of fluorescent signal might be joint tissues other than cartilage, although this does not preclude that the MMP activity is

secreted by the cartilage. In future experiments we would like to localize the source of MMP activity more precisely.

In conclusion, we established experimental parameters to use the MMPSense750 imaging reagent to quantify MMP activity *in-vitro* in cartilage explants, and *in-vivo* in a mouse joint injury model. The advantages of MMPSense750 over other techniques to evaluate MMP activity include its non-destructive nature, enabling repeated measurements on the same samples. This provides an imaging opportunity to monitor the destructive enzymatic processes that contribute to OA progression, and complements traditional imaging technologies such as MRI and CT that quantify the resulting structural changes.

Acknowledgements

Contributions

• Conception and design: TF, JNHY, DRH

• Analysis and interpretation of the data: TF, DRH

• Drafting of the article: TF, DRH

• Critical revision of the article for important intellectual content: TF, ET, JNHY, DRH

• Final approval of the article: TF, ET, JNHY, DRH

• Statistical expertise: TF, DRH

• Obtaining of funding: DRH

• Administrative, technical, or logistic support: JNHY, DRH

• Collection and assembly of data: TF, ET

Role of funding source

Competing interest statement

The authors declare that they have no competing interests.

References

1. Losina E, Weinstein AM, Reichmann WM, Burbine SA, Solomon DH, Daigle ME, et al. Lifetime risk and age at diagnosis of symptomatic knee osteoarthritis in the US. Arthritis Care Res (Hoboken) 2013; 65: 703-11.
2. Nagase H, Fields CG, Fields GB. Design and characterization of a fluorogenic substrate selectively hydrolyzed by stromelysin 1 (matrix metalloproteinase-3). J Biol Chem 1994; 269: 20952-7.
3. Cattano NM, Driban JB, Balasubramanian E, Barbe MF, Amin M, Sitler MR. Biochemical comparison of osteoarthritic knees with and without effusion. BMC Musculoskelet Disord 2011; 12: 273.
4. Mapp PI, Walsh DA, Bowyer J, Maciewicz RA. Effects of a metalloproteinase inhibitor on osteochondral angiogenesis, chondropathy and pain behavior in a rat model of osteoarthritis. Osteoarthritis Cartilage 2010; 18: 593-600.
5. Misko TP, Radabaugh MR, Highkin M, Abrams M, Friese O, Gallavan R, et al. Characterization of nitrotyrosine as a biomarker for arthritis and joint injury. Osteoarthritis Cartilage 2013; 21: 151-6.
6. Vaatainen U, Lohmander LS, Thonar E, Hongisto T, Agren U, Ronkko S, et al. Markers of cartilage and synovial metabolism in joint fluid and serum of patients with chondromalacia of the patella. Osteoarthritis and Cartilage 1998; 6: 115-24.
7. Lozito TP, Tuan RS. Endothelial cell microparticles act as centers of matrix metalloproteinsase-2 (MMP-2) activation and vascular matrix remodeling. Journal of Cellular Physiology 2012; 227: 534-49.
8. Williams A, Smith JR, Allaway D, Harris P, Liddell S, Mobasheri A. Carprofen inhibits the release of matrix metalloproteinases 1, 3 and 13 in the secretome of an explant model of articular cartilage stimulated with interleukin 1beta. Arthritis Res Ther 2013; 15: R223.
9. Pecchi E, Priam S, Mladenovic Z, Gosset M, Saurel AS, Aguilar L, et al. A potential role of chondroitin sulfate on bone in osteoarthritis: inhibition of prostaglandin E(2) and matrix metalloproteinases synthesis in interleukin-1beta-stimulated osteoblasts. Osteoarthritis Cartilage 2012; 20: 127-35.
10. Hufeland M, Schunke M, Grodzinsky AJ, Imgenberg J, Kurz B. Response of mature meniscal tissue to a single injurious compression and interleukin-1 in-vitro. Osteoarthritis Cartilage 2013; 21: 209-16.
11. Moon MH, Jeong JK, Lee YJ, Seol JW, Jackson CJ, Park SY. SIRT1, a class III histone deacetylase, regulates TNF-alpha-induced inflammation in human chondrocytes. Osteoarthritis Cartilage 2013; 21: 470-80.
12. Fuller ES, Smith MM, Little CB, Melrose J. Zonal differences in meniscus matrix turnover and cytokine response. Osteoarthritis Cartilage 2012; 20: 49-59.
13. Schure R, Costa KD, Rezaei R, Lee W, Laschinger C, Tenenbaum HC, et al. Impact of matrix metalloproteinases on inhibition of mineralization by fetuin. J Periodontal Res 2013; 48: 357-66.
14. Gudbergsen H, Lohmander LS, Jones G, Christensen R, Bartels EM, Danneskiold-Samsoe B, et al. Correlations between radiographic assessments and MRI features of knee osteoarthritis--a cross-sectional study. Osteoarthritis Cartilage 2013; 21: 535-43.
15. Hirvasniemi J, Kulmala KA, Lammentausta E, Ojala R, Lehenkari P, Kamel A, et al. In-vivo comparison of delayed gadolinium-enhanced MRI of cartilage and delayed quantitative CT arthrography in imaging of articular cartilage. Osteoarthritis Cartilage 2013; 21: 434-42.

16. van der Esch M, Knoop J, Hunter DJ, Klein JP, van der Leeden M, Knol DL, et al. The association between reduced knee joint proprioception and medial meniscal abnormalities using MRI in knee osteoarthritis: results from the Amsterdam osteoarthritis cohort. Osteoarthritis Cartilage 2013; 21: 676-81.

17. Barber PA, Rushforth D, Agrawal S, Tuor UI. Infrared optical imaging of matrix metalloproteinases (MMPs) up regulation following ischemia reperfusion is ameliorated by hypothermia. BMC Neurosci 2012; 13: 76.

18. Hollis CP, Weiss HL, Evers BM, Gemeinhart RA, Li T. In-vivo Investigation of Hybrid Paclitaxel Nanocrystals with Dual Fluorescent Probes for Cancer Theranostics. Pharm Res 2013.

19. Galligan CL, Fish EN. Circulating fibrocytes contribute to the pathogenesis of collagen antibody-induced arthritis. Arthritis Rheum 2012; 64: 3583-93.

20. Fuchs S, Skwara A, Bloch M, Dankbar B. Differential induction and regulation of matrix metalloproteinases in osteoarthritic tissue and fluid synovial fibroblasts. Osteoarthritis Cartilage 2004; 12: 409-18.

21. Chevalier X, Conrozier T, Gehrmann M, Claudepierre P, Mathieu P, Unger S, et al. Tissue inhibitor of metalloprotease-1 (TIMP-1) serum level may predict progression of hip osteoarthritis. Osteoarthritis Cartilage 2001; 9: 300-7.

22. Mitchell PG, Magna HA, Reeves LM, Lopresti-Morrow LL, Yocum SA, Rosner PJ, et al. Cloning, expression, and type II collagenolytic activity of matrix metalloproteinase-13 from human osteoarthritic cartilage. J Clin Invest 1996; 97: 761-8.

23. Edkins TJ, Alhadeff JA, Kwok V, Kalensky C, Rock MT, Vidmar TJ, et al. Development and validation of novel enzyme activity methods to assess inhibition of matrix metalloproteinases (MMPs) in human serum by antibodies against enzyme therapeutics. J Pharm Biomed Anal 2012; 70: 408-14.

24. Christiansen BA, Anderson MJ, Lee CA, Williams JC, Yik JH, Haudenschild DR. Musculoskeletal changes following non-invasive knee injury using a novel mouse model of post-traumatic osteoarthritis. Osteoarthritis Cartilage 2012; 20: 773-82.

25. Francioli S, Cavallo C, Grigolo B, Martin I, Barbero A. Engineered cartilage maturation regulates cytokine production and interleukin-1beta response. Clin Orthop Relat Res 2011; 469: 2773-84.

26. Campo GM, Avenoso A, Campo S, Ferlazzo AM, Altavilla D, Calatroni A. Efficacy of treatment with glycosaminoglycans on experimental collagen-induced arthritis in rats. Arthritis Res Ther 2003; 5: R122-31.

27. Lee JH, Fitzgerald JB, Dimicco MA, Grodzinsky AJ. Mechanical injury of cartilage explants causes specific time-dependent changes in chondrocyte gene expression. Arthritis Rheum 2005; 52: 2386-95.

28. Lu YC, Evans CH, Grodzinsky AJ. Effects of short-term glucocorticoid treatment on changes in cartilage matrix degradation and chondrocyte gene expression induced by mechanical injury and inflammatory cytokines. Arthritis Res Ther 2011; 13: R142.

Figure Legends

Figure 1

R^2 (R: Pearson correlation coefficient) as indices of correlation of the relationship between MMPs concentration and fluorescent signals at each time point were shown in tables and figures. R^2 greater than 0.8 were shown in the table with bold letters and shaded background.

Figure 2

Normalized average radiant efficiency from MMPs solution with several concentration at 60 minutes and 24 hours after adding 2, 0.7 or 0.2μM of MMPSense750 were shown in graphs. The normalized average radiant efficiency was calculated as difference from the value at 0(m)U. Representative IVIS imaging was shown below each graph with logarithmic scale for average radiant efficiency not normalized average radiant efficiency. Difference between the Normalized average radiant efficiency from MMPs solution with several concentration at 60 minutes and 24 hours after adding 2, 0.7 or 0.2μM of MMPSense750 were shown in graphs. The normalized average radiant efficiency was calculated as difference from the value at 0(m)U. Representative IVIS imaging was shown below each graph with logarithmic scale for average radiant efficiency not normalized average radiant efficiency. Difference between the adjacent normalized average radiant efficiency was analyzed statistically. (n=3) #: normalized average radiant efficiency of MMP concentration required for hydrolysis of equivalent substrate in 1 nmol/minute. (MMP-3: 1mU, MMP-9: 10U, MMP-13: 10U)

Figure 3

The normalized average radiant efficiency of the greatest and the second greatest concentration of each MMP with .7 or 2.0μM of MMPSense750. p-values vs. the second greatest concentrations (MMP-3: 10mU, MMP-9: 1U, MMP-13: 10U) at the same time points. (n=3)

Figure 4

The average radiant efficiency in culture media at day 3 of the IL-β group measured at 60 minutes and 24 hours after adding MMPSense was significantly greater than that of the control group. As for the media collected at day 6, the average radiant efficiency of the IL-1β group measured at 24 hours was significantly greater than the other, while there was no significant difference in the radiant efficiency measured at 60 minutes between the groups. Ctrl: control group. (n=10)

Figure 5

The average radiant efficiency in culture media at day 3 of the mechanical injury group measured at 60 minutes and 24 hours after adding MMPSense was significantly greater than that of the control group. As for the media collected at day 6, there was no significant difference in the average radiant efficiency measured at 60 minutes and 24 hours between the groups. M. Inj.: mechanical injury group, Ctrl: control group. (n=10)

Figure 6

A. Representative IVIS imaging at 48 hours after injury and 24 hours after MMPSense750 injection. The image is a merged picture of fluorescent signal in color and a grayscale picture of the mouse. Blue circles on both knees are regions of interest (ROI) with same shape and size as each other. The right knee (the left side in these pictures) is injured one. The maximum values are indicated in red, medium values in yellow to green, and the lowest values in dark blue in digital color-coded images.

B. Average radiant efficiency in injured knees was significantly higher than that in uninjured knees. (n=8)

Figure 7

mRNA expression of MMP-3 in injured knees were significantly greater than in uninjured knees. No significant difference in mRNA expression of MMP-9 and MMP-13 was shown between the injured and the uninjured knees. (n=8)

R^2 (R: Pearson Correlation Coefficient)

MMP-3

Assay	MMPSense Probe		
Time	2.0μM	0.7μM	0.2μM
0 min	0.0027	0.0033	0.0841
15 min	0.5007	0.3763	0.4709
30 min	0.747	0.6724	0.6559
60 min	**0.9263**	**0.9191**	0.7849
24 h	**0.9561**	0.955	**0.8159**
48 h	**0.9345**	**0.9413**	0.783
72 h	**0.9022**	**0.9247**	0.734
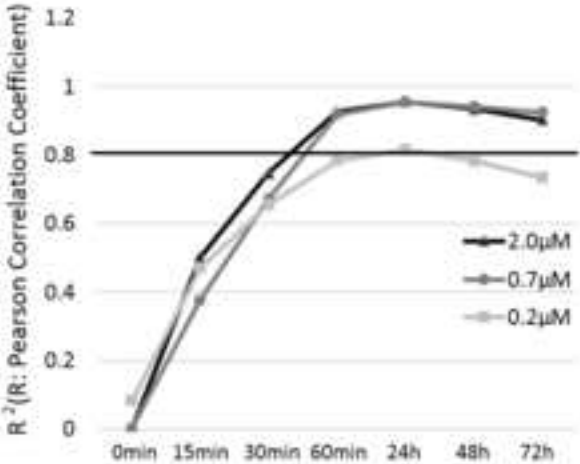
MMP-9

Assay	MMPSense Probe		
Time	2.0μM	0.7μM	0.2μM
0 min	0.1048	0.3791	0.3221
15 min	0.04475	0.1754	0.174
30 min	0.02352	0.2264	0.1958
60 min	0.1129	0.3184	0.257
24 h	**0.9824**	**0.9913**	**0.9682**
48 h	**0.9847**	**0.9964**	**0.9851**
72 h	**0.989**	**0.9966**	**0.986**
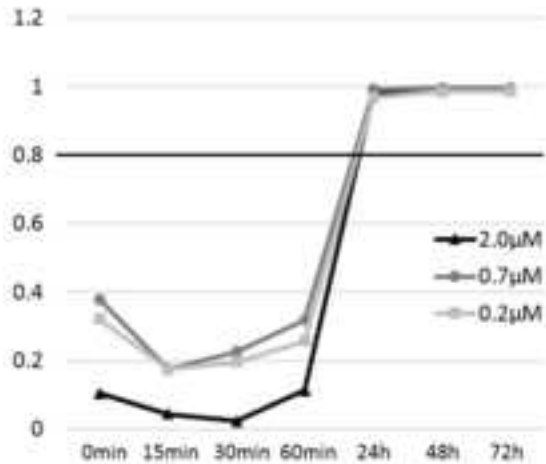
MMP-13

Assay	MMPSense Probe		
Time	2 μM	0.7 μM	0.2 μM
0 min	0.5005	0.5053	**0.827**
15 min	**0.9487**	**0.8453**	**0.8908**
30 min	**0.968**	**0.8625**	**0.9092**
60 min	**0.9607**	**0.8985**	**0.9155**
24 h	**0.9487**	**0.8453**	**0.8908**
48 h	**0.8552**	**0.8926**	0.6739
72 h	**0.8415**	**0.8152**	0.6852
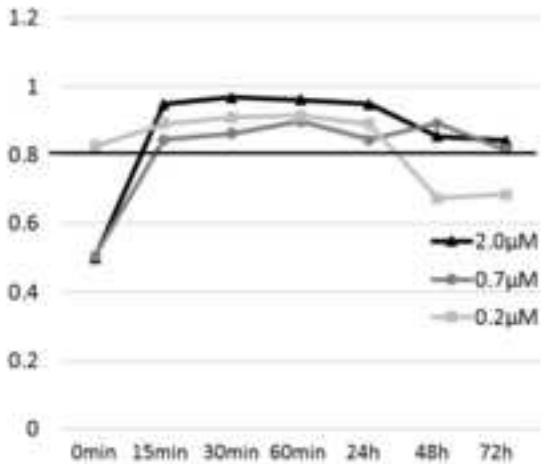
Figure2-1
Click here to download high resolution image
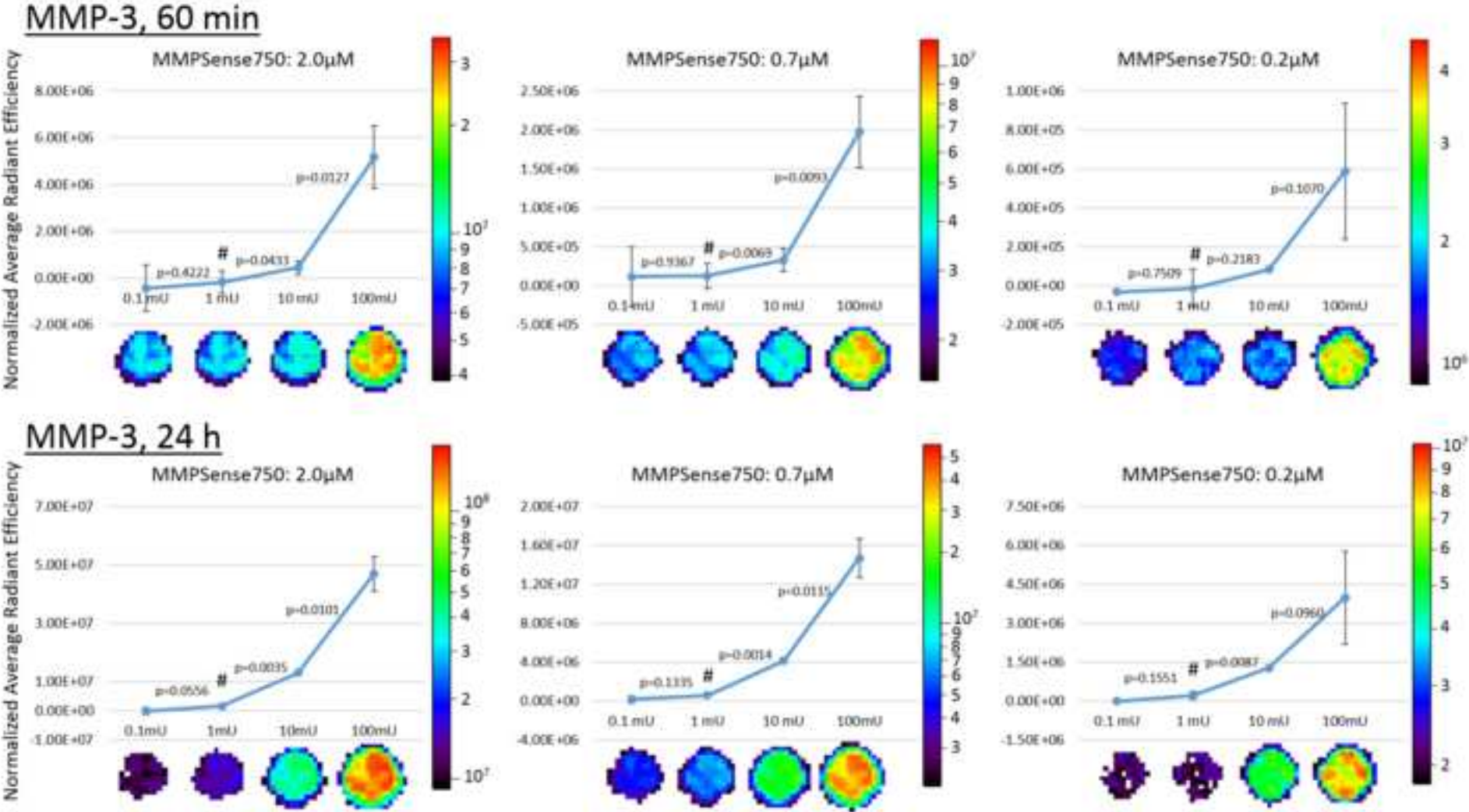
Figure2-2
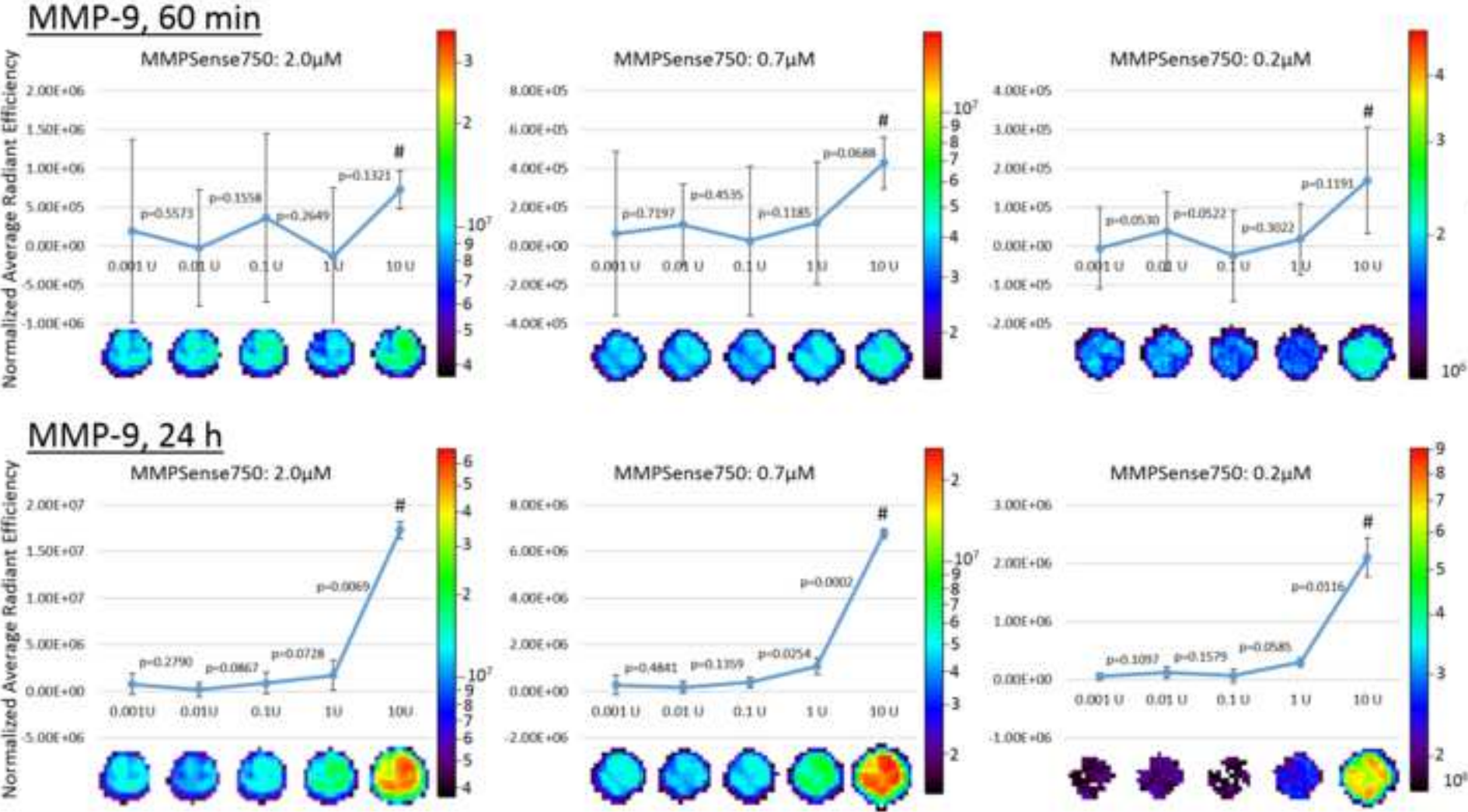
Figure2-3
Click here to download high resolution image

MMP-13, 60 min

MMP-13, 24 h
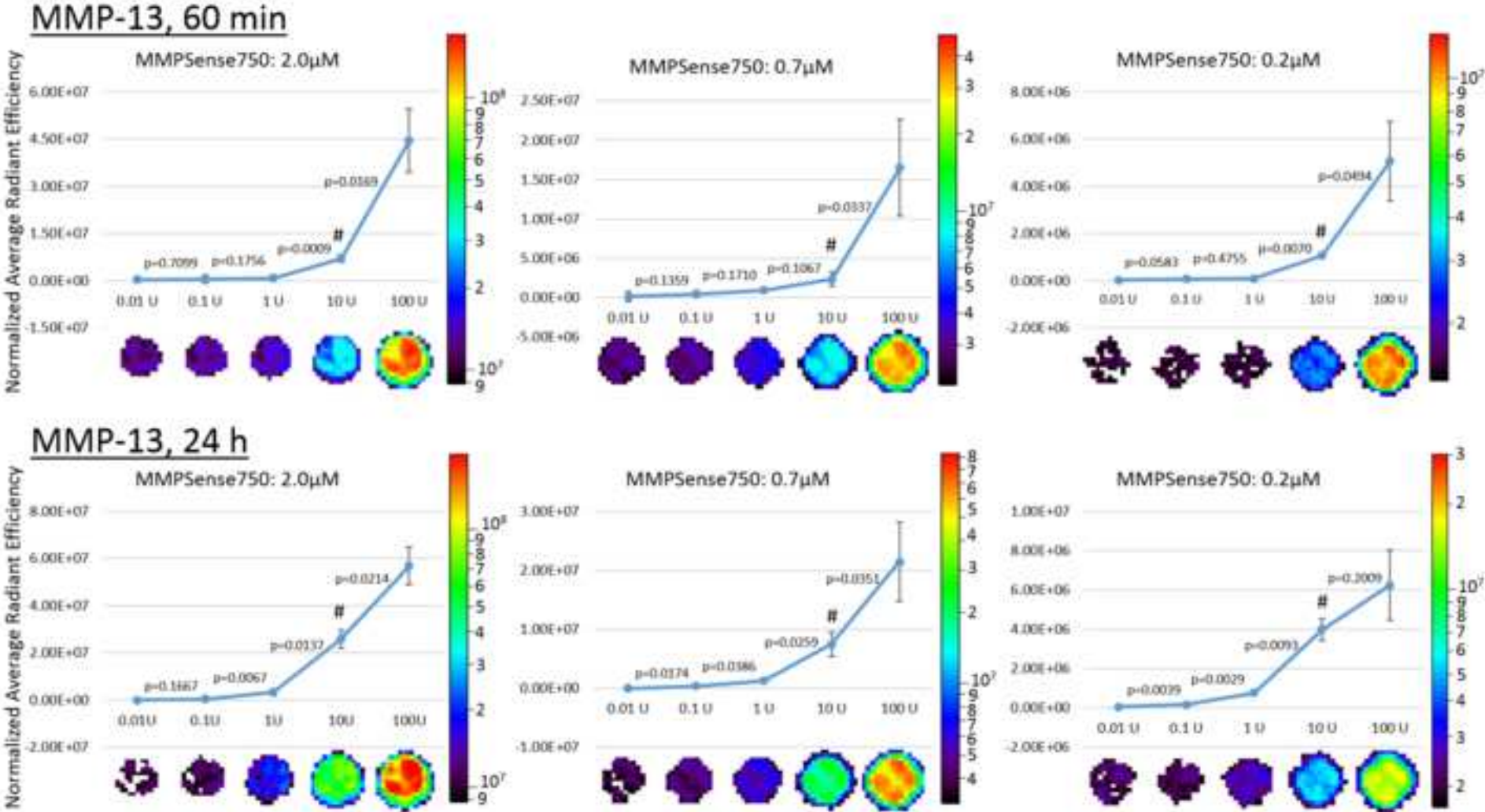
Figure3
Click here to download high resolution image

Figure3

Figure4
Click here to download high resolution image
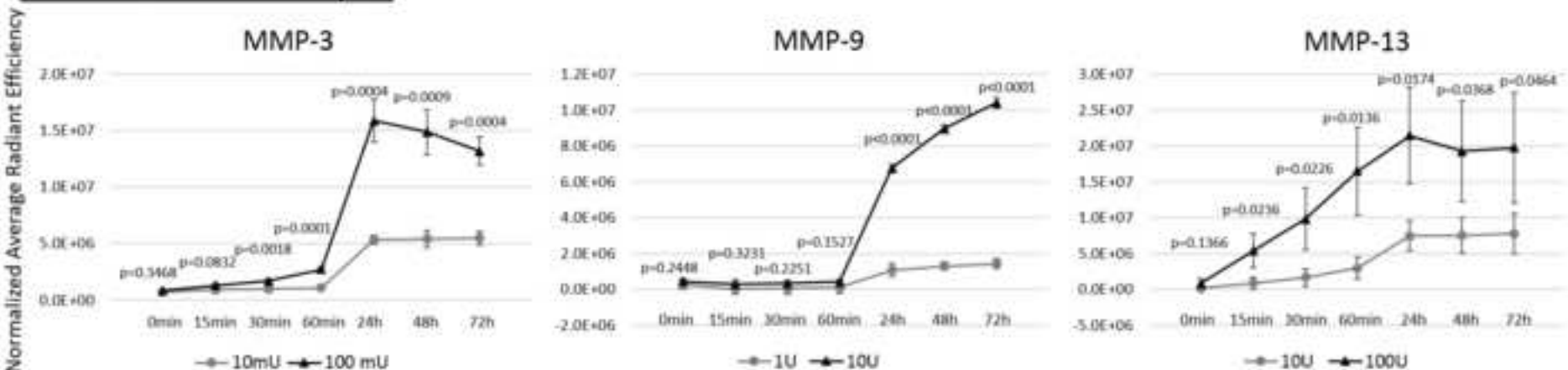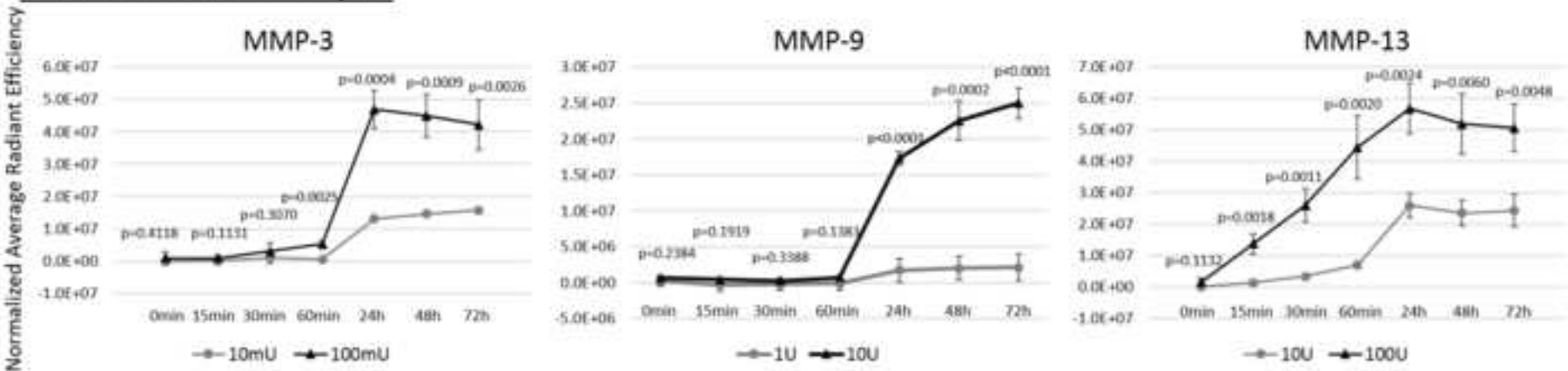
Cartilage explant: IL-1β vs Ctrl

Day 3, 60 min — p=0.0040 (IL-1β, Ctrl)

Day 3, 24 h — p<0.0001 (IL-1β, Ctrl)

Day 6, 60 min — p=0.9961 (IL-1β, Ctrl)

Day 6, 24 h — p=0.0040 (IL1-β, Ctrl)
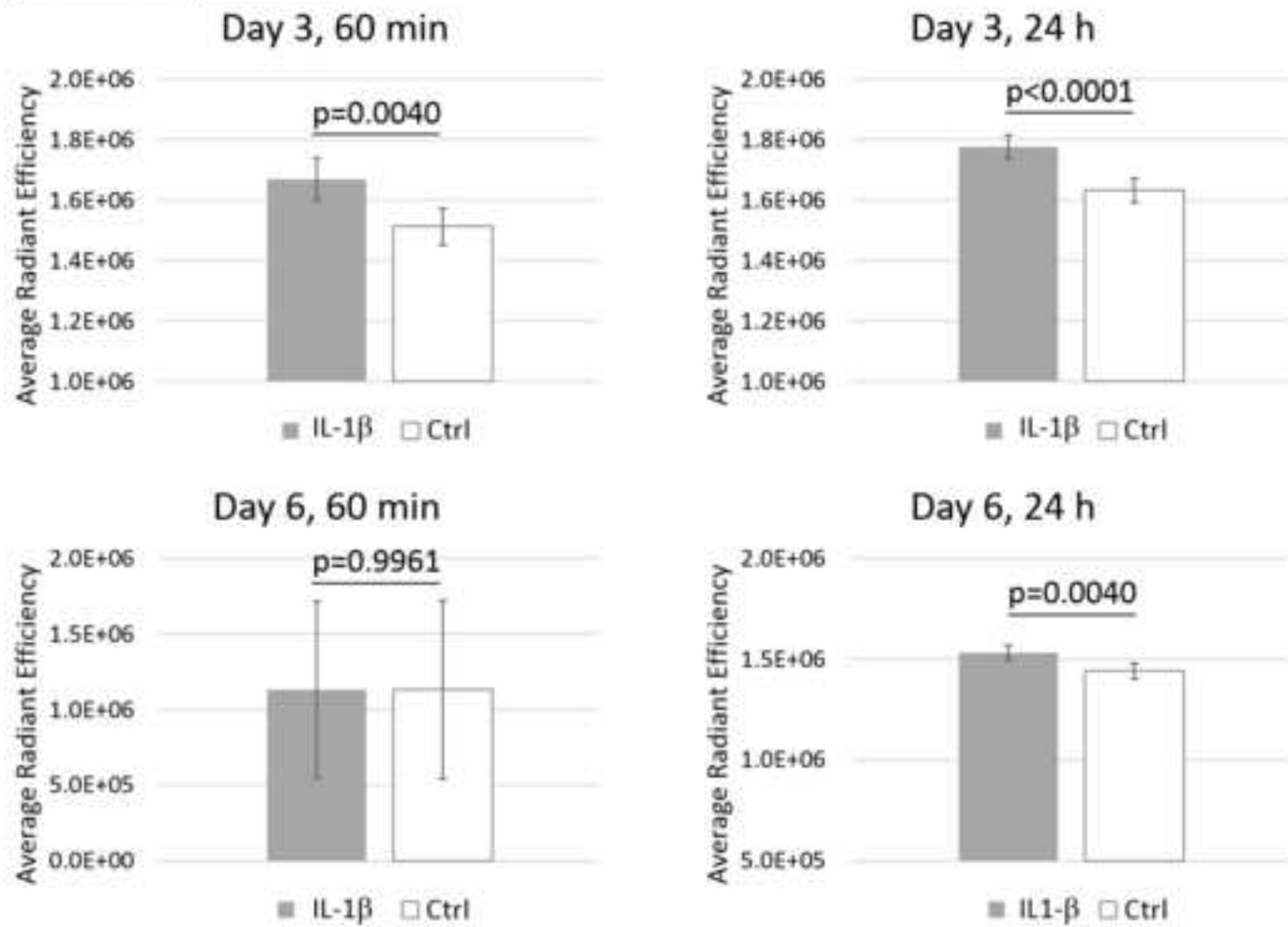
Cartilage explant: M. Inj. vs Ctrl

Figure6

Figure7
Click here to download high resolution image

Real time RT-PCR

UNIVERSITY OF CALIFORNIA, DAVIS

Department of Orthopaedic Surgery
Orthopaedic Research Laboratory

Dominik R. Haudenschild, PhD
Research Building 1 Suite 2000
4635 Second Avenue
Sacramento, CA 95817
Office: (916) 734-5015
Cell: (530) 746-8866
www.ucdmc.ucdavis.edu/orthopaedics

Dr. Stefan Lohmander
Editor-in-Chief,
Osteoarthritis and Cartilage

Dear Dr. Stefan Lohmander,

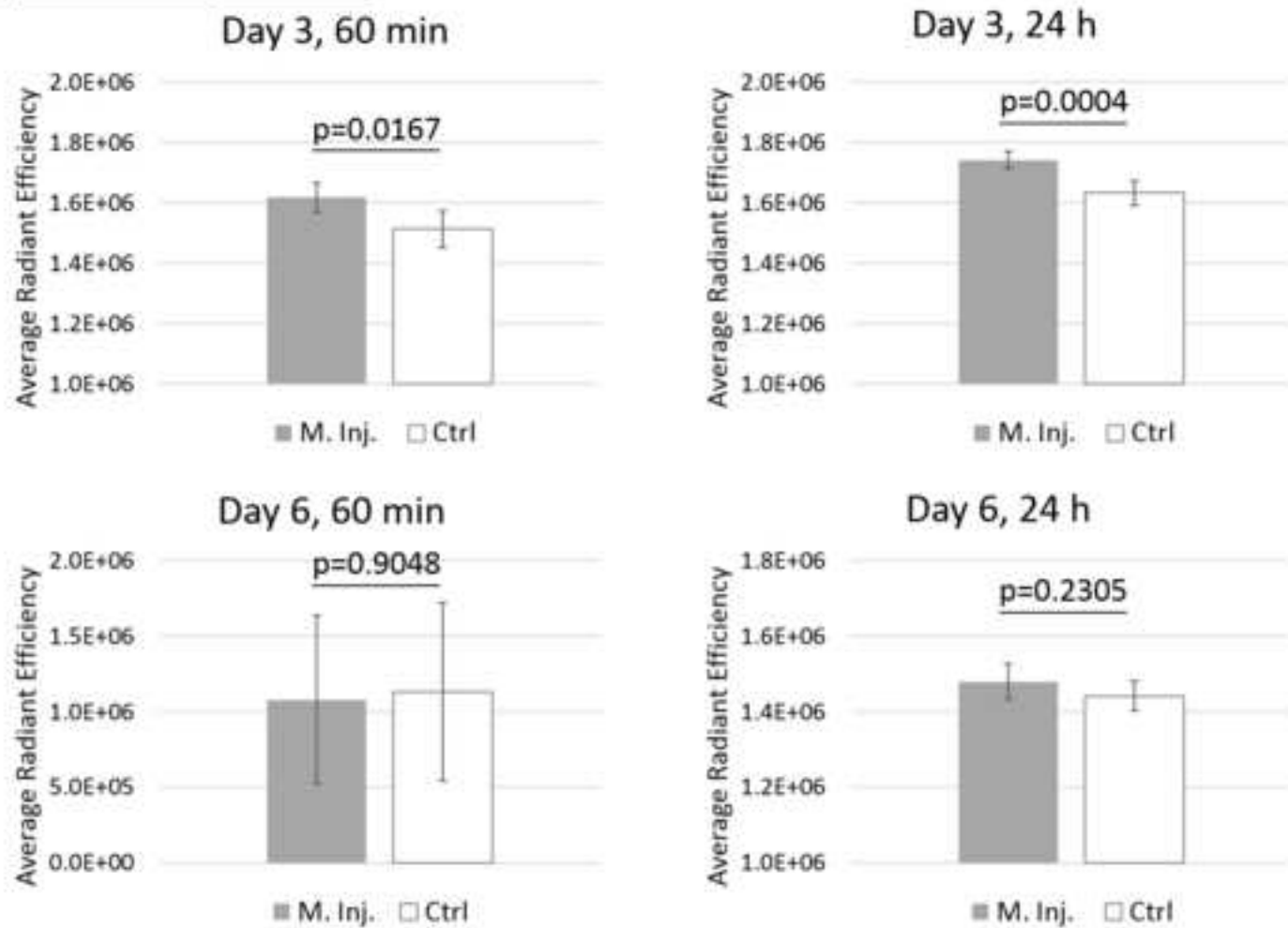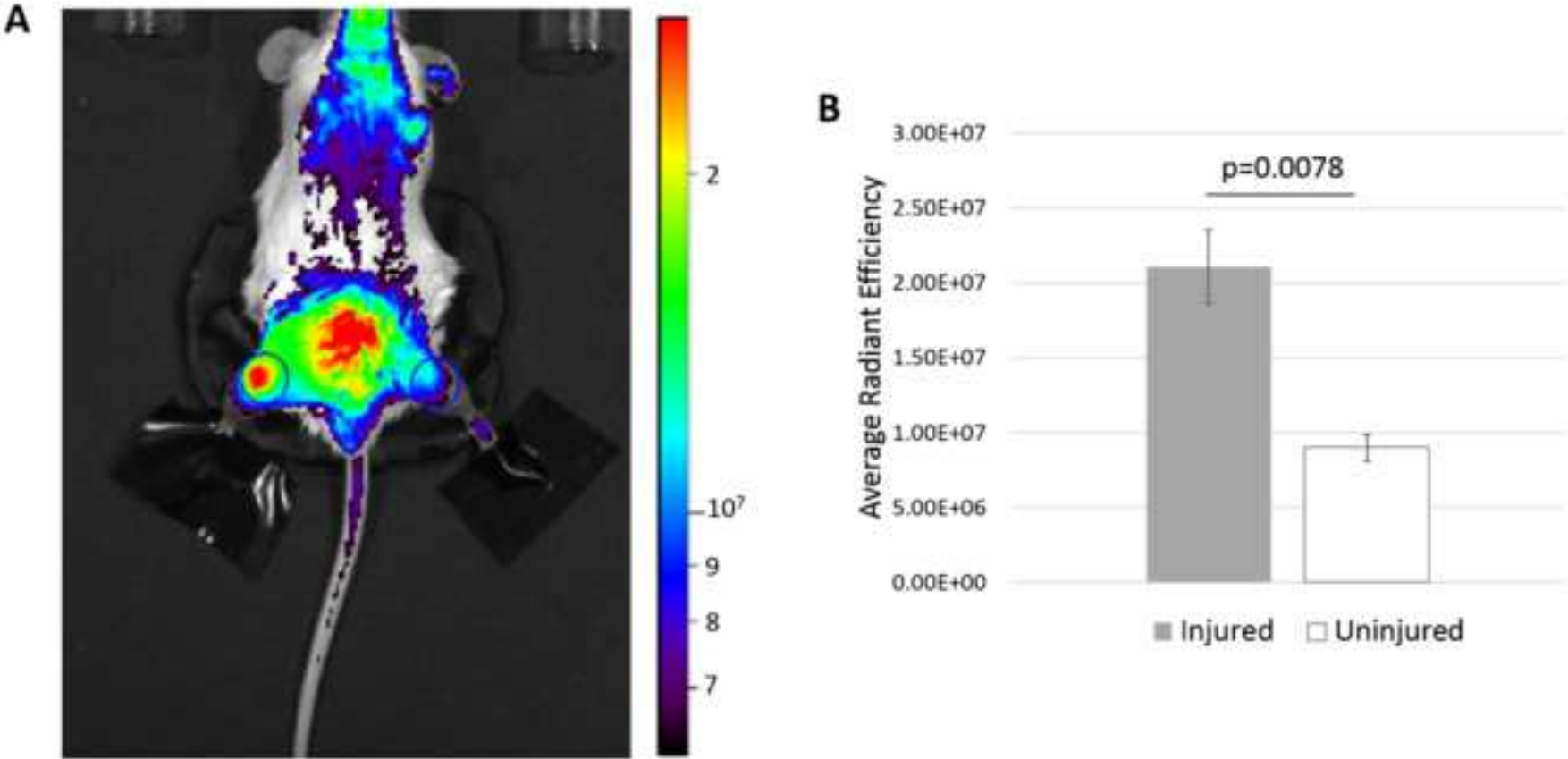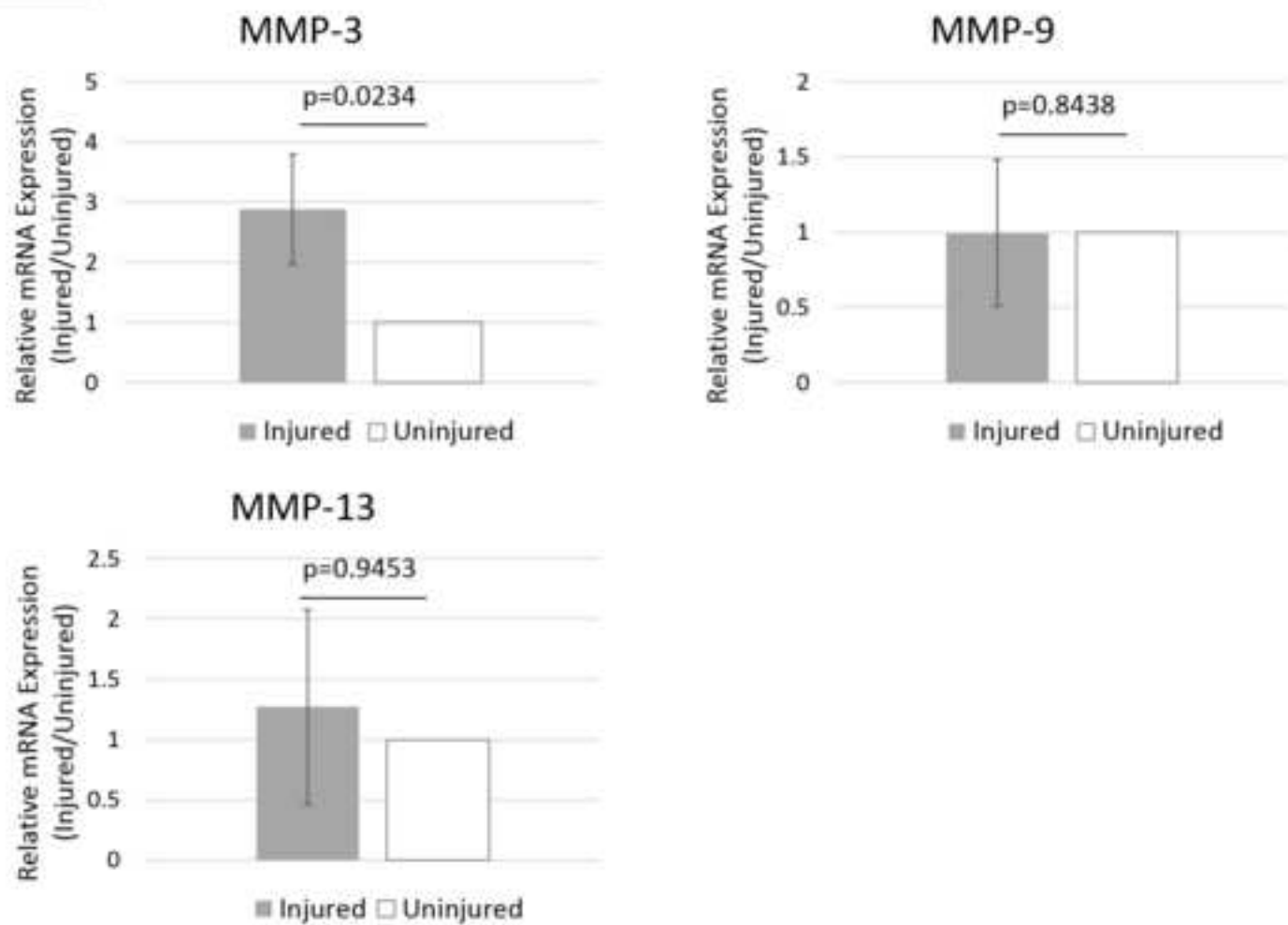My co-authors and I would like to submit an original manuscript entitled "**In-vitro and In-vivo Imaging of MMP Activity in Cartilage and Joint Injury**", which we prepared for publication in the special themed issue of "**Imaging in Osteoarthritis**" in the journal "**Osteoarthritis and Cartilage**".

In this manuscript we use functional imaging of MMP activity in cartilage explants subjected to mechanical impact or cytokine treatment, and in vivo in a mouse model of acute knee joint injury. We further characterize the sensitivity and reaction kinetics of the in-vivo imaging probe to various different OA-related MMP enzymes in-vitro. The development of a non-invasive assay to measure the degradative activity in joints and cartilage explants is an important contribution to the field of OA research, complementing existing imaging technologies that show the resulting structural changes.

The manuscript has been read and approved for submission by all authors. All persons listed as authors have contributed to preparing the manuscript and no person other than the authors listed have contributed significantly to its preparation. The contents of this manuscript are our original work and have not been published, in whole or in part, prior to or simultaneous with our submission of the manuscript to Osteoarthritis and Cartilage. All authors have no conflict of interest to report.

We thank you in advance for consideration of this manuscript.

Sincerely yours,

Dominik R. Haudenschild

Adult Reconstructive Surgery • Foot and Ankle Surgery • Hand, Upper Extremity and Microvascular Surgery • Oncology
Orthopaedic Research • Pediatric Surgery • Spine Surgery • Sports Medicine
Trauma and Post Trauma Reconstruction

Appendix 6 Page 95

OSTEOARTHRITIS AND CARTILAGE

AUTHORS' DISCLOSURE

Manuscript title __*In vitro* and *in vivo* imaging of MMP activity in cartilage and joint injury__

Corresponding author __Dominik R. Haudenschild__

Manuscript number _____

Authorship
All authors should have made substantial contributions to all of the following: (1) the conception and design of the study, or acquisition of data, or analysis and interpretation of data, (2) drafting the article or revising it critically for important intellectual content, (3) final approval of the version to be submitted. By signing below each author also verifies that he (she) confirms that neither this manuscript, nor one with substantially similar content, has been submitted, accepted or published elsewhere (except as an abstract).

Acknowledgement of other contributors
All contributors who do not meet the criteria for authorship as defined above should be listed in an acknowledgements section. Examples of those who might be acknowledged include a person who provided purely technical help, writing assistance, or a department chair who provided only general support. Such contributors must give their consent to being named. Authors should disclose whether they had any writing assistance and identify the entity that paid for this assistance.

Conflict of interest
At the end of the text, under a subheading "Conflict of interest statement" all authors must disclose any financial and personal relationships with other people or organisations that could inappropriately influence (bias) their work. Examples of potential conflicts of interest include employment, consultancies, stock ownership, honoraria, paid expert testimony, patent applications/registrations, and grants or other funding.

Role of the funding source
All sources of funding should be declared as an acknowledgement at the end of the text. Authors should declare the role of study sponsors, if any, in the study design, in the collection, analysis and interpretation of data; in the writing of the manuscript; and in the decision to submit the manuscript for publication. If the study sponsors had no such involvement, the authors should state this.

Studies involving humans or animals
Clinical trials or other experimentation on humans must be in accordance with the ethical standards of the responsible committee on human experimentation (institutional and national) *and* with the Helsinki Declaration of 1975, as revised in 2000. Randomized controlled trials should follow the Consolidated Standards of Reporting Trials (CONSORT) guidelines, and be registered in a public trials registry.

Studies involving experiments with animals were in accordance with institution guidelines

*Author Disclosure2

Please sign below to certify your manuscript complies with the above
requirements and then upload this form at http://ees.elsevier.com/oac/

Author Signature	Date	Author Signature	Date
[signature]	Jan 31, 2014		

OSTEOARTHRITIS AND CARTILAGE

AUTHORS' DISCLOSURE

Manuscript title __*In vitro* and *in vivo* imaging of MMP activity in cartilage and__
__joint injury__

Corresponding author __Dominik R. Haudenschild__

Manuscript number _____

Authorship

All authors should have made substantial contributions to all of the following: (1) the conception and design of the study, or acquisition of data, or analysis and interpretation of data, (2) drafting the article or revising it critically for important intellectual content, (3) final approval of the version to be submitted. By signing below each author also verifies that he (she) confirms that neither this manuscript, nor one with substantially similar content, has been submitted, accepted or published elsewhere (except as an abstract).

Acknowledgement of other contributors

All contributors who do not meet the criteria for authorship as defined above should be listed in an acknowledgements section. Examples of those who might be acknowledged include a person who provided purely technical help, writing assistance, or a department chair who provided only general support. Such contributors must give their consent to being named. Authors should disclose whether they had any writing assistance and identify the entity that paid for this assistance.

Conflict of interest

At the end of the text, under a subheading "Conflict of interest statement" all authors must disclose any financial and personal relationships with other people or organisations that could inappropriately influence (bias) their work. Examples of potential conflicts of interest include employment, consultancies, stock ownership, honoraria, paid expert testimony, patent applications/registrations, and grants or other funding.

Role of the funding source

All sources of funding should be declared as an acknowledgement at the end of the text. Authors should declare the role of study sponsors, if any, in the study design, in the collection, analysis and interpretation of data; in the writing of the manuscript; and in the decision to submit the manuscript for publication. If the study sponsors had no such involvement, the authors should state this.

Studies involving humans or animals

Clinical trials or other experimentation on humans must be in accordance with the ethical standards of the responsible committee on human experimentation (institutional and national) *and* with the Helsinki Declaration of 1975, as revised in 2000. Randomized controlled trials should follow the Consolidated Standards of Reporting Trials (CONSORT) guidelines, and be registered in a public trials registry.

Studies involving experiments with animals were in accordance with institution guidelines

Please sign below to certify your manuscript complies with the above
requirements and then upload this form at http://ees.elsevier.com/oac/

Author Signature	Date	Author Signature	Date
	1/31/2014		1/31/2014
	1/31/2014		

*ICMJE COI form TF
Click here to download ICMJE COI form: ocicmje_TF.pdf

*ICMJE COI form ET
Click here to download ICMJE COI form: ocicmje_ET.pdf

*ICMJE COI form JY
Click here to download ICMJE COI form: ocicmje_JY.pdf

*ICMJE COI form DRH
[Click here to download ICMJE COI form: ocicmje_DRH.pdf](ocicmje_DRH.pdf)

Title: In Vivo Fluorescence Reflectance Imaging to Quantify Sex-Based Differences in Protease, MMP, and Cathepsin K Activity in a Mouse Model of Post-Traumatic Osteoarthritis

Authors: [12]Patrick B. Satkunananthan (psatkun@ucdavis.edu), [1]Matthew J. Anderson (mjanderson@ucdavis.edu), [23]Nicole M. De Jesus (ndejesus@ucdavis.edu), [12]Dominik R. Haudenschild (drhaudenschild@ucdavis.edu), [23]Crystal M. Ripplinger (cripplinger@ucdavis.edu), [12]Blaine A. Christiansen (bchristiansen@ucdavis.edu)

Departments and Institutions:
[1]University of California-Davis Medical Center, Department of Orthopaedic Surgery
[2]University of California-Davis, Biomedical Engineering Graduate Group
[3]University of California-Davis Medical Center, Department of Pharmacology

Correspondence:
Blaine A. Christiansen, Ph.D.
UC Davis Medical Center
Department of Orthopaedic Surgery
4635 2nd Ave, Suite 2000
Sacramento, CA 95817
Phone: 916-734-3974
Fax: 916-734-5750
E-mail: bchristiansen@ucdavis.edu

Running Title: FRI Imaging in a Mouse Model of PTOA

Words: (4000 maximum)

Abstract (250 words maximum)

Objective: Post-traumatic osteoarthritis (PTOA) is a common long-term consequence of ACL rupture. Females are much more likely than males to sustain an ACL injury during increased activity, however males may have an increased tendency to develop PTOA following injury. In this study, we used in vivo fluorescence reflectance imaging (FRI) to quantify protease activity, MMP activity, and bone resorption in mice following ACL rupture. We hypothesized that these early processes of PTOA would be greater in male mice, resulting in more severe terminal PTOA.

Design: Male and female mice were injured via tibial compression overload, and FRI imaging was performed at multiple time points after injury using commercially available fluorescent tracers to quantify protease activity, MMP activity, and bone resorption in injured knees vs. uninjured knees. At 56 days post-injury, terminal PTOA was assessed using micro-computed tomography and whole-joint histology.

Results: Protease activity, MMP activity, and bone resorption were all significantly increased in injured knees relative to uninjured knees at nearly all time points, peaking at 1-7 days post-injury, then decreasing at later time points while remaining elevated relative to controls. No significant differences were observed between male and female mice for any time points using FRI, and no sex-based differences were observed in terminal PTOA at 56 days post-injury.

Conclusions: This study provides crucial information about the time course of inflammation and cellular activity in a translatable mouse model of knee injury, and may inform future studies aimed at targeting early inflammation to reduce the development of PTOA.

Key Words: fluorescence reflectance imaging, post-traumatic osteoarthritis, mouse model, inflammation, bone resorption

Introduction

Osteoarthritis (OA) is one of the primary musculoskeletal health concerns in the nation, affecting almost 27 million Americans [1]. Post-traumatic osteoarthritis (PTOA) is commonly observed within 10-20 years in individuals who sustain an anterior cruciate ligament (ACL) rupture [2-4]. And while female athletes are 4-6 times more likely than male athletes to sustain an ACL rupture during exercise or sports [5-8], studies of both humans and animal models suggest that males may have a greater tendency to develop PTOA following traumatic injury [9, 10]. However, the specific mechanisms contributing to this sex-related disparity are unknown.

Traumatic joint injuries initiate a surge of inflammatory cytokines, matrix metalloproteinases (MMPs), cathepsin proteases, and other degradative enzymes that contribute to cartilage and subchondral bone degeneration [2, 11, 12]. Detecting these early biological processes in animal models of OA typically involves analysis of blood serum or synovial fluid biomarkers, or destructive histological analysis of the joint. Non-invasive in vivo analysis of these processes would be beneficial due to rapid measurement time with relatively low cost, and the capability to perform repeated longitudinal measurements of the same animals at multiple time points. Additionally, non-invasive in vivo analyses preclude the possibility of inflammation or damage as a direct result of the sampling procedure.

Biomolecular imaging techniques such as fluorescence reflectance and bioluminescence imaging have become widely used for quantifying cellular activity by pairing specific pathways or processes with optical tracers that are cleaved simultaneously, producing a measurable signal that can be registered and quantified. These techniques have been extensively used for

applications such as studies of cancer and atherosclerosis [13-18]. They are also potentially useful for applications in skeletal biology, where optical probes can exclusively self-release by targeting markers of inflammation and bone turnover such as cathepsin proteases and matrix metalloproteinases (MMP), which have vital roles in processes such as OA progression. Commercially available fluorescent probes have been validated for use in musculoskeletal applications [14, 19-21]. However, we are unaware of any studies that have utilized these methods to directly measure osteoarthritic biomarkers as a method of quantification of disease severity or progression.

In this study, we used fluorescence reflectance imaging (FRI) along with conventional methods for quantifying articular cartilage and subchondral bone structure (whole joint histology and micro-computed tomography (µCT)) to quantify the time course of PTOA progression in male and female mice. We hypothesized that early inflammatory biomarkers and degradative processes would be elevated in male mice compared to females following traumatic joint injury, resulting in greater development of PTOA at terminal time points. This result would suggest potential mechanisms of sex-related disparities in PTOA progression. This study will also establish FRI imaging as a method for in vivo quantification of early biological processes in a mouse model of PTOA.

Methods

Animals

A total of 54 C57BL/6 mice (27 male, 27 female; 10 weeks old at the time of injury) were obtained from Harlan Sprague Dawley, Inc. (Indianapolis, IN, USA). Twenty-two mice (8

injured male, 8 injured female, 3 sham male, 3 sham female) were used for the ProSense portion

of the study, while sixteen mice (8 injured male, 8 injured female) were used for each of the

MMPSense and CatK portions. Animals were housed in a compliant facility at UCDMC for a 2-

week acclimation period prior to injury. All animals were maintained and used in accordance

with National Institutes of Health guidelines on the care and use of laboratory animals, and the

study was approved by our institutional Animal Studies Committee.

Tibial compression-induced knee injury

Mice were subjected to non-invasive ACL rupture induced by a single overload cycle of tibial

compression as previously described [22]. Briefly, after anesthetization via isoflurane inhalation,

mice were placed in a prone position in a materials testing system (Bose ElectroForce 3200,

Eden Prairie, MN, USA) with tibial compression loading platens (Fig. 1). A single dynamic axial

compressive load was applied at 1 mm/s to the right lower leg to a target compressive force of 12

N to produce ACL rupture. For uninjured mice, sham injury was performed by applying a 1-2 N

preload.

Fluorescent reflectance imaging via IVIS Spectrum

All mice were imaged on days 1, 3, 7, 14, 28, and 56 after injury using *in vivo* fluorescence

reflectance imaging in order to quantify levels of fluorescence from activated probes in injured

knees vs. uninjured knees. Three probes were used in this study: ProSense 680, MMPSense 680,

and CatK 680 FAST (Table 1; PerkinElmer, Waltham, MA). In previous studies, both

MMPSense and ProSense have been shown to localize to sites of inflammation [23, 24], while

CatK has been demonstrated to localize to sites of increased bone resorption and osteoclast activity [25].

Before each imaging time point (24 hours prior for ProSense 680 and MMPSense 680, and 6 hours prior for CatK 680 FAST), mice were anesthetized via isoflurane inhalation, and 10 μL (0.1 mg/kg) of probe was injected retroorbitally to each mouse. Hair was removed from the ventral aspect of both legs, and mice were imaged three at a time (22.5 cm field of view) in the imaging system (IVIS Spectrum, PerkinElmer, Waltham, MA). Each mouse was imaged twice at each time point in two different positions (left, right, or center; Fig.2A), and results from the two images were averaged for each mouse/time point. Mouse legs were positioned such that the anterior-medial aspect of the knees was approximately perpendicular to the epi-illumination source from the top of the imaging cube. The legs were taped down across the ankle, and image processing was performed via LivingImage software.

Filter selection was performed by the IVIS Spectrum after manually entering the excitation and emission wavelengths of each probe. The emission and excitation filters chosen by LivingImage were 675 (±35 nm) and 700 (±35) nm for all probes. The exposure times for each probe were as follows: ProSense 680 – 0.75 sec; MMPSense 680 – 0.75 sec; CatK 680 – 1 sec. Binning of pixels was set at the Medium option, to provide a balance of resolution and sensitivity for the images, while the F/Stop was set at a setting of 2, signifying a relatively wide aperture to allow for greater light collection of signal. Quantification of fluorescence brightness was performed by evaluating the *total radiant efficiency* of the signal within a uniform region of interest (ROI). The region of interest was a uniform circle of 12.3 mm^2 that was anatomically selected around the

knee on a grayscale photograph of the mice (Fig. 2B), such that the selection criteria were unbiased by the fluorescent signals. Subsequently, the total radiant efficiency of the injured knee was normalized against that of the contralateral uninjured knee of each mouse, to remove mouse-to-mouse variation in systemic delivery of fluorescent probes.

We also performed a statistical analysis to assess the effect of position within the imaging system (left, right, center) on the results obtained. We performed repeated-measures ANOVA on radiant efficiencies of mice imaged in the three positions, by delineating both the position on the stage and the position of a mouse leg with respect to the center as additional ordinal variables.

Micro-computed tomography analysis of epiphyseal trabecular bone and osteophyte formation:
Injured and uninjured knees from 8 male and 8 female mice from the MMPSense portion of the study were analyzed with micro-computed tomography (μCT 35, SCANCO, Brüttisellen, Switzerland) to quantify trabecular bone structure of the distal femoral epiphysis and osteophyte formation around the joint. All mice were sacrificed 56 days post-injury following the last time point for FRI imaging. Dissected limbs were fixed in 4% paraformaldehyde for 48 hours, then preserved in 70% ethanol. Knees were scanned according to the guidelines for μCT analysis of rodent bone structure [26] (energy = 55 kVp, intensity = 114 mA, 10 μm nominal voxel size, integration time = 900 ms). Analysis of trabecular bone in the distal femoral epiphysis was performed by manually drawing contours on 2D transverse slices; the distal femoral epiphysis was delineated as the region of trabecular bone enclosed by the growth plate and subchondral cortical bone plate (Fig. 3). Using the manufacturer's analysis software, we quantified trabecular bone volume per total volume (BV/TV), trabecular thickness (Tb.Th), trabecular separation

(Tb.Sp), trabecular number (Tb.N), bone tissue mineral density (Tissue BMD; mg HA/cm^3 BV), and apparent mineral density (Apparent BMD; mg HA/cm^3 TV). Osteophyte volume was calculated for each knee (Fig. 3). For this analysis, manual contours were drawn to quantify all mineralized tissue in and around the joint space, except naturally ossified structures (patella, fabella, anterior and posterior horns of the menisci).

Whole-joint histology of articular cartilage

Following μCT imaging, knees from 8 male mice and 8 female mice were analyzed with whole-joint histology to quantify cartilage and joint deterioration. Knee joints were decalcified for four days in 10% buffered formic acid, and processed for standard paraffin embedding. From each joint, 4 sagittal slices of 6 μm thickness were sectioned from the medial joint, separated by 250 μm. The medial joint was analyzed since this is the primary site of joint degeneration in our previous studies, and in studies by other investigators using similar models [22, 27]. Slides were stained with Safranin-O and Fast Green in order to assess proteoglycan content, articular cartilage degeneration, and overall joint integrity. Slides were blinded and graded by three independent readers using the semi-quantitative OARSI scale [27]. Grades were assigned to the medial tibial plateau and medial femoral condyle. Grades from the three readers were averaged for each section, and all gradable sections were averaged for each knee.

Statistical analysis

For all analyses, paired Student's t-tests were used within each experimental group in order to determine differences in injured vs. uninjured knees. Normalized ratios of total radiant efficiency of injured to uninjured joints were analyzed using two-way ANOVA in order to compare the

longitudinal changes in fluorescent signals in male vs. female mice. µCT data and histology data were compared between male and female mice using unpaired t-test. Differences were considered statistically significant at $p < 0.05$ for all tests. All data is presented as mean ± 95% confidence interval.

Results

FRI quantification of protease, MMP, and cathepsin K activity

Using fluorescence reflectance imaging (FRI), we were able to successfully detect increased inflammation and bone resorption in injured mouse knees compared to uninjured knees following non-invasive joint injury (Fig. 4). For both male and female mice, protease activity (ProSense 680), MMP activity (MMPSense 680), and osteoclastic bone resorption (CatK 680 FAST) were all significantly increased in the injured knee compared to the contralateral (uninjured) knee at all time points except day 3 for CatK males and days 7 and 28 for CatK females (Fig. 5; $p < .001$). Uninjured mice injected with ProSense did not exhibit differences between the right and left knees at any time points.

We were able to successfully establish a time course of activity for all fluorescent probes. Normalized fluorescence levels indicating inflammation (MMPSense and ProSense) were elevated approximately 50% from days 1 through 14, and decreased slightly at later time points while still remaining significantly elevated compared to uninjured limbs (above 1.0), indicating that inflammation is increased in injured joints relative to uninjured joints throughout the experimental period. The normalized data from the CatK probe proved to be much more variable. However, this is likely due to increases in CatK signal in both the injured and

uninjured knees (Fig. 5). A plot of non-normalized data shows a considerable increase in CatK fluorescent signal by day 3 in both knees of injured mice, which gradually decreased to steady state values by day 14. In general, ProSense 680 and CatK 680 FAST displayed the strongest fluorescent signals in both injured and uninjured knees. MMPSense produced the weakest signal, but normalized data from this probe exhibited the least variability, allowing us to demonstrate significant differences between injured and uninjured limbs ($p < .001$). No significant differences were observed between male and female mice for any of the probes at any of the time points.

Analysis of imaging positions within the IVIS Spectrum confirmed that there were significant differences in total radiant efficiency quantified between each of the respective position ($p < .001$). To account for this, mouse position was included as a factor in all statistical analyses. Future studies will utilize only one imaging position (center) in order to eliminate this confounding factor.

Micro-computed tomography of femoral epiphysis

MicroCT analysis of injured and uninjured joints at Day 56 revealed significant loss of trabecular bone in injured joints relative to uninjured joints, consistent with our previous findings [22, 28] (Fig. 6). However, we observed no significant difference between males and females in adaptation to injury, as changes between trabecular bone volume fraction (BV/TV), connectivity density (Conn.Dens), structural model index (SMI), trabecular number (Tb.N), trabecular thickness (Tb.Th), and trabecular separation (Tb.Sp) were similar for female and male mice at day 56. Additionally, we found no significant differences in osteophyte volume around the injured joint between female and male mice. We did, however, observe significant differences in

the absolute values of some trabecular bone parameters between male and female mice (not considering adaptation to injury). For example, males exhibited significantly higher connectivity density (p < .001) and trabecular number (p < .001) than females, while females exhibited significantly higher trabecular thickness (p < .001) and trabecular separation (p < .001) than male mice. This is consistent with previously published findings in mice [29].

Histological analysis of articular cartilage of the medial joint

Whole-joint histology of injured and uninjured knees revealed that injured knees exhibited considerable deterioration of articular cartilage and subchondral bone, often including full loss of thickness and erosion of subchondral bone, representative of severe progressive OA (Fig. 7). Degradation of cartilage extended down to subchondral bone causing bone-to-bone contact, seen by an extensive loss in Safranin-O staining along both the tibia and femur. Osteophyte formation was also observed on the tibia and femur, while the menisci were noticeably hypertrophied. The anterior portion of the tibial plateau was not noticeably damaged, while the posterior tibial plateau exhibited erosion extended down to the growth plate. This pattern of degeneration is similar to what we have seen previously at 12 and 16 weeks post injury [30]. Grading by three independent readers using the OARSI scale revealed significant differences between injured joints and uninjured control joints for both the tibial plateau (p < .001) and femoral condyle (p < .001). However, no significant difference was demonstrated between injured male joints and injured female joints.

Discussion

In this study, we used an integrated multi-modal imaging approach, including fluorescence reflectance imaging, histology, and µCT, to quantify the time course of the early biological response to traumatic joint injury in male and female mice in vivo using highly sensitive activatable fluorescent agents that quantify protease activity, MMP activity, and osteoclastic bone resorption in injured and uninjured knees. We were able to confirm significant differences between injured and uninjured joints using these methods, but contrary to our hypothesis, we observed no significant differences in between male and female mice.

This study establishes fluorescence reflectance imaging as an efficient and successful technique for in vivo quantification of joint-level biomolecular activity following traumatic injury. We were able to demonstrate that injured joints exhibited increased levels of protease activity, MMP activity, and cathepsin K activity compared to uninjured knees. ProSense 680 specifically targets cysteine proteases such as Cathepsins B, L, and S, while CatK solely targets Cathepsin K, and MMPSense targets the family of MMPs involved in inflammation. The family of cathepsins (excluding Cathepsin K) are well established in osteoarthritic progression, though they may not be the prime mechanism of chondrocyte deterioration or bone turnover [31-34]. Cathepsins B and D have been demonstrated to cleave aggrecan *in vitro*, but aggrecan deterioration at neutral pH has not been found to be blocked by cathepsin inhibitors, which may reveal that these cathepsins do not play a major role in pathological aggrecan degradation *in vivo*. However, Cathepsin K plays a major role in bone resorption and aggrecan degradation; it has been recognized as one of the most abundant and primary proteases in osteoclastic activity. Additionally, MMPs are the primary collagenolytic enzymes of osteoarthritic cartilage; MMP-13 is extremely active and MMP-3 is thought to be a collagenase activator [31], and MMP-9 is

highly responsible for initiating osteoclastic resorption by removing the collagenous layer from the bone surface before demineralization begins [35].

Interestingly, we observed increased Cathepsin K activity (osteoclastic bone resorption) in both injured and uninjured knees following knee injury. This is consistent with our previous study [22], which observed a loss of trabecular bone from the femoral epiphysis of contralateral knees by 7 days post-injury. Altogether, these data suggest a systemic loss of bone following a traumatic knee injury. The mechanisms of this systemic bone loss are currently unknown, but may include disuse, systemic inflammation, or utilization of bone calcium stores.

We were able to detect considerable changes in articular cartilage degeneration and subchondral bone turnover through histological analysis and μCT imaging 56 days after injury, including significant joint degeneration on the posterior medial tibial plateau. This is most likely due to the absence of an intact ACL, resulting in a decreased resistance to posterior femoral translation. These results are consistent with our previous studies, which demonstrated similar articular cartilage and bone degeneration at 12 and 16 weeks post-injury [28]. Unfortunately, we were unable to detect any differences in articular cartilage or subchondral bone degeneration between male and female mice. This may be due to examining a single time point (56 days post-injury), when severe terminal OA has been achieved. An intermediate time point may be useful for detecting sex-based differences in OA progression, similar to those observed previously [10]. Alternatively, there may in fact be no sex-based differences in PTOA development using this mouse model. If this is the case, then reported sex-based differences in PTOA progression in

human subjects following injury [9] may be due to mechanisms specific to humans, such as disparate body size or mechanical loading conditions.

Limitations of the in vivo imaging technique used in this study may have had a substantial effect on our capability to observe relatively small differences in fluorescence levels. Quantification of fluorescent signals using the IVIS Spectrum system exhibited large variance and a strong dependence on position of mice within the system. The IVIS Spectrum system produces a circular arc of light from the epi-illumination excitation light source above the stage. Because we imaged three mice at a time, only the centrally located mouse received direct illumination; the mice on the left and right sides received illumination at a skewed angle. An analysis of positional imaging helped elucidate this issue, and by performing a repeated-measures ANOVA on radiant efficiencies on mice imaged in different positions, we confirmed that there was a significant difference in brightness between each respective position on the stage, as well as the position of each leg, with respect to the center line. In addition, typical issues of autofluorescence and attenuation by tissue are continually a concern for imaging studies. In this respect, variations from mouse to mouse can make it difficult to quantify fluorescence with accuracy and reliability, as the depth of penetration of irradiated light can considerably differ. Future studies will minimize measurement variability by using only the center imaging position, however the precision of this imaging technique for detecting small differences in fluorescent signals remains in question.

Using commercially available fluorescent agents we were able to quantify the time course of protease activity, MMP activity, and osteoclastic bone resorption following traumatic injury to

the ACL, with noticeable peaks at early time points (1-7 days post-injury). By identifying this time course of activity, we are able to inform a "window of opportunity" in which treatments may be administered to most efficiently stall the progression of OA. Cathepsin and MMP inhibitors have both been utilized experimentally, both in the molecular and transcriptional pathways, as potential therapies for hindering OA progression [31]. Future studies could further investigate effective time periods for treatment in the murine model, which can then be extrapolated into larger animal models and human subjects.

Conclusions

Using in vivo fluorescence reflectance imaging, we were able to observe substantial increases in protease activity, MMP activity, and bone resorption in injured joints compared to uninjured joints in mice following traumatic knee injury. We successfully described a consistent time course of cellular activity, establishing FRI as a feasible method of quantifying OA progression in mice, although we were unable to detect differences between male and female mice using FRI, μCT, or histology. This study provides crucial information about the time course of inflammation and cellular activity in a translatable mouse model of knee injury, and may inform future studies aimed at targeting early inflammation to reduce the development of PTOA.

Acknowledgments

Author Contributions

All authors were fully involved in this study and in preparation of the manuscript.

Competing Interest Statement

The authors have no potential conflicts of interest to disclose.

References

1. Lawrence RC, Felson DT, Helmick CG, Arnold LM, Choi H, Deyo RA, et al. Estimates of the prevalence of arthritis and other rheumatic conditions in the United States. Part II. Arthritis Rheum 2008; 58: 26-35.

2. Lohmander LS, Englund PM, Dahl LL, Roos EM. The long-term consequence of anterior cruciate ligament and meniscus injuries: osteoarthritis. Am J Sports Med 2007; 35: 1756-1769.

3. Gillquist J, Messner K. Anterior cruciate ligament reconstruction and the long-term incidence of gonarthrosis. Sports Med 1999; 27: 143-156.

4. Myklebust G, Bahr R. Return to play guidelines after anterior cruciate ligament surgery. Br J Sports Med 2005; 39: 127-131.

5. Arendt E, Dick R. Knee injury patterns among men and women in collegiate basketball and soccer. NCAA data and review of literature. Am J Sports Med 1995; 23: 694-701.

6. Powell JW, Barber-Foss KD. Sex-related injury patterns among selected high school sports. Am J Sports Med 2000; 28: 385-391.

7. Hewett TE, Myer GD, Ford KR, Heidt RS, Jr., Colosimo AJ, McLean SG, et al. Biomechanical measures of neuromuscular control and valgus loading of the knee predict anterior cruciate ligament injury risk in female athletes: a prospective study. Am J Sports Med 2005; 33: 492-501.

8. Zelisko JA, Noble HB, Porter M. A comparison of men's and women's professional basketball injuries. Am J Sports Med 1982; 10: 297-299.

9.   Li RT, Lorenz S, Xu Y, Harner CD, Fu FH, Irrgang JJ. Predictors of radiographic knee osteoarthritis after anterior cruciate ligament reconstruction. Am J Sports Med 2011; 39: 2595-2603.

10.   van Osch GJ, van der Kraan PM, Vitters EL, Blankevoort L, van den Berg WB. Induction of osteoarthritis by intra-articular injection of collagenase in mice. Strain and sex related differences. Osteoarthritis Cartilage 1993; 1: 171-177.

11.   Madry H, Luyten FP, Facchini A. Biological aspects of early osteoarthritis. Knee Surg Sports Traumatol Arthrosc 2012; 20: 407-422.

12.   Goldring MB, Goldring SR. Osteoarthritis. J Cell Physiol 2007; 213: 626-634.

13.   Gounaris E, Tung C, Restaino C, Maehr R, Kohler R, Joyce JA, et al. Live Imaging of Cysteine-Cathepsin Activity Reveals Dynamics of Focal Inflammation, Angiogenesis, and Polyp Growth. PLoS ONE 2008; 3.

14.   Kozloff KM, Weissleder R, Mahmood U. Noninvasive optical detection of bone mineral. J Bone Miner Res 2007; 22: 1208-1216.

15.   Jaffer FA, Libby P, Weissleder R. Optical and multimodality molecular imaging: insights into atherosclerosis. Arterioscler Thromb Vasc Biol 2009; 29: 1017-1024.

16.   Jaffer FA, Weissleder R. Seeing within: molecular imaging of the cardiovascular system. Circ Res 2004; 94: 433-445.

17.   Jaffer FA, Kim DE, Quinti L, Tung CH, Aikawa E, Pande AN, et al. Optical visualization of cathepsin K activity in atherosclerosis with a novel, protease-activatable fluorescence sensor. Circulation 2007; 115: 2292-2298.

18.   Sheth RA, Mahmood U. Optical molecular imaging and its emerging role in colorectal cancer. Am J Physiol Gastrointest Liver Physiol 2010; 299: G807-820.

19. Kozloff KM, Volakis LI, Marini JC, Caird MS. Near-infrared fluorescent probe traces bisphosphonate delivery and retention in vivo. J Bone Miner Res 2010; 25: 1748-1758.

20. Kozloff KM, Quinti L, Tung C, Weissleder R, Mahmood U. Non-invasive imaging of osteoclast activity via near-infrared cathepsin-K activatable optical probe. J Musculoskelet Neuronal Interact 2006; 6: 353.

21. Kozloff KM, Quinti L, Patntirapong S, Hauschka PV, Tung CH, Weissleder R, et al. Non-invasive optical detection of cathepsin K-mediated fluorescence reveals osteoclast activity in vitro and in vivo. Bone 2009; 44: 190-198.

22. Christiansen BA, Anderson MJ, Lee CA, Williams JC, Yik JH, Haudenschild DR. Musculoskeletal changes following non-invasive knee injury using a novel mouse model of post-traumatic osteoarthritis. Osteoarthritis Cartilage 2012; 20: 773-782.

23. Nahrendorf M, Sosnovik DE, Waterman P, Swirski FK, Pande AN, Aikawa E, et al. Dual channel optical tomographic imaging of leukocyte recruitment and protease activity in the healing myocardial infarct. Circ Res 2007; 100: 1218-1225.

24. Gounaris E, Tung CH, Restaino C, Maehr R, Kohler R, Joyce JA, et al. Live imaging of cysteine-cathepsin activity reveals dynamics of focal inflammation, angiogenesis, and polyp growth. PLoS One 2008; 3: e2916.

25. Hoff BA, Chughtai K, Jeon YH, Kozloff K, Galban S, Rehemtulla A, et al. Multimodality imaging of tumor and bone response in a mouse model of bony metastasis. Transl Oncol 2012; 5: 415-421.

26. Bouxsein ML, Boyd SK, Christiansen BA, Guldberg RE, Jepsen KJ, Muller R. Guidelines for assessment of bone microstructure in rodents using micro-computed

tomography. Journal of bone and mineral research : the official journal of the American Society for Bone and Mineral Research 2010; 25: 1468-1486.

27. Glasson SS, Chambers MG, Van Den Berg WB, Little CB. The OARSI histopathology initiative - recommendations for histological assessments of osteoarthritis in the mouse. Osteoarthritis Cartilage 2010; 18 Suppl 3: S17-23.

28. Lockwood KA, Chu BT, Anderson MJ, Haudenschild DR, Christiansen BA. Comparison of loading rate-dependent injury modes in a murine model of post-traumatic osteoarthritis. J Orthop Res 2013; 32: 79-88.

29. Glatt V, Canalis E, Stadmeyer L, Bouxsein ML. Age-related changes in trabecular architecture differ in female and male C57BL/6J mice. J Bone Miner Res 2007; 22: 1197-1207.

30. Lockwood KA, Chu BA, Anderson MJ, Haudenschild DR, Christiansen BA. Comparison of loading rate-dependent injury modes in a murine model of post-traumatic osteoarthritis. Journal of Orthopaedic Research 2013; In Press.

31. Troeberg L, Nagase H. Proteases involved in cartilage matrix degradation in osteoarthritis. Biochim Biophys Acta 2012; 1824: 133-145.

32. Woessner JF, Jr. Purification of cathepsin D from cartilage and uterus and its action on the protein-polysaccharide complex of cartilage. J Biol Chem 1973; 248: 1634-1642.

33. Fosang AJ, Neame PJ, Last K, Hardingham TE, Murphy G, Hamilton JA. The interglobular domain of cartilage aggrecan is cleaved by PUMP, gelatinases, and cathepsin B. J Biol Chem 1992; 267: 19470-19474.

34.   Hembry RM, Knight CG, Dingle JT, Barrett AJ. Evidence that extracellular cathepsin D is not responsible for the resorption of cartilage matrix in culture. Biochim Biophys Acta 1982; 714: 307-312.

35.   Logar DB, Komadina R, Prezelj J, Ostanek B, Trost Z, Marc J. Expression of bone resorption genes in osteoarthritis and in osteoporosis. J Bone Miner Metab 2007; 25: 219-225.

Figure Legends

Figure 1: Schematic of tibial compression setup for non-invasive knee injury. Mice were subjected to non-invasive ACL rupture induced by a single overload cycle of tibial compression. A single dynamic axial compressive load was applied at 1 mm/s to the right lower leg to a target compressive force of 12 N to produce ACL rupture. For uninjured mice, sham injury was performed by applying a 1-2 N preload.

Figure 2: (A) Imaging positions for mice in the IVIS Spectrum system. Each mouse was imaged twice at each time point in two different positions, and results from the two images were averaged for each mouse/time point. (B) Regions of interest for quantifying fluorescent signals in each knee. The region of interest was a uniform circle of 12.3 mm^2 that was anatomically selected around the knee on a grayscale photograph of the mice, such that the selection criteria were unbiased by the fluorescent signals.

Figure 3: (Left) Trabecular bone volume of interest from the femoral epiphysis. (Right) Uninjured and injured mouse knees at 56 days post-injury. Considerable osteophyte formation and joint degeneration are apparent on the injured knee.

Figure 4: Representative fluorescent images of male and female mice imaged with each of the fluorescent tracers at 3 and 14 days post-injury. For both male and female mice, protease activity (ProSense 680), MMP activity (MMPSense 680), and osteoclastic bone resorption (CatK 680

FAST) were all significantly increased in the injured knee compared to the contralateral (uninjured) knee at nearly all time points.

Figure 5: (Left column) Normalized time course of total radiant efficiency (injured knee/uninjured knee) for the three probes. (Right column) Measured total radiant efficiency values from each probe, with male and female data combined. Normalized fluorescence levels indicating inflammation (MMPSense and ProSense) were elevated approximately 50% from days 1 through 14, and decreased slightly at later time points while still remaining significantly elevated compared to uninjured limbs (above 1.0), indicating that inflammation is increased in injured joints relative to uninjured joints throughout the experimental period. CatK 680 FAST signals were increased in both the injured and uninjured knees at days 3-7, suggesting a systemic bone loss at these time points. All data presented as mean ± 95% confidence interval.

Figure 6: MicroCT analysis of femoral epiphysis trabecular bone structural parameters from injured and uninjured joints and osteophyte volume (injured joints only) from male and female mice at 56 days post-injury. Consistent with our previous studies, we observed significant loss of trabecular bone in injured joints relative to uninjured joints. However, we observed no significant difference for any parameters between males and females in adaptation to injury. All data presented as mean ± 95% confidence interval. * Injured vs. uninjured ($p < 0.05$), # Male vs. female ($p < 0.05$).

Figure 7: Whole-joint histology of the medial aspect of injured and uninjured joints. Injured knees at 56 days post-injury exhibited considerable deterioration of articular cartilage and

subchondral bone, often including full loss of thickness and erosion of subchondral bone,

representative of severe progressive OA. The anterior portion of the tibial plateau was not

noticeably damaged, while the posterior tibial plateau exhibited erosion extended down to the

growth plate. Articular cartilage grading revealed severe OA on both the tibial plateau and

femoral condyle. However, no significant difference was demonstrated between injured male

joints and injured female joints. All data presented as mean ± 95% confidence interval. * Injured
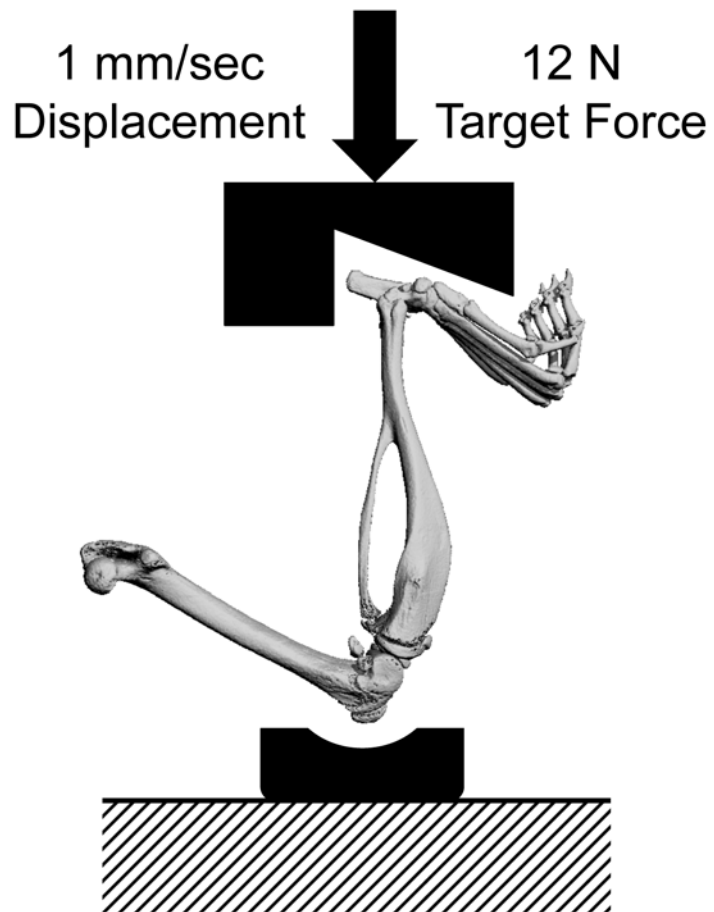
vs. uninjured ($p < 0.05$).
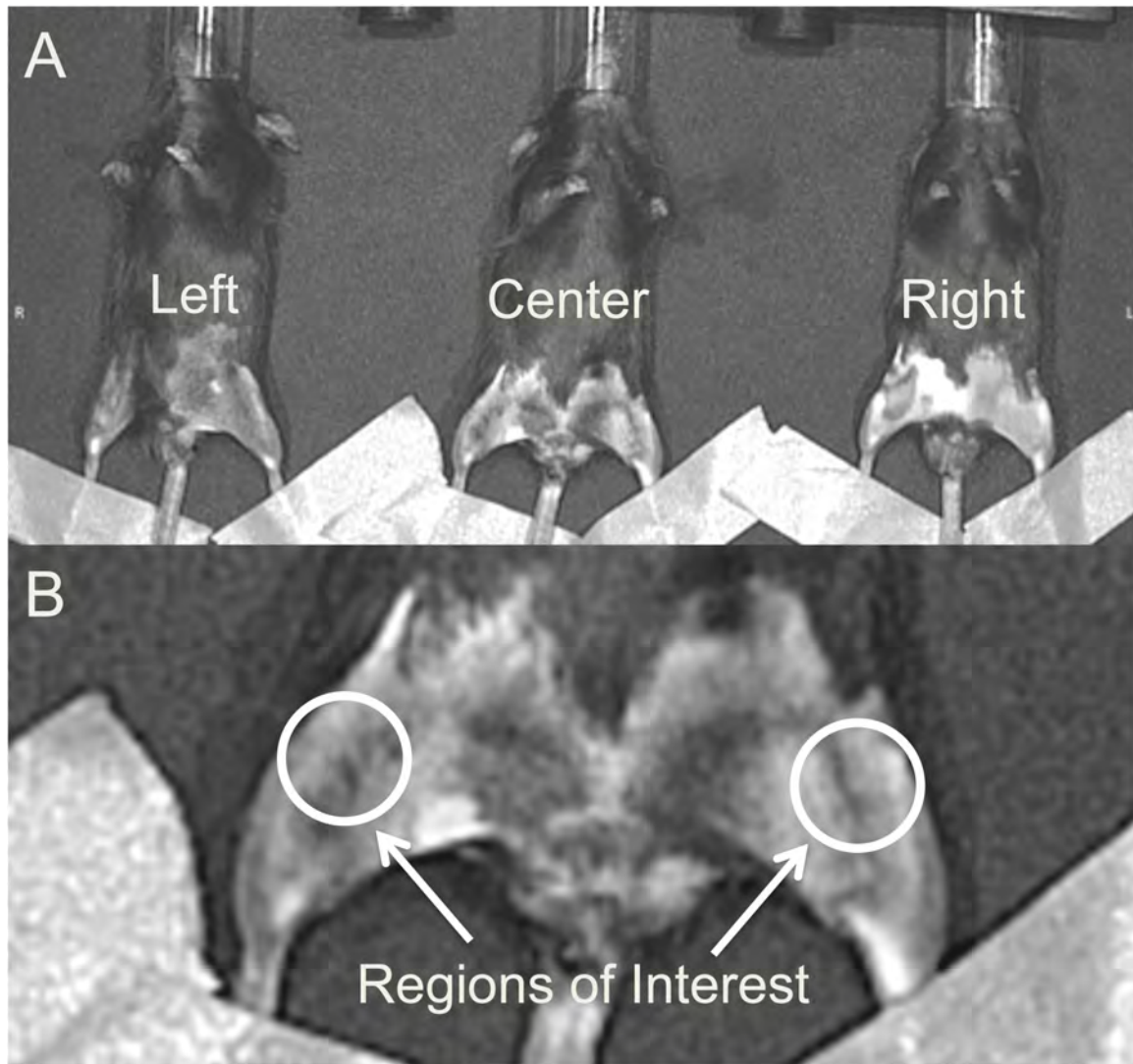
Figure 1

1 mm/sec Displacement
12 N Target Force

Figure 2

A — Left, Center, Right

B — Regions of Interest
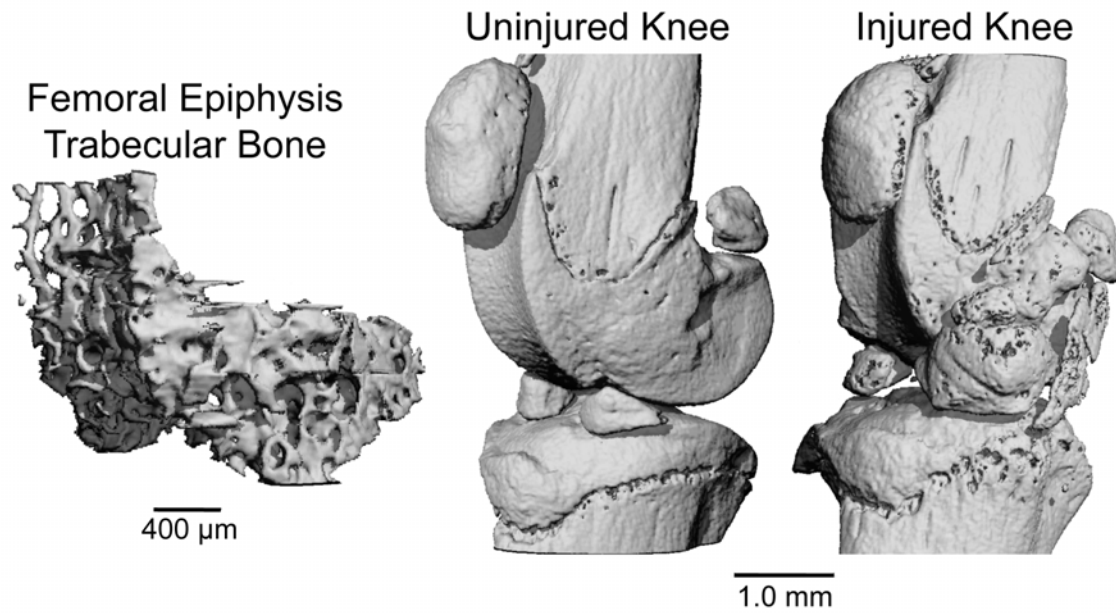
Figure 3

Femoral Epiphysis
Trabecular Bone

400 μm

Uninjured Knee

Injured Knee

1.0 mm
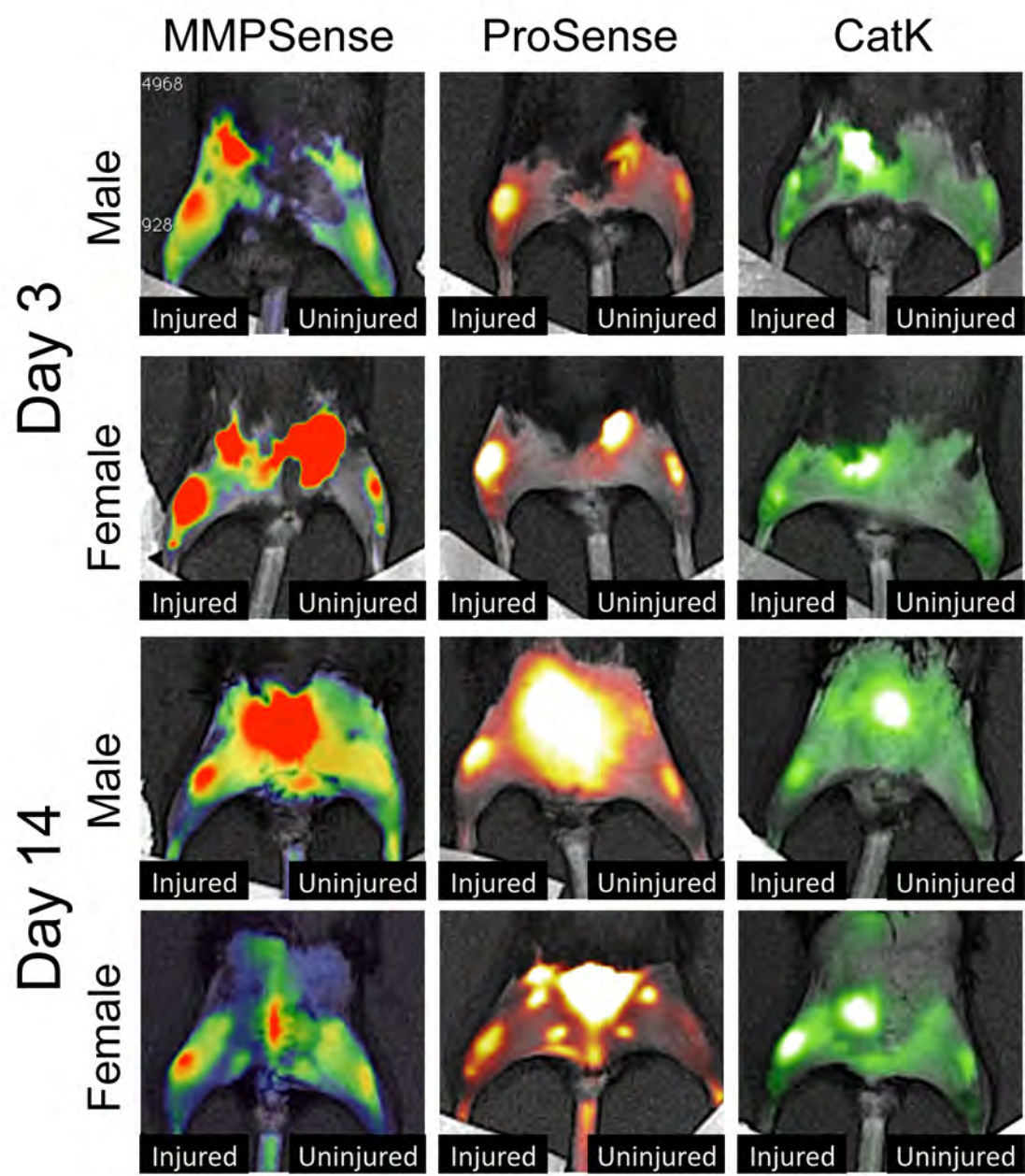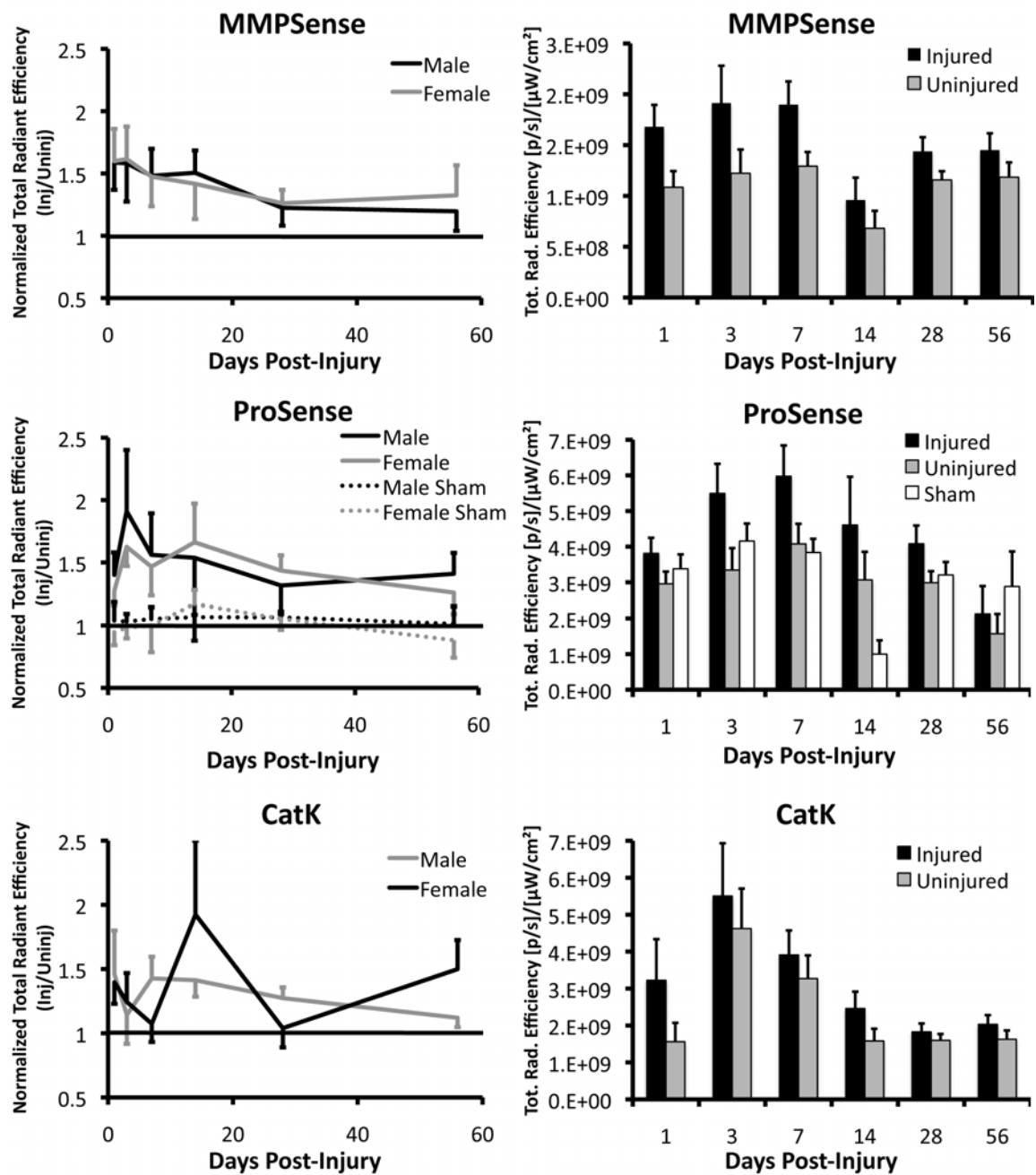
Figure 4

Figure 5

Figure 6
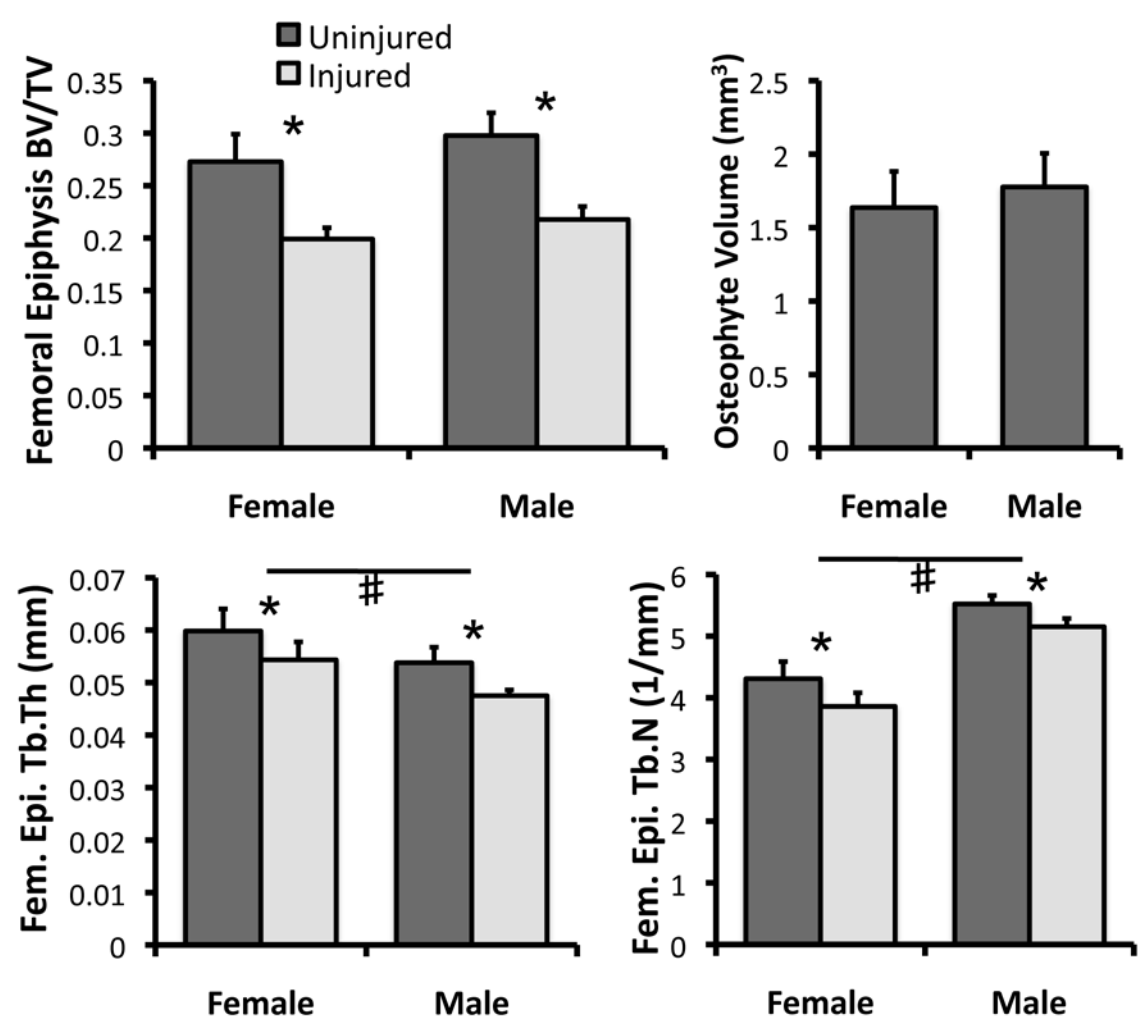
Figure 7
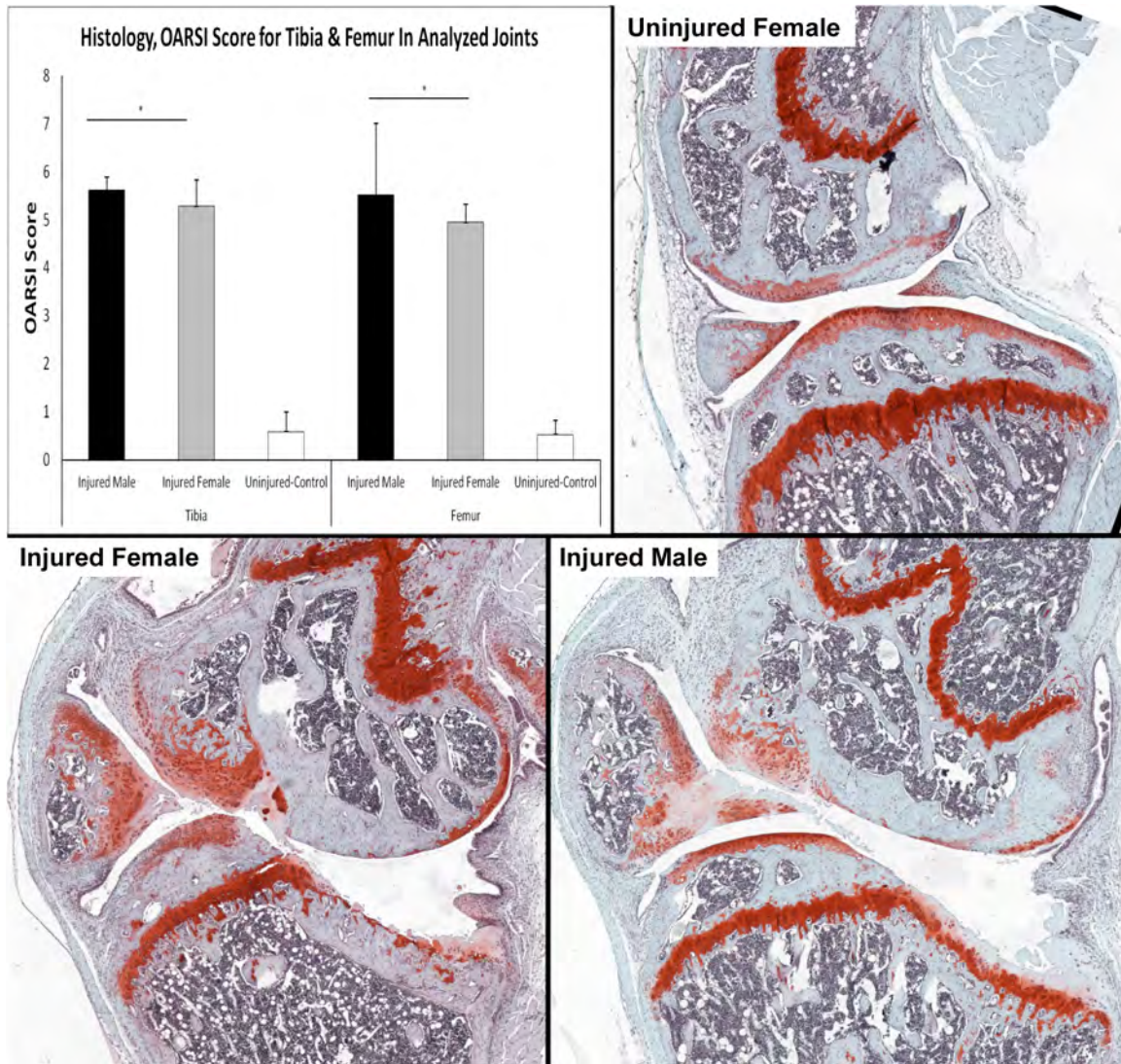
Mouse plasma ELISA

Std(pg/ml)	absorbance	Sample #	50ul 1X absorbance	5ul 1:10 absorbance
		Plasma		
0.00	0.22	UnInjured 1	0.22	0.29
31.25	0.24	UnInjured 1	0.20	0.27
62.50	0.22	UnInjured 2	0.14	0.22
125.00	0.28	UnInjured 2	0.16	0.22
250.00	0.37	8h 1	0.17	0.23
500.00	0.59	8h 1	0.18	0.21
1000.00	0.97	8h 2	0.15	0.22
2000.00	1.68	8h 2	0.19	0.27

Std(pg/ml)	absorbance	Sample #	50ul 1X absorbance	5ul 1:10 absorbance
		Plasma		
0	0.039	JnInjured 1	0.04	0.041
31.25	0.044	JnInjured 1	0.041	0.041
62.5	0.042	JnInjured 2	0.039	0.039
125	0.038	JnInjured 2	0.039	0.039
250	0.039	8h 1	0.039	0.041
500	0.036	8h 1	0.036	0.04
1000	0.043	8h 2	0.039	0.039
2000	0.046	8h 2	0.039	0.04

single-analyte ELISArray kit
Qiagen

Post-Injury Subchondral Bone Volume by μCT

Significant
p=0.0014

N.S.
p=0.1551

N.S.
p=0.4211

Error bars represent 95% Confidence Interval of the Mean
Statistical comparisons using Oneway Anova with Tukey's
post-hoc correction for multiple comparisons

Untreated
Flavopiridol

Bone Volume / Total Volume (BV/TV)

Control   3 days   7 days   8 weeks